

DOI: 10.1002/ ((please add manuscript number))

Article type: Review

Programmable and Multifunctional DNA-Based Materials for Biomedical Applications

Yuezhou Zhang^{1,}, Jing Tu¹, Dongqing Wang¹, Haitao Zhu, Sajal Kumar Maity, Xiangmeng Qu, Bram Bogaert, Hao Pei, and Hongbo Zhang**

Dr. Y.Z. Zhang, Dr. J. Tu, B. Bogaert, Prof. H. Zhang

Department of Pharmaceutical Science Laboratory, Åbo Akademi University, 20520, Turku, Finland

E-mail: hongbo.zhang@abo.fi

Dr. H.T. Zhu, Prof. D. Q. Wang, Prof. H. Zhang

Department of Radiology, The Affiliated Hospital of Jiangsu University, 212001, Zhenjiang, P. R. China

Dr. S. K. Maity

Department of Chemistry, University of Turku, 20014, Turku, Finland

Dr. X.M. Qu, Prof. H. Pei

Shanghai Key Laboratory of Green Chemistry and Chemical Processes, School of Chemistry and Molecular Engineering, East China Normal University, 200241, Shanghai, P. R. China

Prof. H. Zhang

Turku Center for Biotechnology, Åbo Akademi University, 20520, Turku, Finland

¹The authors contribute equally to this work.

Keywords: aptamer, DNA hydrogel, DNA nanostructure, DNA-Based hybrid materials, biomedical applications

Programmable and Multifunctional DNA-Based Materials for Biomedical Applications	1
Abstract	4
2. Evolution of DNA nanotechnology and DNA-based Materials	14
2.1. DNA Tile-based Nanostructures.....	18
2.2. DNA Aptamer.....	23
2.3. DNA Origami.....	27
2.4. DNA Robotics.....	33
2.5. DNA based devices and hybrid DNA nanostructures with other materials.....	35
3. Biomedical applications.....	40
3.1. Drug-DNA adducts	42
3.2. DNA aptamer	42
3.3. DNA hydrogel.....	59

3.4. DNA nanostructure	69
3.5. DNA-Nanoparticle superstructures.....	111
4. Conclusion and perspective	114
Acknowledgements.....	119
References.....	120
Table of Content:	Error! Bookmark not defined.

Abstract

DNA encodes the genetic information; recently it has also become a key player in material science. Given the specific Watson-Crick base-pairing interactions between only four type of nucleotides, well-designed DNA self-assembly can be programmable and predictable. The stem-loop, sticky end, Holiday junction, DNA tile and lattice are the typical motifs for forming DNA-based structures. The oligonucleotides experience thermal annealing in a near-neutral buffer containing divalent cation (usually Mg²⁺) to produce variety of DNA nanostructures. These structures not only show beautiful landscape, but can be endowed multifaceted functionalities. This review begins with the fundamental characterization and evolutionary trajectory of DNA-based artificial structures, but concentrates on their biomedical applications. The coverage spans from controlled drug delivery, to high therapeutically profile and accurate diagnosis. Variety of DNA based materials, including aptamer, hydrogel, origami and tetrahedron are widely utilized in different biomedical fields. In addition, to achieve better performance and functionality, material hybridization is widely witnessed, and the DNA nanostructures modification is also discussed. Although impressive advances and high expectation, the development of DNA-based structures/technologies is still hindered by several commonly recognized challenges, such as the nucleases instability, lacking of pharmacokinetics data and relatively high synthesis cost.

1. Introduction

Deoxyribonucleic acid (DNA) is the exquisite design of nature which acts as the central genetic carrier of life for billions of years.^[1] DNA-based materials represents a forefront frontier for the biomedical field by making programmable and multifunctional materials or hybrid materials with nanoscale features with DNA.^[2] To fabricate DNA-based materials, the fundamental understanding of the physical and chemical properties of DNA is demanded.

As presented in many text books, DNA is built up with monomeric nucleotides, which is made of nitrogenous base, pentose sugar and a phosphate. The covalently bonding between pentose sugar and phosphate forms the backbone of DNA and four types of nitrogenous base, cytosine (C), thymine (T), guanine (G), adenine (A) can selectively bind to each other through hydrogen bonds (HB) to form Watson-Crick double-strand helix.^[3] The two purines (A and G) have double heteroaromatic rings and two pyrimidines (T and C) have single ring. The base pairs are complementary connection of adenine-thymine (A-T) and guanine-cytosine (G-C) in DNA, and adenine-uracil (A-U) and guanine-cytosine (G-U) in RNA, which derive from hydrogen bonds (H-bonds). The atom covalently connected with hydrogen atom designate H-bonds donor while another one is H-bonds acceptor. It seemed not only the amount of HBs determinants DNA structure stability, the distance (between two electronegative atoms) and angle of HB also play important roles. H-bonds between amide C=O and OH have a median distance of 2.75 Å in Cambridge Structural

Database (CSD), with NH donors, the median distance increases by about 0.15 Å.

Within protein binding site regions of the Protein Data Bank (PDB), the median distances reserved by the distributions are significantly broader.^[3] The base pairs are selective in complementary manner mainly due to the favorable distance between purines and pyrimidines in DNA double helix and the matching of HB donors and acceptors in the nitrogenous bases' molecular structure. It is believed that two HBs are to form when A-T and A-U coupled, while the perfect recognition of G to C is favored by three HBs, which lead to a straightforward conclusion that G-C pair rich nucleoid acids structures feature high thermostability.^[4] The calculated HB distances are as following: 1) A-T pair, 2.85 Å (N6-H6 \cdots O4), 2.81 Å (N1 \cdots H3-N3); 2) G-C pair, 2.73 Å (O6 \cdots H4-N4), 2.89 Å (N1-H1 \cdots N3), 2.87 Å (N2-H2 \cdots O2).^[5] However, the NMR dipolar data indicated time-averaged distance between hydrogen atom and acceptor nitrogen atom with lengths of 1.80 ± 0.03 Å for A-T and 1.86 ± 0.02 Å for C-G in double stranded DNA.^[6] A significant discrepancy between theory and experiment H-bonds lengths in Watson-Crick base pairs was contributed to molecular environment (water, sugar hydroxyl groups, counterions) in the crystals.^[5] In addition, these H-bonds are not perfect linear and the deviation from the acceptor plane is generally 0.6-4.2° in theory.^[5] Eley and Spivey reported the H-bonded nucleobase pairs within the double helix of the DNA π - π stack with a distance of 3.4 Å,^[7] disclosed another crucial contributor of DNA specific structure. Theoretically, it is possible to have other bases combinations than the canonical Watson-Crick pairs, but

the hydrogen bond donors and acceptors would not match. Donor/acceptor pair at each position is needed. The empirical H-bonds between two pyramids T and C was too far to form H-bonds while two purines A and G was too close and repel each other. Therefore, base pairing between complementary strands and π -stacking between adjacent bases within single strand are predominant factors to maintain unique DNA double helix and their individual contribution responsible for the stability of the structure has been detailed.^[8] Utilizing those biological features, single stranded DNA (ssDNA) long chain was folded with hundreds of staple ssDNA to create non-arbitrary two- and three-dimensional DNA origami nanostructures.^[9] Such programmable and well-organized nanoplatform is an ideal harbor for polycyclic aromatic hydrocarbon containing entities, which rationalize doxorubicin (DOX) to be classical a model candidate for DNA-based drug delivery systems to circumvent its unwanted side effects.^[1]

The alternating sugar and phosphate groups from backbone of DNA define directionality of the molecule. In double-stranded DNA, the molecular double-helix shape is formed by two linear sugar-phosphate backbones that run opposite to each other and twist together in a helical shape.^[10] The sugar-phosphate backbone is negatively charged and polar, which allows the DNA backbone to hydrate by water and therefore enable DNA to assemble into hydrogel-like structures in aqueous circumstance.^[11]

One DNA double-helix has two grooves that not equal in size. The major groove occurs where the backbones are far apart, when they are close together the minor groove occurs. The grooves twist around the molecule on opposite sides. Proteins^[12] and other molecules that bind DNA specifically recognize either the major or minor groove. Certain proteins bind to DNA to alter its structure or to regulate transcription or replication. Beside the double helices, DNA can also form triplexes and quadruple helices. Cellular DNA is stored in a confined space to form the chromosomes, designating as tertiary structure vary among different organisms. In prokaryotes, the DNA is folded into super-helix and entangled with few proteins.^[13] Eukaryotic chromosome contains very large amount of DNA, the packing is more complex and compact with the help of the proteins such as histones.^[14] The DNA can be twisted in a process called DNA supercoiling. In a “relaxed” state, a strand usually revolves around the double helix axis with one complete turn of every 10.4 base pairs. If the DNA is positively supercoiled, the bases are held together more closely, *vice versa*. Inspired by nature, different types of hybrid DNA based materials and DNA superstructures are created and utilized in biomedical applications.^[13] Metal ions stabilize DNA double helix into a particular conformation for storage and propagation of genetic information. Metal ions, however, can interact with various sites on nucleic acids. The relative affinity of metal ion coordinates to the negatively charged phosphodiester backbone or other donor sites related with the nucleobases mediated interactions.^[15] The applications of metal-DNA interactions in nanotechnology,

biosensor, bioelectronics as well as therapeutic applications have been reviewed.^[16]

Transition metal ions are of particular interesting because they may lead to DNA mutations and participate the cross-linking between DNA chains. Among versatile metal ions, gold nanoparticles (AuNPs) are getting more attractions because of their size-dependent optical and electronic properties.^[17] Hybrid materials prepared with DNA and AuNPs have been studied for many years since thiol-ssDNA can be absorbed to the gold surface via the thiol group mediated interactions.^[18] Besides, magnetic nanoparticles, such as cobalt ferrite nanoparticles can efficiently bind to DNA in aqueous solutions, forming bionanocomposite.^[19] The combination of metal nanoparticles with DNA open new window to understand hybrid DNA-based materials from different horizon and endow them broader applications.

Comparing to protein-based ligands, nucleobases comprising DNA provides less chemical variety since only four building bases are available. The introduction of functional groups at just one of the four bases has been of considerable interest because diversifying the nucleic-acid-based ligands can minimize the diversity gap between nucleic acid- and protein-based ligands and fabricate a new class of ligands with favorable characteristics of both. The catalytic activity of aptamers binding properties were enhanced by introducing nucleobase functional groups such as amino acid side chains^[20] or small molecules fragments^[21] at either the 5-position of pyrimidines or the 7- or 8-position of purines. Among several types of chemical moieties, large, hydrophobic functional groups that resemble amino acid residues,

such as benzyl, naphthyl and isobutyl were the most effective modifications for slow off-rate modified aptamer target to a wide range of proteins.^[22] Comparing to single modification, the aptamer with two modified bases assess higher binding affinity, specificity with species cross-reactivity and nuclease resistance for proprotein convertase subtilisin/kexin type 9.^[23] The aptamer implies not only HB, but also hydrophobic interactions for the aptamer-protein recognition.

The replacement of DNA phosphodiester by amide give rise to an artificially synthesized polymer peptide nucleic acid (PNA) with higher binding strength than same length of DNA due to the lack of electrostatic repulsion.^[24] The relative instability of mismatch PNA/DNA bases pairing comparing to DNA/DNA duplex seems to account for the PNA's binding specificity. Besides, PNA is more insistent to nuclease, and enzymes then DNA. Few studies also discussed the potential to replace phosphodiester by squaramide not only in small nucleoside-like ligand^[25] but also in macro-molecules such as lipid^[26] and DNA^[27] since squaramide was considered as a bioisostere of phosphate.^[28] To fulfill multiple functionalities, ssDNA structures often covalently link with other functional units. Therefore, chemically active moieties, such as amine, carboxylic acid, azide, alkyne and thiol, were often attached at the terminal base of the specific DNA strand to facilitate some easy-going amide coupling, click chemistry and disulfide-thiol exchange reactions. The flexibility in chemical modification allows the tailor fabrication of multifunctional and programmable DNA materials or hybrid DNA materials for different types of biomedical applications. It

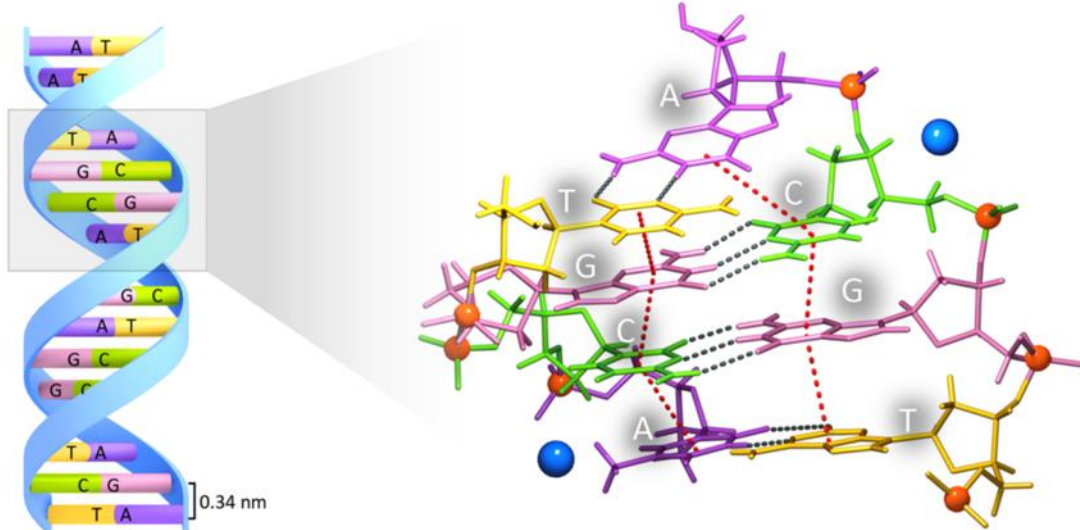
also enables the specific surface alignment of different probes mediated by DNA materials, to enhance the super sensitive biomarkers detection with DNA based biomedical devices.^[29]

There is a growing interest in structural studies of DNA by both experimental and computational approaches. Often, 3D-structural models of DNA are required for the analysis and design of nucleic acid structures, devices, and systems.^[30] The regularity of the double-stranded DNA structure makes it especially suitable for modelling, which is of great value for rational design of DNA nanostructures. Various software packages are available that model user specified base-pair sequences into 3D structure.^[31] NUPACK was one of most utilized web server, which allows the user to specify the components and conditions of the solution of interest, such as temperature, number of strand species, maximum complex size, strand sequences and strand concentrations.^[32] Wolfe et al described a nucleic acid structure design algorithm based on test tube ensemble defect optimization.^[33] By adjusting the equilibrium base pairing properties of interacting nucleic acid strands,^[33] a framework was created to guild the hybridization of multiple nucleic acid strands with different sequences in solution,^[34] therefore unified and generalized the complex design, multistate complex design, test tube design, and multistate test tube design tools provided by the NUPACK. The first analysis algorithm for calculating the partition function^[35] of an unpseudoknotted complex of multiple interacting nucleic acid strands was proposed

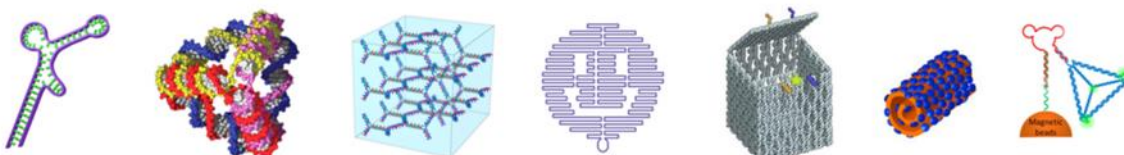
by Robot et al, based on extension of secondary structure models to the multi-stranded cases.^[35]

In this review, we first summarize the evolution of DNA-based materials, from natural primary, secondary and tertiary structures to artificial assembles such as DNA aptamer, origami, hydrogel, dendrimers, molecular beacon, protein or nanoparticles' hybrid DNA materials etc. Then we elucidate the specific and different biomedical applications of individual DNA structure, including (bio)sensing, targeted imaging, intracellular drug delivery, diagnostics, gene therapy, tissue engineering as schematically represented in **Figure 1**.

Chemical and physical characterization of DNA



DNA-based materials



Biomedical applications



Figure 1. DNA nanostructures and their biomedical applications. Aptamer, reprinted with permission

from ref.[36], Copyright © 1992 Nature Publishing Group. Tetrahedron, reprinted with permission

from ref.[37], Copyright © 2005 American Association for the Advancement of Science. Hydrogel,

adapted with permission from ref.[38], Copyright © 2006 Nature Publishing Group. DNA origami

(smile face), adapted with permission from ref.[9a], Copyright © 2006 Nature Publishing Group. DNA

origami (box with lid), reprinted with permission from ref.[39], Copyright ©2009 Nature Publishing Group. DNA origami-protein complex, reprinted with permission from ref.[40], Copyright © 2014 American Chemical Society. DNA nanodevices, reprinted with permission from ref.[41], Copyright © 2016 American Chemical Society. Targeted drug delivery, adapted with permission from ref.[41], Copyright © 2015 American Chemical Society. DNA nanodevice for diagnostic, reprinted with permission from ref.[42], Copyright © 2010 WILEY-VCH Verlag GmbH & Co. KGaA, Weinheim.

2. Evolution of DNA nanotechnology and DNA-based Materials

In this section, the diverse self-assembled DNA nanostructures and DNA nanotechnology from the material perspectives are discussed, arranged according to their usage wideness and commonality.

Over the past few decades, molecular self-assembly processes have been utilized to fabricate various nanostructures including nanofibers, nanotubes and vesicles from self-assembling nucleic acids, peptides, lipids and polymers.^[43] However, it remains a challenge to develop powerful assembly algorithms to achieve programmable structural design with precisely nanoscale control, which will contribute to the multi-functional materials fabrication with improved fidelity and yield. Undoubtedly, DNA nanotechnology is among the most promising algorithms^[44] since DNA has excellent features such as self-assembly, molecular recognition, programmability, predictable nanoscale structure etc.^[45] Moreover, modern technologies such as automated solid phase synthesis, polymerase chain reaction and molecular cloning

enable the robust synthesizing of oligonucleotides and long nucleic acid stands at affordable price.^[46] DNA is a natural self-assembling biopolymer directed by canonical Watson-Crick base pairing, which form predictable, double helical secondary structures stabilized by hydrogen-bonding, π-π stacking, and hydrophobic interactions.^[47] Unique geometries can be formed by regulating the assembling of complementary single-stranded DNA molecules. Artificial DNA nanostructure was first proposed by Nadrian C. Seeman in the 1980s.^[48] Since then, DNA nanotechnology has become one of highlights in this area. To date, various DNA nanostructures and nanodevices with diverse geometry and topology have been designed and fabricated. Multiple landmark examples were chronologically sorted and showed in **Figure 2**.

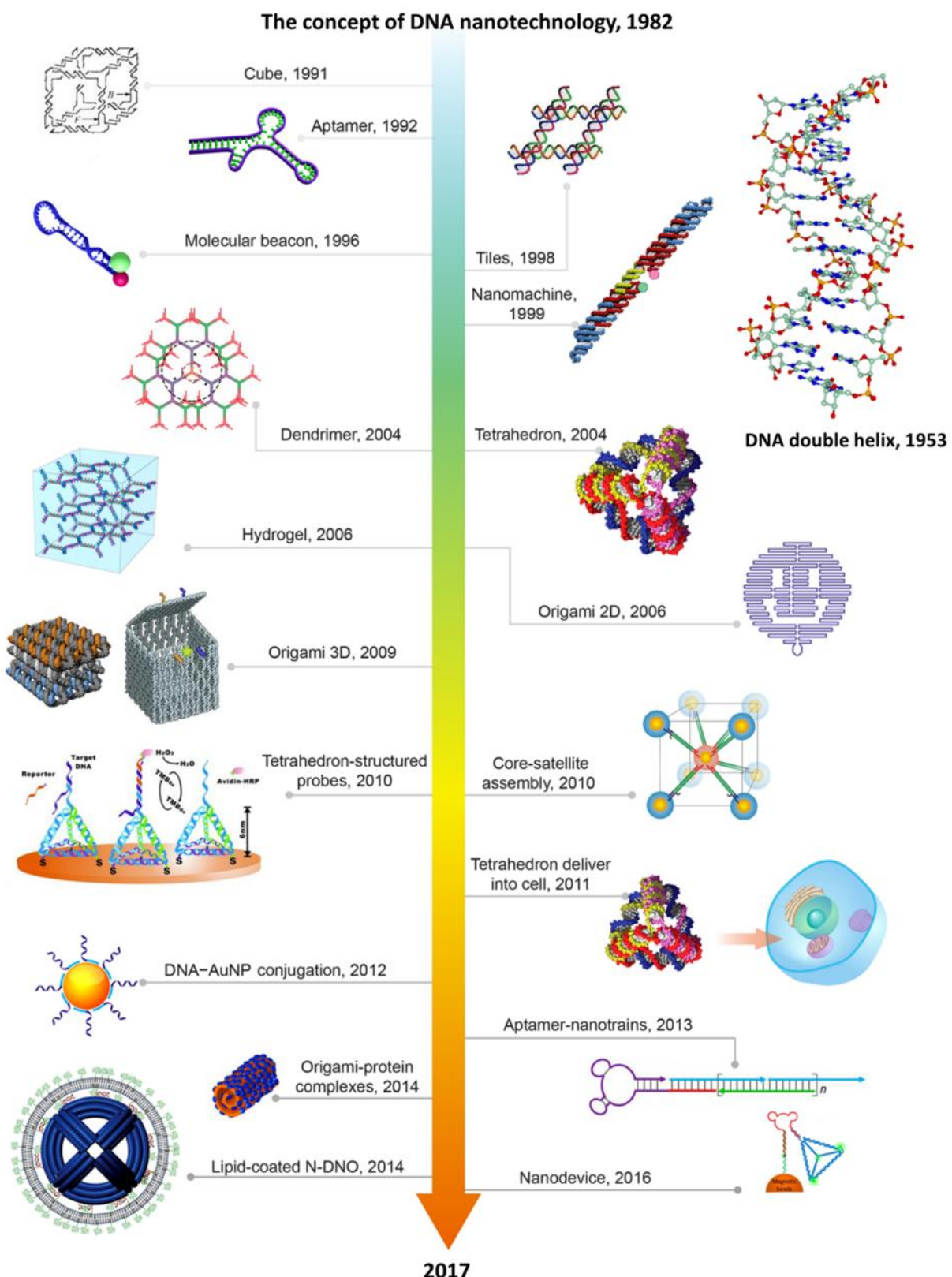


Figure 2. Evolution of DNA nanotechnology for past several decades. DNA cube, reprinted with permission from ref.[49], Copyright © 1991 Nature Publishing Group. Aptamer, reprinted with permission from ref.[36], Copyright © 1992 Nature Publishing Group. Molecular beacon, adapted with permission from ref.[50], Copyright © 1996 Nature Publishing Group. Tiles, adapted with permission from ref.[51], Copyright © 1999 American Chemical Society. Nanomachine, adapted from ref.[52], Copyright © 1999 Nature Publishing Group. Dendrimer, reprinted with permission from ref.[53], Copyright © 2004 Nature Publishing Group. Tetrahedron, reprinted with permission from ref.[37], Copyright © 2005 American Association for the Advancement of Science. Hydrogel, adapted with permission from ref.[38], Copyright © 2006 Nature Publishing Group. DNA origami (smile face), adapted with permission from ref.[9a], Copyright © 2006 Nature Publishing Group. DNA origami (box with lid), reprinted with permission from ref.[39], Copyright © 2009 Nature Publishing Group. DNA origami, reprinted with permission from ref.[47], Copyright © 2009 Nature Publishing Group. DNA nanodevice for diagnostic, reprinted with permission from ref.[42], Copyright © 2010 WILEY-VCH Verlag GmbH & Co. KGaA, Weinheim. Core-satellite assembly, reprinted with permission from ref.[54], Copyright © 2010 Nature Publishing Group. Tetrahedron delivery into cells, adapted with permission from ref.[55], Copyright © 2011 American Chemical Society. DNA-AuNP conjugation, reprinted with permission from ref.[56], Copyright © 2012 American Chemical Society. DNA origami-protein complexes, reprinted with permission from ref.[40], Copyright © 2014 American Chemical Society. Lipid-coated N-DNA, reprinted with permission from ref.[57], Copyright © 2014 American Chemical Society. Aptamer nanotrains, reprinted with permission from ref.[58], Copyright ©

2012 National Academy of Sciences. DNA nanodevices, reprinted with permission from ref.[41],

Copyright © 2016 American Chemical Society.

2.1. DNA Tile-based Nanostructures

The journey of self-assembled DNA nanostructures began with Seeman's construction of artificial branched DNA nanostructures, inspired by Holliday Junction which occurs during genetic recombination in the cell.^[59] The four sequence specific oligomeric nucleic acid strands with extended overhangs (also known as sticky ends) at each arm of ssDNA stands, self-assembled into an immobile four-way junction.^[60]

(Figure 3a) Since then, immobile DNA arm junctions have become a building block for designing more complex and stable DNA nanostructures. Later on, Seeman's group created various DNA nanostructures based on DNA branched junctions with more arms, including three-arms,^[61] five-arms, six-arms, eight-arms and even twelve-arms.^[62] Apart from Seeman's work, another important DNA geometrical structure (triangles) has been introduced by Mao and co-workers.^[63] This rigid DNA triangles from flexible DNA four-arm junctions which are promising for the building up “tensegrity” structures.^[63] The structures were made of rigid rods connected by short “tendons” that were connected by short tensegrity segments.^[63] (Figure 3b) However, branched DNA junctions have low rigidity, and DNA branched junction based assembly does not often yield a regular structure.

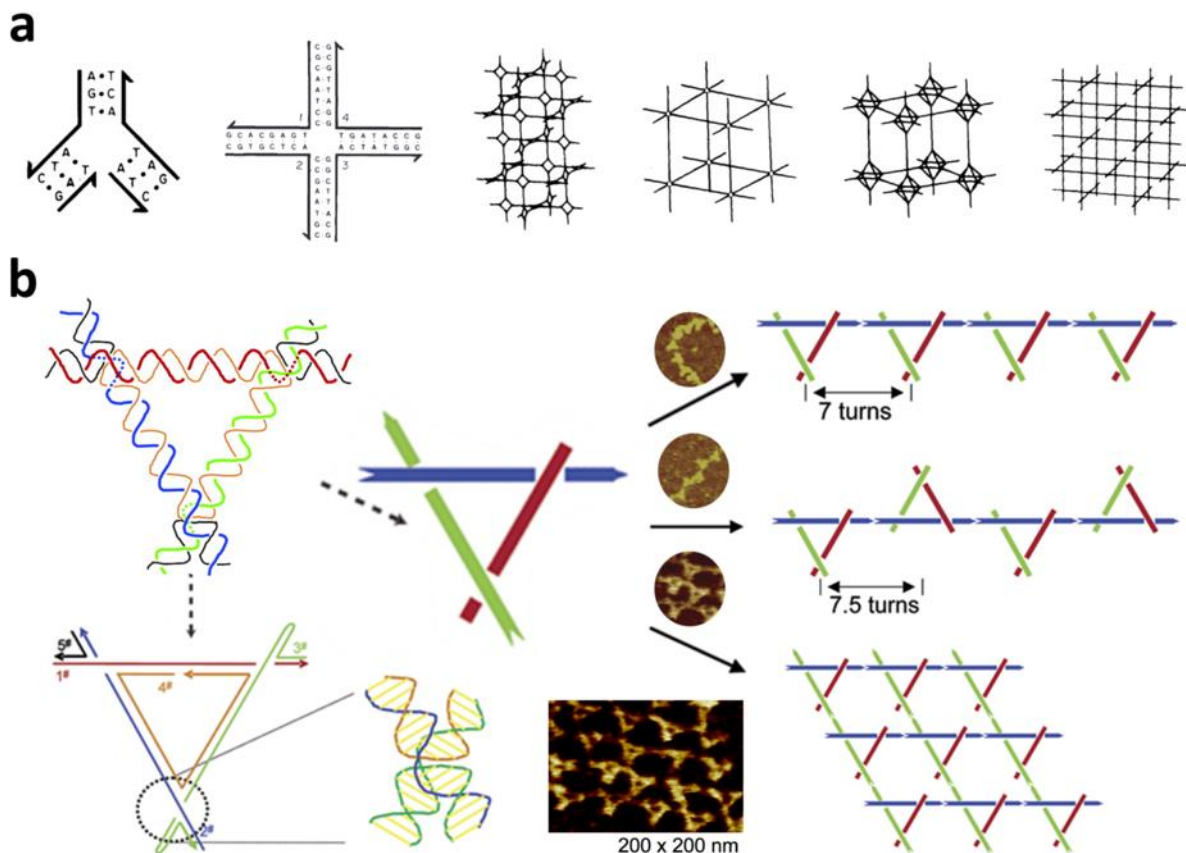


Figure 3. DNA tile for nanostructure. a) DNA junctions and lattices, reprinted with permission from ref.[60], Copyright © 1982 Academic Press Inc. (London) Ltd.; b) Fabrication of a rigid triangle structure from DNA four-arm junctions, reprinted with permission from ref.[63], Copyright © 2004 American Chemical Society.

To address these issues, researchers have established modified branched DNA junctions to generate rigid and defined nanostructures. Primarily, Seeman and co-workers came out with an innovative idea by creating the double crossover (DX) motif consisting two parallel double-stranded helices with individual strands crossing between the helices at two crossover points, each of which was a topologically

four-arm junction.^[64] Owing to constraints between two four-arm junctions in a single orientation, DX tiles were rigid enough to act as structural building blocks for more complex DNA nanoarchitectures and became the most fundamental motif in DNA nanotechnology. Extensively, scientists were trying to construct tile-based 3D DNA nanostructures. The first tile based 3D DNA structures, the cube^[49] and truncated octahedron^[65] were constructed by Seeman and co-workers. However, the study only provided indirect evidence for the formation of the 3D structure. And those structures were obtained with low yield. A few years later, a remarkable study was carried out by Shih et al. They reported the formation of an octahedron with DX-like edges and PX-motifs:^[66] a 1.7 kb single-stranded DNA (heavy strand) folded with five 40-mer octahedron (ODN) smaller strands (light strands).^[67] Seeman's group successfully constructed crystals from a continuous 3D lattice formed by the self-assembly of a DNA 13-mer in 2004.^[68] This work represents a milestone in fulfilling Seeman's original vision of using 3D DNA lattices as hosts to organize guest protein molecules and facilitate protein crystallography. Later, Seeman's group also assembled 3D DNA crystals by purposely designing sticky-end connections^[69] rather than through simple, nonspecific base stacking. They used self-assembling tensegrity triangle motifs to generate 3D crystals with diverse unit dimensions. In parallel, several groups fabricated DNA nanostructures using DX DNA tiles, which includes periodical one dimensional tubes^[70] and ribbons, two dimensional crystal,^[71] triangle,^[72] quadrilateral^[73] and pseudohexagonal trigonal arrays.^[73] Goodman et al. reported

construction of a chiral tetrahedron DNA structure.^[74] With this approach, it was found that adding programmable linkers gave structural stability and resistance to deformation. In another experiment, Yan's group replaced DNA strands in a DX motif with locked nucleic acid (LNA) strands in the formation of 2D arrays.^[75] After huge success of the DX tile in the fabrication of DNA nanostructures, Seeman and co-workers designed and fabricated triple-crossover (TX) tiles that consists of three adjacent helical domains lying in the same plane, connected at two or more sets of crossover points,^[76] as found in linear lattices, 2D arrays,^[76] and DNA tubes.^[77] Paramecic crossover (PX) tile,^[78] another important class of DNA tile, was also synthesized by Seeman's group, which was composed of two flanking parallel double helices, holding together exclusively by Watson-Crick base pairing. Various other tiles have also been executed. For example, triangle tensegrity DNA tiles which involves rigid struts and flexible tendons.^[63] The balance between two forces ends up with stable and rigid nanostructures. This strategy has been explored for the fabrication of 2D regular DNA arrays. For example, triangular DNA tiles with three four-arm junctions connected together in single DNA motif was fabricated,^[63] and in other examples hexagonal patterns are formed.^[79] Three-point or Y shaped,^[80] and six-point star^[81] motifs have also been used by Mao's group for the construction of two dimensional arrays. Just recently Ke's group reported the DNA "domino" nanoarrays that were able to transform in a stepwise relay process initiated by the

hybridization of a trigger strand, empowering the DNA nanodevice the potential to mimic cellular information relay at the molecular level.^[82]

Another type of DNA tile, known as 4×4 tile, consisting of four four-arm junctions oriented with square aspect ratio was designed and fabricated by LaBean's group.^[83]

These are readily self-assembled into two distinct lattice forms: nanoribbons or 2D nanogrids. He et al. assembled larger two-dimensional arrays from 4×4 tile by introducing two new ideas.^[84] Firstly, for the generation of 4×4 tile, they used symmetric sequences and secondly, it followed a "corrugation strategy", consisting of two adjacent building blocks face up and down alternatively in each growing direction, such that small curvatures of the individual motif are canceled instead of accumulating throughout the structure.

More complex and modified polyhedra were also constructed in a single step.^[85]

Knudsen reported a covalently closed and efficiently assembled octahedral DNA cages^[86] that were resistant to thermal and chemical denaturation. These unique properties make them as a promising candidate as delivery systems. In addition, formation of various 3D structures such as prism, cubic, pentameric and hexameric prisms, heteroprism, and a biprism were reported by Sleiman.^[87] By controlling the flexibility and the concentration of the three-point star tiles and adjusting the length of central single-stranded loop, Mao's group created a tetrahedron, a dodecahedron, a buckyball and a DNA octahedral structure.^[88] Using the same strategy, a five point star tile was designed and self-assembled into icosahedra.^[89]

In a recent work, Yin and co-workers described a method for the synthesising of 1D,^[90] 2D,^[91] and 3D^[92] nanostructures based on single-stranded tile (SST), also called DNA bricks. In this method, the sequence of each single-stranded DNA and their sticky-end associations were deliberately designed. With increased number of single-stranded DNAs in SST assembly, DNA nanopores could be constructed through the formation of circular bundle which contained varied number of DNA duplexes. One of the nanopores consisting of six DNA duplexes could be synthesized using 14 SS DNAs.^[93] Each of these DNA brick had the ability to bind four neighboring DNA bricks, thus allowing the precise control of the shape, size, and sophisticated surface properties of the DNA nanostructures.^[94] The beauty of this method relies on the fact that it can form any prescribed 3D shapes by single step annealing reactions without considering the purification and stoichiometry of DNA strands.

2.2. DNA Aptamer

Aptamers are short, single-stranded oligonucleotides (DNA or RNA). The word aptamer coined by Eligton and Szotw,^[95] derived from the latin “aptus-fit” and greek “merous-part”. In 1990, several research groups independently developed the first RNA aptamers.^[96] Most aptamers binding to proteins with equilibrium constant (K_d) in the range of 1 pico Molar to 1 nano Molar.^[97] Similar to monoclonal antibodies, these nucleic acid ligands bind to nucleic acids, proteins, small organic compounds, even entire organisms.^[98] Aptamer are often identified by using a technique called

Systematic Evolution of Ligands by Exponential enrichment (SELEX), which was developed by several independent groups^[95, 99] for generating various DNA and RNA ligands. Through this technique, aptamers with high affinity and specificity to the targeting molecules can be isolated from sequence pool after several rounds of selection. The binding mechanisms include induced fit, structure compatibility, electrostatic interactions and hydrogen bridges.^[98] To date, more than 250 aptamers had been sequenced.^[100] DNA aptamers are 16-50 oligonucleotides bases long. Interaction of aptamer to the target is based on three dimensional folding patterns.^[101] The complex three dimensional structure of single stranded oligonucleotides is driven by the intramolecular hybridization, thus resulting in the folding of aptamer into particular shape.^[102] In theory, it is possible to select aptamers against any molecule target. Aptamers have been selected for various targets by incubating the target molecules in a pool with 1010 to 1020 oligonucleotides. Aptamer can distinguish between closely related protein analogous, or different conformational states of the same protein.^[103] Commonly used aptamer selection methods include purified protein-, cell- and live animal-based SELEX.^[104] (**Figure 4**) While aptamers are homologues to antibodies in the range of targeting recognition and variety of applications, they possess several advantages over the protein counterparts: 1) can be easier and economical produced; 2) low toxicity and low immunogenicity of particular antigen do not interfere with the aptamer selection; 3) are capable of greater specificity and affinity than antibodies; 4) can be readily modified chemically to yield

improved, custom tailored properties; 5) can specifically bound to either small molecules and complex multimeric structures; 6) are much more stable at ambient temperature than antibodies and yield much higher shelf life; 7) small size of aptamer may improve transport properties allowing cell specific targeting and tissue penetration; 8) combination therapy can be achieved by conjugate aptamer with other drugs. Aptamers have got variety of medical applications in the following fields: new drug development, bio-imaging, as therapeutic tool and drug discovery, disease diagnosis.^[105]

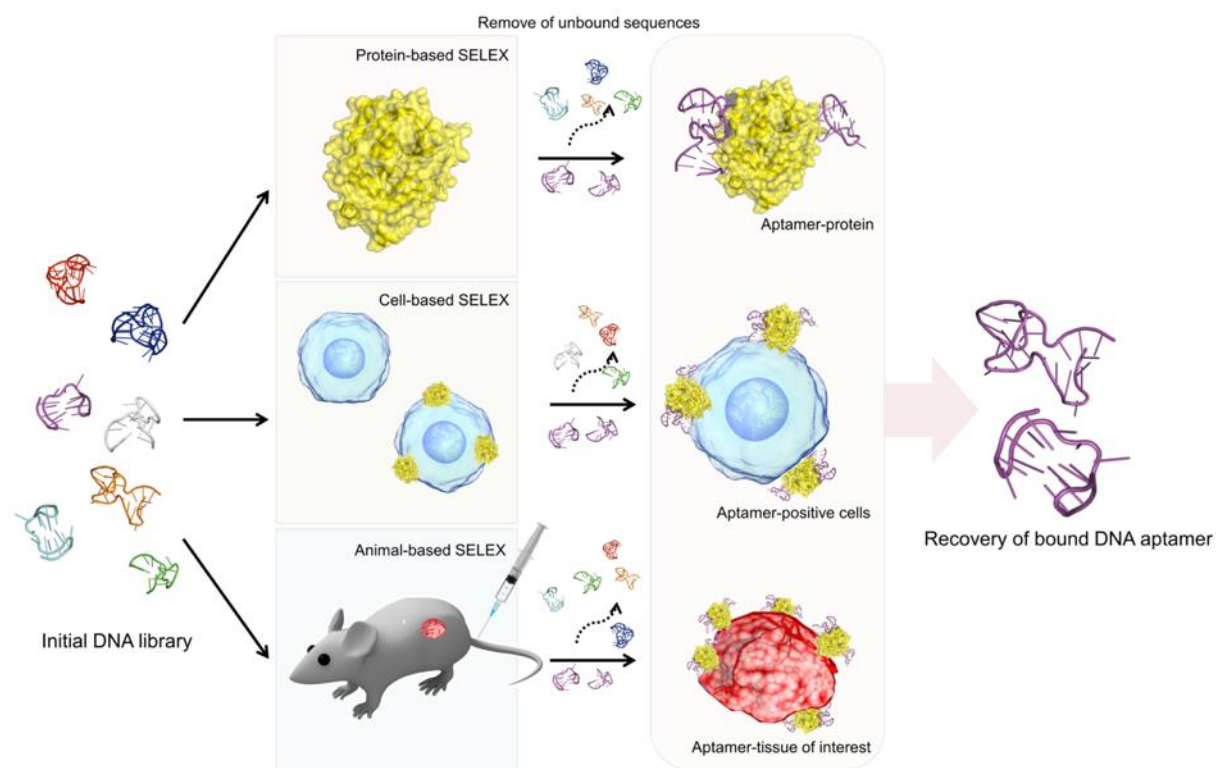


Figure 4. Schematic illustration of protein-, cell- and animal-based SELEX for aptamer identification, adapted with permission of ref.[104], Copyright © 2017 Nature Publishing Group.

Apart from aptamer-therapeutic agent conjugates,^[106] aptamer-nanoparticle conjugates have drawn a widely attention for targeted pharmacotherapy^[107] Many nanoparticles such as liposome,^[108] micelle,^[109] graphene,^[110] DNA icosahedral^[111] have been functionalized with cell-specific aptamer for high efficiency targeted delivery.^[112] Inspired by the former researches, oligonucleotide can be used as biological-gates.^[113] In other work, to fabricate targeted- and controlled-release systems, DNA aptamers were further employed as both a lid and a targeting agent.^[114] Aptamer binding region identification is of critical significance since not all the nucleotides in the full length aptamers contribute to the binding with their targets and non-binding residues maybe canceled out if SELEX methodology needs to be applied for aptamer generation. Alhadrami et al mapped key progesterone aptamer residues by using truncated aptamers/DNA duplex structures following fluorescence switching mechanism. As a result, one of the truncated sequences have shown 16-folds binding affinity increase compared to the parents aptamer.^[115] DNAzyme and aptamer conjugations have been used for molecules detection, while it is worth mentioning that orientation also should be considered. For instance, Jafari et al reported DNAzyme-Aflatoxin B1 aptamer has more catalytic activity and efficiency than reverse version^[116] since specific binding between aptamer and DNAzyme would possibility change the 3D conformation therefore influence the catalytic activity of enzyme.^[117]

2.3. DNA Origami

In 2006, the emerging of a DNA origami^[9a] changed the scenery of structural DNA nanotechnology (**Figure 5a**). “DNA origami” has transfigured the field of structural DNA nanotechnology by significantly enhancing the complexity and size of self-assembled DNA nanostructures to a simple “one-pot” reaction.^[39] The DNA origami method uses a number of short single-stranded DNA (ssDNA) oligonucleotides, also known as “staple strands”, to direct the folding path of a long circular ssDNA strand. The term origami refers to the Japanese folk art of folding paper into a diverse shape. The method is called DNA origami as one long scaffold of single strand DNA is folded to generate the desired structure with the aid of smaller staple strands.^[9a] Rothemund’s original experiment involved the folding of a genomic ssDNA derived from the M13mp18 bacteriophage, as the scaffold strand (composed of 7249 nucleotides) into arbitrary 2D shape, directed by a set of designed short “staple” strands that are complementary to different regions of the scaffold.^[39] (Figure 5b) The specific matching of the scaffold and staple strands provides well-shaped nanostructures, with high yield and reproducibility. Several of the limitations in DNA tile based methods have been addressed by DNA origami. For instance, it does not require stoichiometric equivalence, therefore eliminating the need for purification and exact determination of the concentration of the oligonucleotides, and thus reducing the time and effort required for its assembly. Another most attractive advantage of this technique is the addressability of the surface, thus allowing the attachment of different

biomolecules or nanoparticles by the modification of specific staple strands at definite

positions on DNA origami nanostructures.^[118]

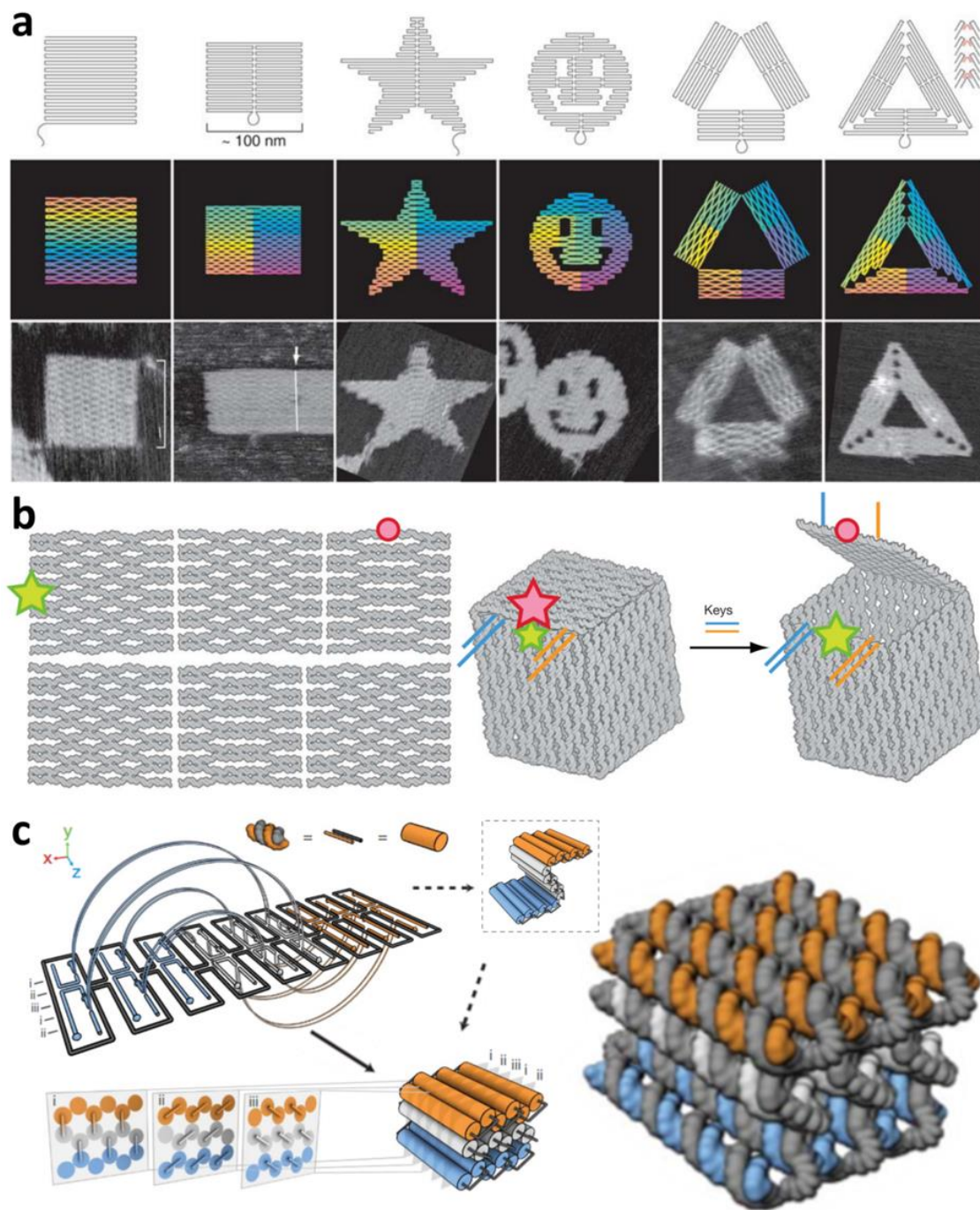


Figure 5. DNA origami structure. a) DNA origami shapes and their atomic-force microscopy (AFM)

images, reprinted with permission from ref.[9a], Copyright © 2006 Nature Publishing Group; b)

Fabrication of an addressable DNA origami box with lid, reprinted with permission from ref.[39], Copyright ©2009 Nature Publishing Group; c) Design of DNA origami, reprinted with permission from ref.[119], Copyright ©2009 Nature Publishing Group.

After the revolutionary work on DNA origami, Rothemund demonstrated construction of various arbitrary structures such as stars, squares, rectangles, smiley faces, triangles and some other complex nanostructures. Since then, scientists are using DNA origami technique to construct complex 2D and 3D DNA nanostructures (Figure 5). (Figure 5c) In 2009, Shih and co-workers^[120] reported the fabrication of DNA origami from a double stranded DNA (dsDNA) scaffold. This report unfastened a new door in the DNA origami technique. Li et al. reported a rectangular-shaped DNA origami tiles for the construction of higher order self-assembled DNA nanostructures.^[121] Sugiyama and co-workers^[122] reported the construction of 2D self-assembly from multiple DNA origami and in a very similar work Endo et al. reported formation of multi-domain DNA origami by using origami four-way junctions.^[123] The assembly of 2D DNA origami structures showed temperature-dependent dynamic characteristics, which was observed by using thermally controlled atomic force microscopy (AFM) and theoretically modelling.^[124] By combining nanomechanical spectroscopy with forces, controlled in the pico Newton range, it was unveiled that the local hybridization rate of DNA origami could be accelerated by adding a higher concentration of the staples.^[125] And DNA origami was self-assembled at room temperature under optimized condition.^[126]

The DNA origami approach has been further exploited for the construction of 3D nanostructures. In contrast to tile-based 3D self-assembly, the nanostructures synthesized by origami technique derive from several crossover events between neighboring duplexes, and their complicity and rigidity are much higher than in the former cases due to the large number of crossover points existed in the relatively solid structure.^[39, 127] Gothelf and co-workers constructed a box with a controllable lid from a combination of six origami sheets.^[39] At the same time, Kuyuza and Komiyana designed and fabricated another box-shaped origami by selective closing of a preformed open motif.^[128] Ke et al described a strategy of a scaffold DNA origami for the construction of a closed DNA tetrahedron which resembled the icosahedral structure of many viral particles.^[129] Shih and co-worker fabricated a 3D DNA-origami nanotube that is based on a honeycomb lattice.^[130] In this nanotube, six DNA helices were stapled together at consecutive 240° angles (*i.e.*, every 21 base-pairs) to form a hexagonal tube. Later, Shih and colleagues extended the honeycomb lattice approach more universally in 2009, describing a honeycomb shaped cross-sectional lattice in the X-Y plane looking end-on at DNA helices with the helical axis extending in the Z-direction as the basis for an array of 3D nanostructures including monolith, square nut, railed bridge, genie bottle, stacked cross, slotted cross.^[47] The same group also revealed a close-packed lattice strategy which was based on a square lattice that allowed for structures with more rectangular cross-sections.^[131] Later, Shih et al. also constructed tensegrity 3D origami structures

with high strength-to-weight ratios and great flexibility.^[132] They used multiple segments of unpaired scaffold for connecting rigid DNA helix-bundle units in the fabricating of 3D nanostructures. Shih and coworkers later described insertion of twists or bends into the 3D nanostructures by addition or deletion of base pairs at specific positions in a block of honeycomb duplexes to create regions of local strain.^[133] The honeycomb lattice DNA-origami could further form either tubes or flat 2D planar lattices, that were utilized for constructing plasmonic metamaterials,^[134] exhibiting tailored optical activity in the visible spectral range.^[135] Ke and coworkers also constructed an artificial DNA-protein hybrid nanoswitch whose fluorescence signal could be turned on and off by tuning the DNA origami ‘connecting strut’.^[136] In another work, DNA origami clamp was utilized to modify the surface of gold nanorods (AuNRs) at site-specific manner.^[137] And on the basis of octahedral DNA origami frame, prescribed nanoparticle cluster architectures and low-dimensional array were built.^[138]

The Yan’s group developed a method based on the organization of concentric DNA rings of different radii to fabricate 3D nanostructures with complex curvatures.^[139] This group also developed a strategy which involved the tuning of the curvatures in 3D objects to control their topology. For example, they successfully constructed a Möbius strip, a topological ribbon-like structure, as the first example of topological DNA 3D nanostructure, by precisely tuning the bending and twisting of a DNA 2D

origami.^[140] These novel 3D structures further exhibit the robustness and potential of the origami technique in different kinds of applications.

Although DNA origami technique has lots of impact in the advancement of 3D nanostructures, it still suffers from some limitations which include lacking of large surface area and limitation in the length of the standard scaffold. In some cases, the origami surface might not be sufficient for the precise positioning of functional molecules or for other applications. To overcome these limitations, scientists came up with new ideas of assembling large structures, including approaches such as algorithmic assembly from origami seeds,^[141] origami oligomerization^[121] and polymerization,^[142] the use of eight-helix bundles as staples,^[143] long single-stranded PCR amplification products,^[144] and double-stranded viral genomes^[145] as scaffolds. Nowadays, several computational tools including SARSE-DNA,^[146] caDNAno,^[120] and CanDo^[147] have been developed to facilitate the design of DNA nanostructures, making structural DNA nanotechnology more accessible to researchers from other fields.

The shape diversity of nanoscale DNA assemblies is also critical. Veneziano and coworkers developed a fully automatic inverse design procedure named as DAEDALUS (DNA Origami Sequence Design Algorithm for User-defined Structures), which could program arbitrary wireframe DNA origami exemplified by four polyhedral, six asymmetric and 35 Platonic, Archimedean, Johnson, and Catalan solids.^[148]

2.4. DNA Robotics

The structural properties of DNAs that allow them to serve as a versatile construction material have been exploited to create dynamic nanomachines by appropriate design. Since 1990s, different group of scientists have constructed various type of dynamic nanodevices ranging from small switchable structures^[149] and reconfigurable systems^[150] to structures that display complex movements such as rolling, rotating, and walking. The cell, natural protein-based molecular machines transform chemical energy (getting from ATP) into mechanical energy to facilitate a variety of biological functions like cell division, transportation, and motility to enzymatic activity.^[151] For a long time, DNA nanotechnologists have been working on the preparation of DNA based molecular machines to mimic the ability of natural proteins machines to walk along intracellular tracks and achieve controlled motion.

In 2000, Yurke and Turberfield et al. reported first example of DNA nanomachine driven by fuel DNA molecule. They used DNA building block, called DNA tweezer, to construct DNA nanomachines by hybridization. Subsequently, an auxiliary stand “fuel DNA” and “antifuel DNA” were used to close and open the assembled tweezers. Since then, many variations of the tweezers system have been developed. By connecting the arms of the tweezers with a single-stranded loop, an “actuator” device was realized that could both stretch^[152] and contract,^[153] depending on the type of set strands used. In another system, the phenomenon that happens during the DNA

transcription was exploited to control the nanomachine,^[154] in which an mRNA fuel strand was used to trigger the switch from open to the close conformation. Recently, Firrao and co-workers developed a new “tweezer” concept to control the motion of a 2D DNA origami structure.^[155] They designed and fabricated a 2D DNA circular origami consisting of external ring and an internal disk, which was connected to ring in two opposite points. The internal disk was made with relative flexible two halves (named “wings”), which could be bent out of the plane by the loop's fully complementary to the central part of the “probe”. Seeman and co-workers developed a more complex hybridization-driven device than the tweezers-related structures,^[156] known as “PX-JX₂” nanomachine based on “paranemic-cross-over” DNA. PX and JX₂ are basically topoisomers. The only difference is that two parallel double helices in PX are joined by reciprocal exchange (cross over) of strands at every possible point while JX₂ contains two adjacent sites where backbones juxtapose without cross over. When parts of PX structure are removed and replaced by DNA sections without cross-overs, molecules in a “juxtaposed” structure result in which two helices are rotated by 180° with respect to the paramedic structure. This motion can be used to rotate molecular structures attached to the nanodevice and the change in the morphology can be measured by atomic force microscopy (AFM). Later, Seeman's group exploited this technique to develop more complex molecular nanomachines such as PX-JX₂-BX device.^[157] In addition to the rotation of the PX section, the central part of the device could be made to contract and extrude two double-cross-over sections,

which results in an overall crosslink conformation. Further, a system containing a pair of PX-JX₂, in which the pair could be operated in parallel by using the same set of effector strands.^[158] The functional operation in this device is that one device is switched from the PX to the JX₂ conformation, while the other is switched in the opposite direction, thereby resulting in a reciprocating motion of the two structures. In other experiments, Seeman and co-workers introduced PX-JX₂ “cassette” into a supramolecular network made from triple cross-over (TX) DNA tiles, in which PX and JX₂ state could be switched by fuel and set strands. By using marker TX tile attached to the cassettes, the switching between the PX and JX₂ states could be impressively visualized for the whole supramolecular array on AFM.^[159] Recently, Pei and Fan reported an exonuclease III-(Exo III) powered stochastic DNA walkering system consisting of a 21-base sequence using a burnt-bridge mechanism.^[160] This walker can move on a spherical nucleic acid-based track with the driving force from digestion of tracks with Exo III.

2.5. DNA based devices and hybrid DNA nanostructures with other materials

Due to the unique structural morphology and advantage of precise modification at the definite sites on DNA nanostructure by various chemical conjugation strategies, many guest nano-objects can be arbitrarily decorated at predesigned positions on DNA scaffolds. Recently, DNA nanostructures have been widely utilized as ideal templates to construct new materials with hallmark properties by organizing multiple

nanomaterials, such as proteins, lipid molecules, inorganic nanoparticles, etc.^[161] DNA nanostructures bear high density of probes at specific distances defined by deliberately designed internal features.^[162] These probes can be confined molecules with diagnostic and therapeutic significance and thus potentially, can be useful in biomedical applications.

By introducing specific interactions, individual protein particles were immobilized on DNA polyhedron scaffolds to form highly ordered DNA-protein hybrid structures.^[161] For example, Park et al. utilized the biotin-streptavidin interactions to pattern streptavidin protein molecules at nanometer spatial resolutions.^[73] By selectively functionalizing DNA tiles with biotin, 2D arrays of streptavidin with programmable inter-protein spacing were achieved. Based on the same principal, Mao and coworkers created antibody arrays with a vision of potential applications in immunodiagnostics or catalysis.^[163] As a model system, they used a grid like scaffold to conjugate fluorescein which bonded to anti-fluorescein antibody to form periodic arrays of antibodies with a periodic spacing of ~20 nm. Yan and co-workers developed a general strategy to produce high-density peptide arrays that rely on the addressable information encoded in the nucleic acid portion of a DNA-tagged peptide.^[164] They showed that Myc-epitope peptide was covalently conjugated to DNA oligonucleotide and upon self-assembly, peptides were displayed on the DNA scaffold at periodic distances. Functionality of the peptide array was then demonstrated by addition of anti-myc antibody which bonded to the peptides displayed on the DNA scaffold.

Owing to the fact that DNA or RNA aptamer can binds nucleic acid, proteins, small organic compounds, and even entire organisms,^[165] they have been incorporated in the DNA nanoarray for diagnostic and therapeutic significance. Due to the broad availability of nucleic acid aptamers and their compatibility with DNA nanostructures through simple strand hybridization, the aptamer-protein binding approach has demonstrated to be a highly programmable way for DNA directed self-assembly of protein nanoarrays.^[166] For example, Yan and co-workers have demonstrated that spatially addressable multi-protein nanoarrays can be constructed by incorporating different aptamer sequences into complex DNA nanostructures.^[167]

Another important side of self-assembled DNA nanoarchitectures as scaffolding elements lies in their potential to organize various nanoparticles (NPs) into discrete structures. For example, Mirkin et al demonstrated the nano-patterning of colloidal gold nanoparticles using DNA nanoarchitectures as scaffolds to synthesized DNA hybrid (DNA-AuNPs) nanodevice.^[168] Thiol-terminated ODNs readily react with the surface of AuNPs and subsequent hybridization provided access to assemblies of higher order.^[169] DNA-Au-NPs offer some extra features like plasmonic effects or the ability of fluorescence quenching, which represent a significant extension to the functionality of 3D DNA nano-objects.^[170] These characteristics are important in the field of bio-imaging and biomedicine; therefore DNA-AuNPs have become a very Three gold nanorods (AuNRs) were positioned onto a reconfigurable DNA origami

tripod. imaging, detection and as transfection agents and gene regulation materials.^[171]

The surface assembly of DNA probes on the Au has been studied. In 2003, Fan et al. developed an electronchemical DNA (E-DNA) sensor with a sensitivity of 10 pM. This sensor was fabricated by hybridizing the 2D DNA stem-loop structure onto Au electrode via Au-thiol chemistry for electronchemical sensing.^[172] Recently, Ke's group assembled gold nanorods (AuNRs) onto a reconfigurable DNA origami tripod and realized tunable angle and distance between DNA arms.^[173] In 2010 Fan's group first reported a 3D DNA nanostructure-based E-DNA biosensor by employing a highly rigid DNA tetrahedron. The tetrahedron-structured probe (TSP) consisting of three thiolated single-stranded and one probe-containing DNA fragments that can self-assemble onto planar gold surface via thiol-gold chemistry. This TSP was prepared with high yield (>85%) and applied in detection of biological environment.^[42] In 2011, Fan's group and Turberfield's group individual exploited the cellular behavior after treating with DNA tetrahedron.^[55, 174] The DNA tetrahedron showed excellent properties, such as biocompatibility, structural stability, efficiently internalization, which guarantee its potential applications as nanodevice. Recently, Pei's group developed a rapid and sensitive DNA-nanostructured microarray (DNM) aiming the detection of heavy-metal ions.^[175] Target specific DNA tetrahedral-structural probes were self-assembled and distributed evenly along the microchannel, allowing the sensitive and selective multiplex detection of metal ions.

All classes of DNA nanomaterials described above have in common that the size and shape are very well defined, probably better than in any other bottom-up fabricated material. This feature has dramatic consequences for applications in the field of biomedicine where multifunctional nanoparticles start to play an increasingly important role, especially in the areas of drug delivery and bio-imaging. In the next section, we will discuss the use of self-assembled DNA nanostructures and DNA-hybrid nanomaterials in pharmaceutical applications.

3. Biomedical applications

DNA nanotechnology overlook its genetic function of DNA, but instead focuses on physicochemical properties of the molecule and exploits the predictable self-assembly of DNA oligonucleotides to design and assemble novel nanostructures. The programmability of DNA oligonucleotides base paring allows researcher to build the structures purely made of DNA: simple 2D lattices to more complicated 3D nanostructures. Because DNA nanostructures inherit most of DNA molecule's unique characteristics, they can easily be applied in biomedical research areas and definitely offer new perspective on analytics, diagnostics and therapy to confront potential biomedicine challenges.

Similar to other type of materials, DNA assembles also abide by the principle of structure itself to determine corresponding applications, which imply that particular DNA structure may specialize in certain applications. As a nucleic acid antibody, DNA aptamers mainly functionalize as specific targeting ligand for delivery, but many of them also work exclusively well as either the antagonist or agonists.^[98] Although DNA origami serve as molecules cargo carrier/vehicle for triggered drug delivery, it has been used in applications such as bio-sensing, enzyme cascades and biomolecular analysis.^[176] DNA hydrogel often experience reversible solution↔hydrogel↔solid transitions under various stimuli, therefore they were utilized as carriers for controlled drug release and as shape-memory matrices.^[3] The enzyme resistant structures, superior mechanical properties, rich modification sites,

and convenient fabrication methods with high yield of DNA tetrahedron enable its applications on molecular diagnosis, bio-imaging and targeted drug delivery. Typically, MBs contain a target-binding region (loop) flanked by two complementary stem sequences and terminated with signal reporter, therefore they are primarily used for bio-sensing and bio-imaging, but therapy alike.^[177] Unlike other DNA-based structures depending upon conventional Watson-Crick base paring, DNA nanoflowers (NFs) assemble is driven by liquid crystallization and dense packing of building blocks. As a result, many different functional modules such as aptamers, bio-imaging agents and drug-loading sites could be introduced into NF particles, offering NFs compelling potential for many biomedical applications.^[178] DNA nanotubes hold great promise as drug delivery vehicles and as programmable scaffold for protein organization, as template of nanowires and photonic systems.^[179] DNA dendrimer can be functionalized as nanocarrier for molecular sensing, cell imaging and drug delivery.^[180] DNA nanopore/chanel buried in lipid bilayer aimed to simulate the function of cell membrane proteins.^[181] As such, not only selective but active intracellular transportation can be accomplished.

Here, we particularly focused on DNA-based artificial structures' biomedical applications from controlled drug delivery to high therapeutical profile and accurate diagnosis. Additionally, we discussed the material hybridization and DNA modification to achieve better performance and functionality. The contents of this part

was successively compiled depending upon complexity of the DNA based structure combination.

3.1. Drug-DNA adducts

Unlike DNA adduct as predictive biomarkers of carcinogenesis,^[182] anticancer drug-DNA adducts (DDAs) aim to successfully treat cancer. Platinum-based anticancer drugs cisplatin and oxaliplatin covalently bind to DNA to form DDAs, which is associated with their recognition by repairing HMGB1a proteins.^[183] DNA was site specifically conjugated with anthracycline anticancer drug. It has been known that the anthracyclines (particularly DOX) are capable of adduct formation while the formaldehyde serving as a bridge primarily at GC sequences.^[184] In a tumour xenograft mouse mode, DOX was covalently bond to deoxyguanosine of DNA through heat labile cleavable methylene linkage. In doing so, this DDA considerably inhibited the target tumour growth without reducing tissue deformation and apoptosis in the heart, which is the most dangerous side effect of DOX.^[106]

3.2. DNA aptamer

Nucleic acid aptamer, especially single-stranded DNA (ssDNA) or RNA oligonucleotides, are designed to specific bind to a target, which have great potential for disease diagnosis^[185] and therapy.^[186] Nucleid acid aptamers offer several advantages, including small physical size (6-30 kDa, 2 nm), flexible structure, versatile for chemical modification and high stability.^[104] The aptamers are selected from a large

random sequence pool or identified from nature.^[187] They can fold into distinct secondary or tertiary structure that capable of specific, high affinity binding to a target molecule.^[186]

3.2.1. Drug DNA Aptamer Conjugation

The fundamental benchmark of successful drug development are potency and specificity. Or in other word, we expect that the drug endows remarkable efficacy without triggering unpleasant side effects. Unfortunately, this is not always the case. Often, the drugs end up with obtaining high potency while compromising the specificity to acceptable degree, for example in the case of anticancer chemotherapy. Chemotherapy can cure cancer because it kills cells, yet it also impairs normal cells therefore lead to the side effects. These side effects deriving from off-target can be offset/balanced by smart drug delivery systems which aim to pinpoint diseased tissue and only release drug there. The classical drug transfer system skeleton is to integrate a molecular navigator with “weapon” drug molecules. The design of an ideal drug delivery system with targeted recognition, zero premature and spatial-temporal controlled release remain great challenges in biomedicine.^[188] The DNA aptamers are short single-stranded oligonucleotides that are biocompatible, stable, and importantly they are able to specifically recognize and effectively bind to their targets.^[189]

DNA aptamers can be generated using SELEX for specific targeting of various molecules at high affinity.^[104] Currently, DNA aptamers with a wide range of binding targets have been applied for different therapeutic purposes. Unlike the antibodies, the

generation of DNA aptamers is much cheaper and easier and those aptamers show no immunogenicity.^[104] Many efforts made by some research groups demonstrated that DNA aptamers are ideal candidates for biomedical applications, especially for targeted drug delivery to cancer tissues.^[111, 190a, 114, 190b, 109, 112, 190c, 190d] The conjugation of antitumor drugs to aptamer is a promising method that can increase the efficacy of chemotherapy and reduce the overall toxicity of the drugs. The conjugation was believed to position the drug molecules in the right place at the right time.^[191]

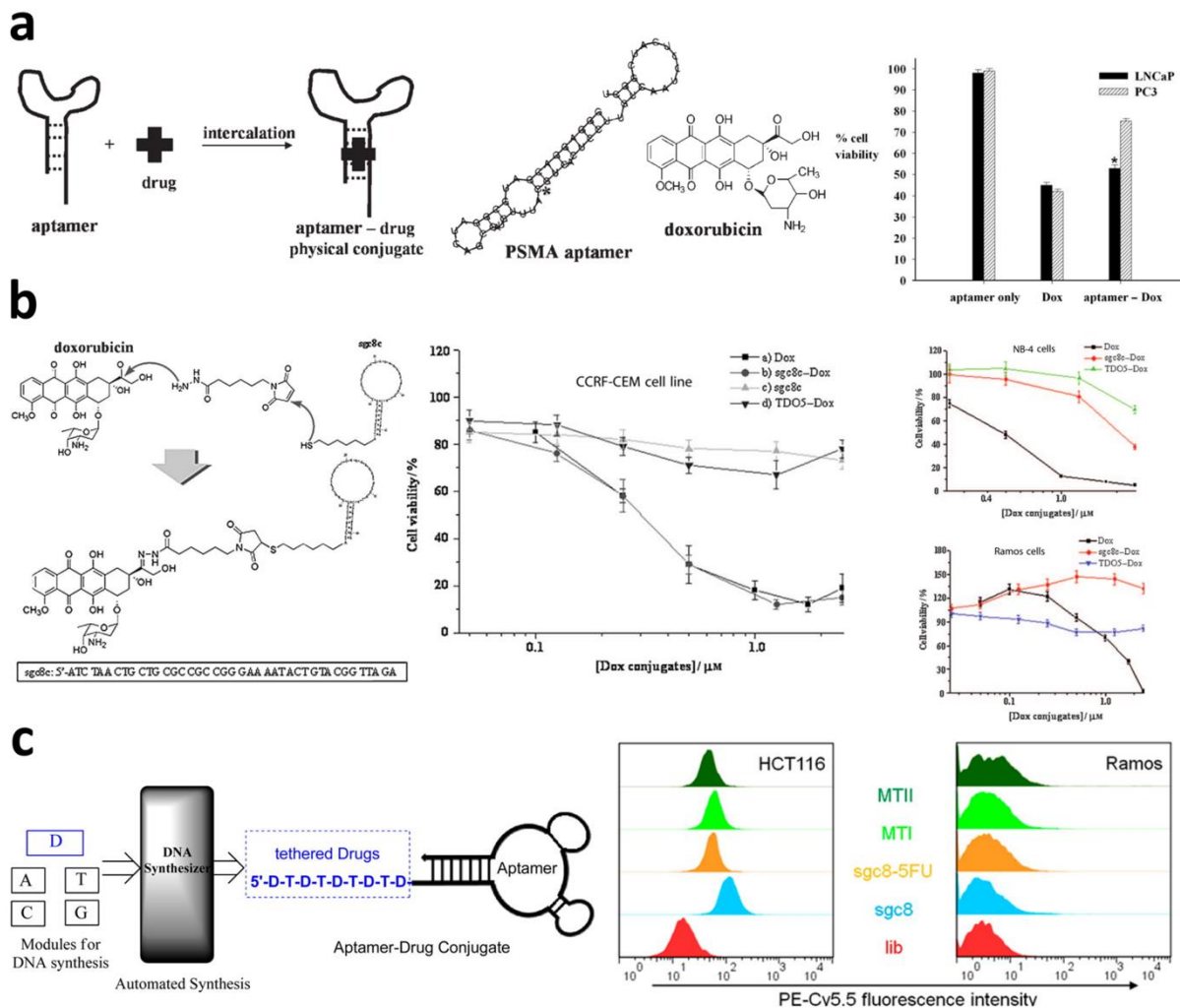


Figure 6. Aptamer-adduct conjugates as targeted drug delivery platform. a) schematic illustration of an aptamer-doxorubicin conjugates for targeted drug delivery, reprinted with permission from ref.[192], Copyright © 2006 Wiley-VCH Verlag GmbH & Co. KGaA, Weinheim; b) Conjugation of doxorubicin to aptamer sgc8c for targeted delivery, reprinted with permission from ref.[193], Copyright © 2009 Wiley-VCH Verlag GmbH&Co. KGaA, Weinheim; c) Conjugation of aptamer sgc8c-fluorouracil (5-FU) for cancer cell delivery, reprinted with permission from ref.[194], Copyright © 2014 American Chemical Society.

Recent advances and progress of aptamer targeting systems rely on aptamer-drug conjugates (ApDCs) or aptamer-nanomaterials. ApDCs are structurally similar to molecular trains, where drugs are loaded into the aptamers and selectively transmitted to target cells.^[195] ApDCs aim to reduce adverse drug effects and increase the efficacy of chemotherapy. Ideally, conjugated drug should depart from the ApDCs after cell internalization without deteriorating the drug's potency. The ApDC technologies have been evolved from the physical association to chemical coupling of drugs to aptamer. The dissociation constant ($K_d = 600$ nm) of the aptamer A10 PSMA-DOX suggested a spontaneously formed stable conjugate, but through noncovalent conjugation.^[192] (**Figure 6a**) Notwithstanding, the high DOX loading to DNA is sequence dependent, known to preferentially bind to double-stranded 5'-GC-3' or 5'-CG-3' segments, due to the π - π interaction.^[196] The stability of the noncovalent conjugate remains in concern as covalent coupling is often thought to be more stable in particular when the ApDCs are subjected to *in vivo* circumstance and controlled delivery and release are in demand.

Therefore, covalently linked DNA ApDCs are drawing more and more attentions. The sgc8c-DOX conjugate was reported to not only remain high binding affinity and high internalization efficiency of T-cell acute lymphoblastic leukemia (CCRF-CEM), but also possessed potency similar to unconjugated DOX.^[197] It has also been confirmed that internalization of sgc8c into the target cells was driven by the strong binding ($K_d = 0.8$ nm) of its target protein tyrosine kinase 7 (PTK7), which is a transmembrane receptor highly expressed on CCRF-CEM cells.^[198] When the anti-cancer drugs gemcitabine and fluorouracil (5-FU) were incorporate with pancreatic cancer aptamer P19,^[199] the conjugation significantly inhibited cell proliferation in PANC-1 cells by 51-53% and by 34-54% in the gemcitabine-resistant pancreatic cancer cell line AsPC-1.^[200] To readily dissociate the drug moieties from ApDC and remain the drug as intact as possible, a stimulus-responsive chemical linker is needed for aptamer-drug conjugate. Several types of linkers have been investigated. Acid-sensitive hydrazine linker was introduced to bridge DOX and aptamer sgc8c for targeted drug delivery to tumor cells,^[201] (Figure 6b) based on the fact that acidic extracellular pH was a major feature of tumor tissue^[202] and hydrazine could be easily cleaved at pH 4.5-5.5.^[203] The aptamer sgc8c has also been conjugated with anticancer drug 5-FU through photocleavable nitrobenzene derivatives linker and the efficient photocontrollable release of the 5-FU moiety was achieved in responsive of UV irradiation at 365 nm.^[194] (Figure 6c) In another work, the DOX functionalized aptamer complex TLS11a-GC-DOX could effectively lead to HepG2 cells apoptosis by gradually

damaging of relevant proteins and DNA in nuclei.^[204] The aforementioned examples demonstrated drug-aptamer conjugate with controlled chemotherapy release performed by using both internal and external stimulus.

The co-loading and delivery of drugs aim to achieve synergistic anticancer treatment without deteriorate the potency of individual drug candidate, yet combination of the co-loaded drug and aptamer will further strengthen the synergistic. DOX and paclitaxel (PTX) are commonly used chemotherapeutic drugs with distinct solubility characteristics and different anticancer mechanisms. Hydrophilic DOX binds to DNA, while PTX is a highly hydrophobic drug, which inhibits microtubule disassembly.^[205] Clinical studies shown that antitumor efficiency was synergized when incorporating both DOX and PTX compared to individual drug.^[206] To co-deliver DOX and PTX to target cancer cells with high specificity and efficiency, a therapeutic aptamer-lipid-poly(lactide-co-glycolic acid) (PLGA) hybrid drug delivery system was prepared in which the molecular recognition moiety, DNA aptamer sgc8 coated PLGA NPs, together with PTX constituted the hydrophobic core structure, while lecithin, distearoylphosphatidylethanolamine-PEG and lipid-PEG-aptamer loaded with DOX form the hydrophilic shell. As result, co-delivery of DOX and PTX was confirmed and significantly reduced the target CEM cell viability.^[205-206]

Beside the classical ApDCs, aptmer also showed considerable potential to conjugate with other therapeutics. Singlet oxygen (${}^1\text{O}_2$) is one of the most important cytotoxic agents generated during photodynamic therapy (PDT), and is gaining wide acceptance

as a noninvasive treatment of cancers.^[207] PDT involves two-step process whereby photosensitizer was delivered to specific tissues then was activated by exogenous light source.^[208] The photosensitizer transferred the light energy to tissue oxygen to generate highly active $^1\text{O}_2$ which reacted with cellular molecules and led to cell apoptosis.^[209] Given the limited lifetime and diffusion distance of $^1\text{O}_2$, a controllable singlet oxygen generation (SOG) is in demand. It was believed that DNA aptamer can act as an effective $^1\text{O}_2$ generation mediator. An aptamer-photosensitizer-single walled carbon nanotubes (SWNT) complex has been built such that photosensitizer Chlorin e6 was covalently linked to DNA aptamer which wrapped onto the SWNT surface through π -stacking interactions to quench SOG while led to significant restoration of SOG when the target molecule thrombin protein binds to the complex.^[210] One challenge of PDT was that it was often hurdled by inefficient delivery of photosensitizer to target cell and the limited depth cell penetration of photosensitizer. Recently, aptamer-derived G-quadruplex (GQ) has merged as a novel class of cargo molecule to address these challenges. GQ was stabilized by the porphyrin illuminophore contained cationic photosensitizer, such as 5,10,15,20-tetrakis-(1-methyl-4-pyridyl)-21H,23H-porphine (TMPPyP4) through intercalation process, which suggested the application of GQ DNA sequence as a carrier for porphyrin type of photosensitizers.^[211] Wang et al proposed a method to generate GQ-aptamer-drug platform which takes advantage of the target-recognition function of DNA aptamer and the TMPPyP4-loading ability of GQ. By doing so, not only the selectivity of G-quadruplex–aptamer module was achieved,

but the CCRF-CEM cells' toxicity of TMPyP4 delivered by Gquadruplex-TMPyP4 was doubled comparing to by TMPyP4 itself.^[211] When this conjugate was attached to upconversion nanoparticles, both CCRF-CEM cancer cells image and therapy were achieved.^[212]

Multimodality is promising strategy in cancer diagnosis, therapy, and targeted molecular imaging. To achieve multimodality with molecular specificity, an aptamer switch probe linked with a photosensitizer molecule chlorin e6 (Ce6) to the surface of AuNRs was used to target cancer cells for photodynamic therapy (PDT) and photothermal therapy (PTT).^[213] Consequently, this multimodal conjugate offered a significantly improved and synergistic therapeutic effect compared to PTT or PDT alone.^[213]

Due to N-Heterocyclic carbenes' (NHC) strong δ -donating properties, it can form NHC-Au^I complexes with induced cell apoptosis by targeting mitochondrial-related cellular pathways.^[214] However, the cell unspecificity still represented main hurdle of successful therapeutic application of NHC-Au^I complexes. Yet, NHC-Au^I-aptamer sgc8c conjugates were 13 to 27 folds more cytotoxic than the NHC-Au^I complex alone for targeted CCRF-CEM leukemia cells.^[140]

3.2.2 Functionalize Drug Carriers with Aptamer

Apart from the direct physical conjugation and indirect chemical conjugation of aptamer with chemotherapy drug, aptamer was also attached to big drug carriers to fulfill targeted drug delivery. Based on the observation that the ATP levels between

extracellular (<5 μ M) and intracellular (1-10 mM) differ significantly,^[153] more attention has been paid to design ATP-responsive drug carriers constructed by ATP aptamer. In the presence of high concentration of ATP, the ATP aptamer assembled DNA duplex with preloaded DOX underwent conformational change to the aptamer/ATP complex therefore triggered DOX delivery.^[153] Polymeric nanogel functionalized with an ATP-binding aptamer-incorporated DNA motif could release the intercalated DOX through the dissociation of DOX/DNA duplex to favor ATP aptamer cDNA to form stable tertiary structure in an ATP-rich environment.^[153]

The specific cellular uptake of drug carrier with high loading to diseased tissue is crucial. Normally these types of delivery are passive or in another words it concentration gradient dependent. To improve the specificity and make the transportation active, install DAN aptamer in the drug carrier is commonly used strategy. Wu et al fabricated a multifunctional and programmable DOX-loaded aptamer-based DNA nanoassembly (AptNAs) platform that featured of easy modular design, facile assembly, integrated multifunctionality, high programmability, good biostability and excellent biocompatibility. With these properties, AptNAs showed specific cytotoxic against leukemia cells, the inhibition of drug efflux pump as well as decreased drug resistance.^[141b] In another work, the A10 aptamer, which can specifically recognize the extracellular domain of the prostate-specific membrane antigen expressed on the surface of the prostate cancer cells, was conjugated to DOX-loaded unimolecular micelles to achieve targeted therapy of prostate cancer.^[153]

Furthermore, aptamer sgc8 tethered DNA nanotrains was constructed such that aptamer functioned as “locomotive” which drove “boxcar” made of two complementary DNA hairpin monomers, and the “passenger” DOX intercalated with short DNA strand.^[43] The advantage of this structure is that long “boxcar” is readily achieved from short building block due to the programmability of DNA sequence.

It was believed that negatively charged NPs own better biocompatibility, reduced protein surface adsorption and antigenicity, and longer circulation half-lives compared to positively charged NPs. Hence the negatively charged DNA aptamer AS1411, a DNA aptamer targeting nucleolin under phase II trial,^[215] was selected to invert surface charge of drug loaded porous silicon (PSi).^[216] As an example, the surface modified PSi nanoparticles were efficiently internalized by nucleolin-positive MDA-MB-231 breast cancer cells, with around 5.8 times higher efficiency than that of nucleolin-negative cells (NIH 3T3 fibroblasts) and the major mechanism of the internalized nanoparticles in MDA-MB-231 cells was due to the receptor-mediated surface charge inversion process.^[216]

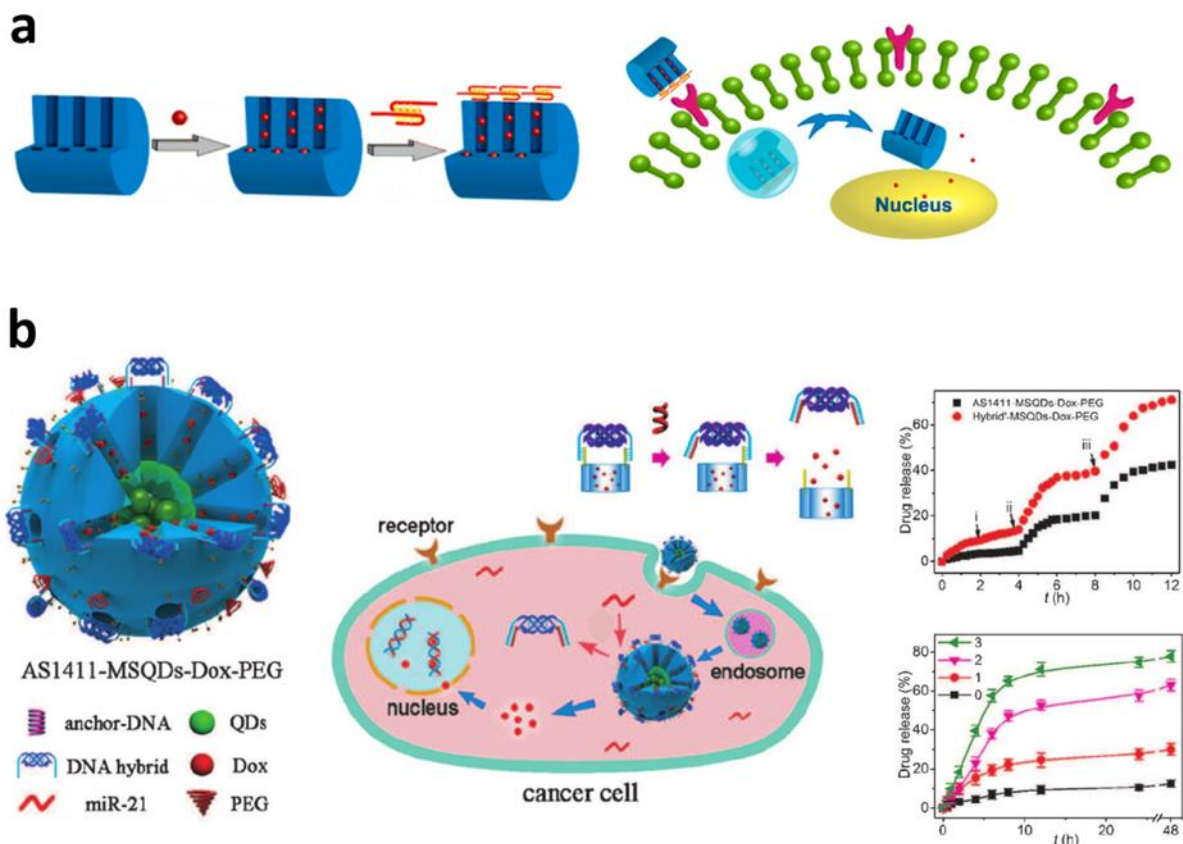


Figure 7. Aptamer functionalized nanocarriers. Schematic illustration of a) cancer cells-triggered release of drugs from the pores of Gd:SrHap capped with aptamer, reprinted with permission from ref.[114], Copyright © 2012 American Chemical Society; b) miRNA-responsive controlled release drug delivery nanocarriers, reprinted with permission from ref.[188], Copyright © 2014 Wiley-VCH Verlag GmbH & Co. KGaA, Weinheim.

Porous materials are widely used in drug delivery applications, owing to their high drug loading capability,^[217] however those systems suffer with premature drug release.^[218] Apart from providing a general route for targeted drug delivery and aptasensor, DNA aptamer can also be used as a capping agent to protect the premature

release of drugs loaded in porous materials.^[190d] Li *et al.* employed DNA aptamers as caps on the surface of gadolinium-doped mesoporous strontium hydroxyapatite (SrHap) nanoparticle for targeted DOX delivery.^[114] DOX-loaded and Gd-doped SrHap nanoparticles (Gd:SrHap-Dox) interact with negatively charged AS1411 aptamer via electrostatic forces, resulting in the closure of the mesopores (Gd:SrHap-Dox-aptamer).^[114] (**Figure 7a**) After internalization into specific tumor cell, the aptamer AS1411 showed high binding affinity to nucleolin, resulting in the pore opening and drug releasing. Zhu et al. reported a traceable and dual-targeted drug delivery system based on DNA-hybrid-capped mesoporous silica-coated quantum dots (MSQD).^[188] (Figure 7b) Since microRNA-21 (miR-21) was overexpressed in the cytoplasm of various cancer cells, the delivery of antisense miR-21 can be an efficient way to inhibit and further eradicate of tumor cells.^[219] DOX was loaded into MSQDs and then capped with the DNA hybrid consisting of anti-miR-21 and AS1411 aptamer. The nanocarriers exclusively entered the targeted tumor cells with the help of AS1411 aptamer.^[220] Subsequently, the overexpressed miR-21 triggered the on-command release of DOX by complementary base-pairing with the anti-miR-21 gating strands, which further enhance the selectivity and efficacy of chemotherapy.^[188]

3.2.3. Aptamer functions as therapeutics

Moreover, DNA aptamers, also termed 'chemical antibodies', are functionally comparable to classical antibodies, but host multiple advantageous features.^[104] Therefore the feasibility of using aptamers as an alternative to traditional antibodies in

vaccine potency assay has been exploited. For instance, Merck recently published that a slow off-rate modified DNA aptamer HPV-07 selectively bind to the Type 16 virus-like-particle with high sensitivity (EC_{50} of 0.1 to 0.4 $\mu\text{g.mL}^{-1}$ depending on assay format) and also met the standard requirements for precision (intermediate precision of 6.3%) and linearity in a format mimicking a previously developed antibody-based enzyme-linker immunosorbent assay (ELISA).^[221]

Apart from targeting functionality, DNA aptamer may also manipulate the functions of its targets after binding, especially for biologically important macromolecules, such as receptor proteins. After nearly a decade of preclinical development to optimize and characterize its biological effects, pegaptanib became the first aptamer therapeutic shown in clinical trials to be effective in treating choroidal neovascularization associated with age-related macular degeneration.^[222]

Given high binding capacity in combination with very high degree of specificity, DNA aptamers are promising ligands for not only analytical but preparative-scale affinity chromatography applications. Forier et al exemplified aptamer affinity chromatography for the purification of three human therapeutic proteins whose purity increase from 0.5% to 98% within one step.^[223] Comparing to the traditional Ni-NTA based protein purification technology, aptamer affinity chromatography resulted in a 3.6-fold higher L-selectin yield with increased purity.^[224]

3.2.4. DNA aptamer in biosensor

Due to the advantages of DNA aptamer in size, stability and reproducibility,^[252] aptamers labeled with a number of reporter molecules have shown great potential for bio-sensing applications.^[186] The goal of applying aptamers in bioanalysis is to report the presence of target molecules or cells with simple operation, thus they can act as sensitive probes for diagnostic applications.

Taking credit of the discovery of panels of cancer biomarkers, a DNA aptamer based logic platform can realize multicellular marker-based cancer analysis on modular AND, OR, and NOT boolean logic gates.^[225] Besides good affinity and specificity obtained, the aptamer J3 labeled with Cy5 fluorescent group was able to image metastatic cancer cells at high detection rate of 73.9%, but showed low detection rates to tissue with no metastasis or the cells in cancer adjacent tissue.^[226] Hong et al first reported a triply amplified cancer-related protein platelet-derived growth factor BB aptasensor with detection limit of 0.11 fM based on three ways amplification: 1) nanoparticles in device had large surface areas, providing greater aptamer payload, 2) each ionic nanocrystal could release thousands of Zn²⁺ into solution by cation exchange reaction and 3) the 8-17 DNAzyme could catalyze the cleavage of several substrates.^[227] As an intercellular signal transmitter in biofluids, the potential of cancerous exosomes as tumor biomarkers has been recognized, but desired detection barely match. However, it has been observed that aptamer-based DNA nanoassemblies was able to selectively recognize exosomes.^[228] In order to direct capture and detect liver cancer exosomes,

Wang et al integrated the aptamer technology, DNA-based nanostructure, and portable electrochemical devices to fabricate a nanotetrahedron-assisted aptasensor, which increased 100-folds sensitivity compared to the single-stranded aptamer-functionalized aptasensor.^[229] (**Figure 8a**) The ultrasensitive mucin 1 detection with detection limit of 0.62 fg mL^{-1} was achieved by using the electrochemiluminescence biosensor based on a 3D DNA nanomachine signal probe powered by protein-aptamer binding complex.^[230]

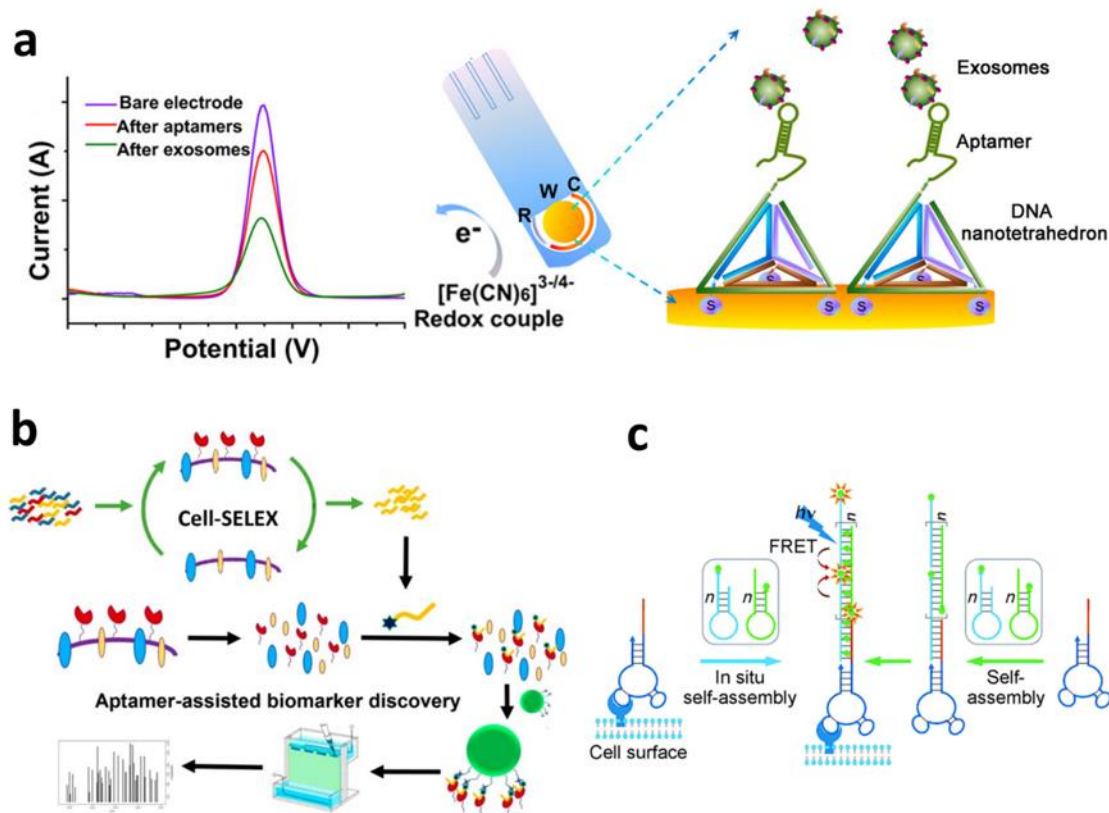


Figure 8. Aptamer-based biosensors. a) Schematic illustration of the nanotetrahedron-assisted electrochemical aptasensor Reprinted with permission from ref.[229], Copyright © 2017 American Chemical Society; b) Cell-SELEX procedure and aptamer-assisted biomarker discovery, reprinted with permission from ref.[231], Copyright © 2017 American Chemical Society. c) DNA nanotrain, these

DNA nanodevices underwent fluorescence resonance energy transfer (FRET) on living cell surface, reprinted with permission from ref.[232], Copyright © 2013 Wiley-VCH Verlag GmbH & Co. KGaA, Weinheim.

Tan *et al.* report that aptamer can also serve as novel molecular probe in biomarker studies, especially in identification and validation of disease-related biomarkers.^[231] (Figure 8b) Two DNA aptamers sgc8 and TDO5 were used to construct model aptamer-tethered DNA nanodevices (aptNDs), in which fluorophores were either chemically or physically incorporated with aptNDs for targeting the receptor TDO5 of living cell by *in situ* self-assembly. The devices fulfill the long-term goal of pinpoint bioanalysis or manipulation of biological activities on targeting living cell membranes.^[232] (Figure 8c)

Aptamers are used for detecting other human health related molecules. For example, phthalic acid esters (PAEs) and its ubiquitousness, exist in environment, are potential toxic for human. Thus PAE skeleton-binding DNA aptamers were identified to detect bis(2-ethylhexyl) phthalate with exceptional sensitivity (LOD: 10 pM) and selectivity (> 10⁵-fold) against potential interferences commonly existing in the soft drinks and environmental waters, such as glucose, ethanol, and antibiotics.^[233] The label-free, bio-sensing of salmonella enterica serovars from food source was carried out at single-cell level attributing to aptamers with specific binding affinity to the membrane proteins on foodborne pathogens surface.^[234] The fungicide carbendazim was detected

with a limit of detection of 8.2 pg/mL by relating the conformational change of aptamer with its accessibility of ferrocyanide/ferricyanide on the surface.^[235]

Aptamer-based fluorescent biosensor platform can also detect cells,^[236] bacteria,^[237] protein,^[238] glycoprotein,^{[239] [238]} antibiotics,^[240] and neurotransmitter.^[241]

3.2.5. DNA aptamer as template

DNA aptamers can act as template in nanofabrication to preserve the necessary structure for therapeutic action and stabilize the nanoparticles, in the meanwhile those aptamers can also be extended to have therapeutic effects. Strano and colleagues^[2a] developed a facile method named “oligonucleotide-passivated” to synthesize semiconductive nanocrystal-quantum dots (QDs). With the DNA termination, the as-prepared QDs are biocompatible and water soluble. The thrombin targeting DNA aptamer acted as a nucleation and capping reagent for QDs’ synthesis, while the aptamer retained its structure during the capping process. Once the aptamer binds to the protein target, the QD’s fluorescence quenches, resulting in the optical reporting of specific protein recognition.^[242] Furthermore, a class of aptamers for targeting cancer cells can be used as templates for synthesizing and stabilization of nanocrystals.^[243] Not only the therapeutic effects have been greatly improved, the details of action pathways could also be optically observed by utilizing QDs. This multifunctional DNA aptamer-nanocrystal shows great potential in diagnostic and therapeutically applications.

3.2.6. DNA aptamer as Growth factor mimetics

In general, the main function of DNA aptamer is for cell recognition and targeting, but some of them possess therapeutic features as well. Ueki *et al* reported that a 50-mer DNA aptamer inhibited cancer cell migration through binding to c-Met protein.^[244] Another potent aptamer dimer, composed solely of 100-mer single stranded DNA, was reported to exhibit nanomolar potency to Oligonucleotide-based hepatocyte growth factor,^[245] which enriched the functionality of DNA aptamer.

Santo *et al.* utilized DNA aptamers as a novel chemical entity for the designing of hepatocyte growth factor (HGF) mimetics for regenerative therapy.^[244] They applied the SELEX methodology to generate a HGF receptor (known as Met)-binding DNA aptamer (CLN003_SL1).^[244] Subsequently, DNA aptamer-based hepatocyte growth factor mimetics (Di-SL1) were produced through hybridization of two SL1 monomers with a complimentary strand at 5' termini. Di-SL1 acts as a Met agonist and shows Met activation potential.

3.3. DNA hydrogel

Hydrogels are crosslinked hydrophilic polymers that can absorb a large amount of water,^[29] leading to swelling of the hydrogel matrices, while undergo a volume change in aqueous phase.^[38] Over the last several decades, DNA has received great attentions as an excellent building material.^[246] With the development of DNA synthesis and modification, a hydrogel made of DNA also coincidentally obtained increasing interests.^[247] These DNA hydrogels (Dgels) are susceptible to physicochemical

changes responding to stimuli such as pH, molecular electromagnetics, and temperature, and the different triggers have been used to induce reversible hydrogel-to-solution or hydrogel-to-solid transitions. Dgel shows excellent biocompatibility, biodegradation, molecular recognition property, nanometer scale architecture and programmability.^[162] Dgels can easily encapsulate biological components during the enzymatic gelation process under physiological conditions. By optimizing initial concentrations and selecting different DNA monomers input, the Dgel output can be easily turned,^[248] allowing them to be tailored for specific applications such as controlled drug delivery, 3D cell culture, scaffolds for tissue engineering, and other biomedical applications.

3.3.1. Fabrication of DNA hydrogel

Usually DNA hydrogel is created by bottom-up strategies via ligase-mediated crosslinking reactions, enabling the gelling processes to occur under physiological condition. Depending on the input components, versatile of the outcome can be accomplished. Tan's group developed a general self-assembly method to create DNA nanohydrogels with controllable size.^[249] (**Figure 9a**) The DNA hydrogel is formulated through a self-assembly process using three kinds of building units: Y-shaped monomer A (YMA), Y-shaped monomer B (YMB), and a DNA linker (LK). Both YMA and YMB assembled from three single-stranded DNAs (ssDNAs). The YMA serves as a building unit with three “sticky end” segments, while YMB has one “sticky end” and one strand consists of an aptamer. The LK is a linear duplex with two “sticky end” complementary segments for these Y-shaped monomers. To design

stimuli-responsive DNA hydrogel, different functional groups, including aptamer, antisense oligonucleotides, disulfide linkages and therapeutic genes can be incorporated into the building units. By varying the ratio of YMA to YMB, the size of DNA hydrogel nanoparticle can be controlled.^[249] Luo's group confirmed that the higher the initial concentration of the branched DNA monomers (BDM), the higher the degree of swelling in hydrogel and the type of BDM also influenced the degree of swelling, even the stability of hydrogel: X-DNA gels were most resistant to degradation comparing to T-and Y-DNA gels.^[38] Although hydrogel was characterized as soft and wet matter but lack of fluidity, consequently the administration required breaking them down bulk hydrogel into small pieces for injection. More importantly, the untreated ligase residue during hydrogel formulation may lead to undesired effect, including allergy related shock. Therefore, the development of ligation-free and injectable DNA hydrogels would dramatically improve the feasibility of it as delivery systems. Nishikawa et al has reported such DNA hydrogel DNA hydrogel can efficiently deliver tumor antigens with higher potency and less toxicity than clinically available vaccine adjuvants.^[246] The controlled size of nano-hydrogels is also desired since the size of the nano-hydrogels is determinant to their fate in the bloodstream. By adjusting the single-stranded DNAs monomer ratio, 144 nm sized nanohydrogels, self-assembled by monomer and DNA linker with sticky ends, were achieved to extend their blood circulation time.^[249]

3.3.2. Dgels for Drug Delivery Application

Dgel are promising drug delivery system for a vast number of drug candidates due to the mild condition of Dgel gelling processes and the convenient encapsulation procedures. Luo's group encapsulated the anticancer drug camptothecin (CPT) and observed that drug loaded Dgel was more resistant to enzymatic degradation than empty gels. The drug release followed zero-order release profile for long term, presumably attribute to CPT's high affinity to the grooves of the DNA molecules and the internal structures of the Dgel.^[38]

To enable the controlled or accelerated release of encapsulated cargo in hydrogel on demand, the contents for responding external stimuli and triggers were usually co-loaded beforehand, which could initiate the burst release of drug loaded in Dgel utilizing the unique characteristics of Dgels, for example melting by thermal denaturation. Gold nanostructures have excellent photothermal effects upon NIR irradiation and have been widely used for efficient thermotherapeutics, however most gold nanostructures are nonporous and they have limited elasticity surfaces thereby lost conjugation capability and hardly attained synergistic thermo-chemocombination cancer therapy. The combination of gold nanostructures and Dgel enables the loading of drug, and photothermal responsive drug release. The DOX and positively charged gold nanostructures were co-loaded into the Dgel by electrostatic attractions and when the laser was applied, energy transformed by either gold nanoparticles^[250] (Figure 9b) or gold nanorods^[251] melt the Dgel, and triggered the DOX release.

Often, the high-performance hydrogel was developed through the combination of different materials since it is quite rare that an individual material can realize cutting-edge multi-functionality. After confirmation of aptamer-based nanohydrogels (Y-gel-Apt) degradability in the intracellular reductive environment and targeting recognition, its ability for targeted gene regulation therapy was also investigated by conjugating the therapeutic antisense oligonucleotide against c-raf-1 mRNA and DNAzyme targeting matrix metalloproteinase-9 individually. It was showed that the A549 cancer cell proliferation was remarkably inhibited in a dose dependent manner after treatment with Y-gel-Apt, suggesting that Y-gel-Apt could be selectively internalized into cells and that the antisense transported by Y-gel-Apt played an important role in inhibiting cell proliferation.^[249] (Figure 9a)

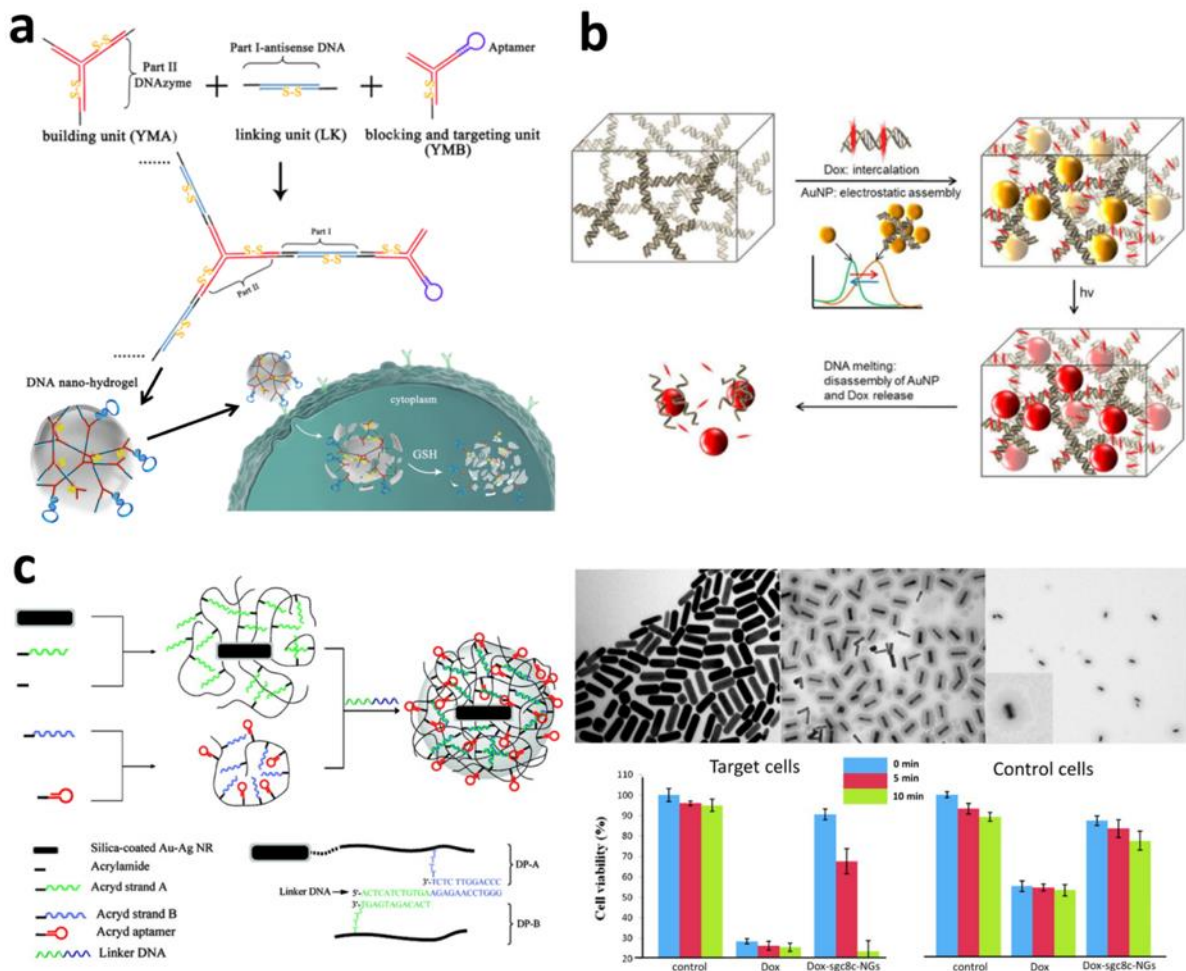


Figure 9. Dgel for drug delivery. Schematic illustration of a) stimuli-responsive Dgel formation, YMA and YMB and linker are designed to crosslink by hybridization of their “sticky end” segment, leading to Dgel formation, reproduced with permission from ref.[249], Copyright © 2015 American Chemical Society; b) DOX-AuNP-Dgel, external light triggering induces the DOX by DNA melting, reproduced with permission from ref.[250], Copyright © 2014 The Royal Society of Chemistry and c) light-responsive drug delivery system based on Au-Ag coated DNA cross linked nanogel, ref.[252], Copyright © 2011 American Chemical Society.

More comprehensive hydrogel can be prepared by conjugating multiple elements. The silica-coated gold-silver-based nanorods core (Au-Ag NRs), DNA cross-linked polymeric shells, polyacrylamide linker and guider aptamer sgc8c form a nanogel in which DOX intercalated with DNA nanoshell. Under the guiding of sgc8c, the core-shell nanogel entered the target, CCRF-CEM cells and exposed to a near-infrared light (NIR) laser to burst release DOX molecules, triggered by the solid-to-gel transition of the hydrogels due to Au-Ag NRs' capability of photon energy conversion to heat mechanism.^[252](Figure 9c)

Immunoinhibitory oligodeoxynucleotides (INH-ODNs) are promising inhibitors of Toll-like receptor 9 ((TLR9). To efficiently deliver INH-ODNs to TLR9-positive cells, Dgel consisting of two partially complementary ODNs as the main component was generated and significant cellular uptake was observed. As result, TLR9-mediated hyperinduction of proinflammatory cytokines release was efficiently inhibited by the Dgel.^[253]

Nishikawa et al. reported biodegradable Dgel with immunostimulatory unmethylated cytosine-phosphate-guanine (CpG) motifs was more effective than CpG-free counterpart in terms of the production of tumor necrosis factor- α and realized sustained delivery immunostimulatory CpG in tumor-bearing mice.^[254] The work was extended to produce an injectable Dgel containing sequences with immunostimulatory CpG dinucleotides motifs which was used to stimulate innate immunity through Toll-like receptor 9, a receptor for CpG DNA. Gel formation significantly increased the

immunostimulatory activity of CpG DNA, hindered the clearance after intradermal injection into mice, and increased the immune responses of ovalbumin (OVA) incorporated in hydrogel as a model antigen.^[246]

3.3.2. Dgels for other Application

Besides small molecules, macromolecules or nanostructures, for instance insulin,^[48] green fluorescent protein and drug loaded cargos^[255] can also be encapsulated and controlled release from Dgel. Supercharged green fluorescent protein (ScGFP) was chosen as model protein to be encapsulated into the Dgel during the gelling process.

Once treated with DNase I on the whole system, the digestion of the Dgel was proceeded within 10 h with a concomitant release of ScGFP.^[255]

Strikingly, protein-producing gel (P-gel) provided the foundation of cell free expression system in which a linear expression plasmid was incorporated into a DNA hydrogel to produce proteins. The P-gel system could produce up to 5 mg.mL⁻¹ of protein in a single expression, which was about 300 times higher than current commercially available solution phase systems.^[256] (**Figure 10a**) Depending on the quantity expectation of protein, the entire process can spend 1-3 days.^[257] (Figure 10b)

Hydrogel are promising for cell culture as the cell culture media, nutrients, and waste products generated during cell metabolic processes can freely transport through the gel matrix.^[258] Luo and his team first developed a bulk-scale hydrogel entirely from DNA.

The Dgel formation and cell loading was accomplished solely by an enzyme, T4 ligase. The release of cells can be easily triggered by using nucleases to degrade this Dgel to

non-toxic nucleotides as by-products. The biomaterials composed Dgels co-incorporated with endothelial cells (OEC), neuropeptides and growth factors can be injected into the diabetic wound margins for better healing outcome without obvious adverse effect comparing to the delivery of OEC alone.^[259]

The strong affinity of DNA to transition metals makes it template for synthesizing inorganic particles, for example DNA cross-linked hydrogel is used for synthesizing AuNP. Zinchenko and coworkers reported the formation of ultrasmall, non-aggregated AuNPs of 2-3 nm size inside DNA hydrogel.^[247] (Figure 10c) It was also observed that the catalytic activity of AuNPs for same reaction in DNA hydrogel heavily depended on the swelling degree of Dgel which could be easily controlled by changing of ionic strength in the solution. In 0.1 mM of NaCl, the Dgel swollened and completely converted *p*-nitrophenol into aminophenol within 10 min while in 100 mM of NaCl the Dgel only converted less than half of *p*-nitrophenol after 40 min,^[260] indicating that diffusion of reactants toward catalytic centers inside hydrogel is determining step for the soft-matter-based hybrid material catalysis.(Figure 10d)

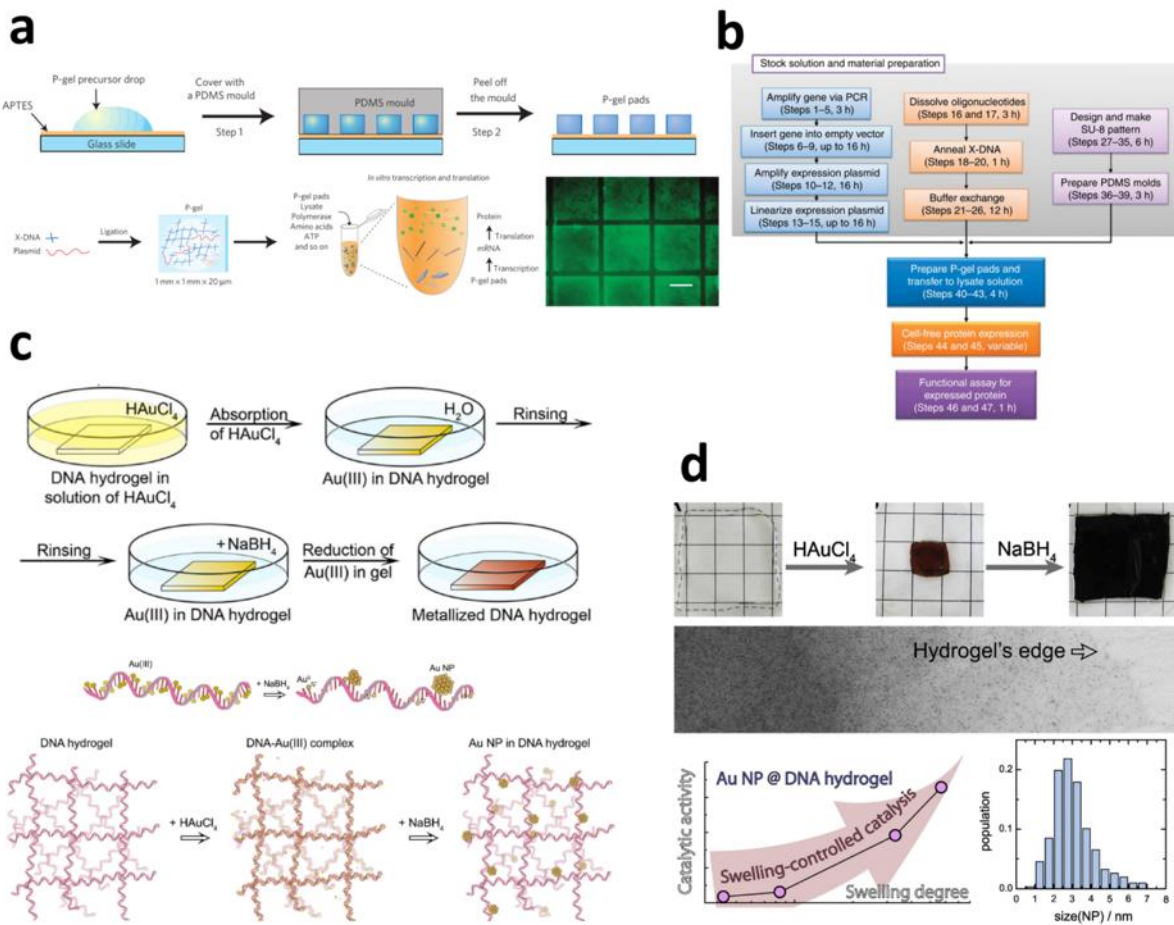


Figure 10. DNA hydrogels as scaffold. Schematic illustration of a) the formation of protein-producing gel (P-gel) micropads and the gelation process through enzymatic crosslinking and cell-free expression with P-gel pads, reproduced with permission from ref.[256], Copyright © 2009 Nature Publishing Group; b) Flowchart for protein-producing gel formation and protein production, reproduced with permission from ref.[257], Copyright © 2009 Nature Publishing Group; c) preparation of hybrid hydrogel, reproduced with permission from ref.[247], Copyright © 2014 American Chemical Society and d) the catalytic activity evaluation, reproduced with permission from ref.[260], Copyright © 2015 Elsevier Inc.

Taking the excellent molecular recognition properties and editability of Dgel, aptamer-functionalized Dgel has been applied to selectively detect thrombin using preloaded AuNPs in Dgel as signal indicators.^[261] A recently published Account highlighted bioresponsive Dgel will play an irreplaceable role in the development of future evolvable materials such as soft robots and point out cell-like material which might be the ultimate goal of Dgel^[262] and now it is on the way.^[263]

3.4. DNA nanostructure

DNA nanostructures are nanoscale artificial nucleic acid structures synthesized by folding of DNA. The 2-dimensional and 3-dimensional nanostructures can be built through complementary binding of DNA strands in programmable manner and the simple DNA structure as “DNA-brick” can grow bigger through designing complementary sticky ends.^[264] Currently, isothermal enzymatic amplification process is a powerful tool for large-scale preparation of DNA nanostructures, which increased the production of DNA nanostructures for more than 200-fold comparing to normal rolling circle replication with PCR.^[265] Due to the unique programmable structural design, multi-functionality and biocompatibility, DNA nanostructures have been widely applied in bio-sensing, bio-imaging, drug delivery, molecular computation and as macromolecular scaffold.^[266] A variety of strategies have been developed to functionalize these nanostructures, paving the way to more comprehensive and yet unmet clinical applications.

3.4.1. DNA origami

DNA origami, the nanoscale structure in which the long strand of linear DNA is folded into a flat “sheet” by introducing short oligonucleotides that partially base pairing with the long DNA strand and form crossovers to hold the structure together, which was first reported as cover story of *Nature* more than a decade ago.^[9a] Since then, DNA origami has been widely used in drug delivery systems and in biosensors.

3.4.1.1. DNA origami for drug delivery

With enhanced size and controllable shape, DNA origami can be used for drug delivery. Besides, it has many features including the *in vitro* stability,^[267] biodegradability,^[268] no detectable cytotoxicity or immunogenicity,^[269] which are important features for drug delivery carriers.

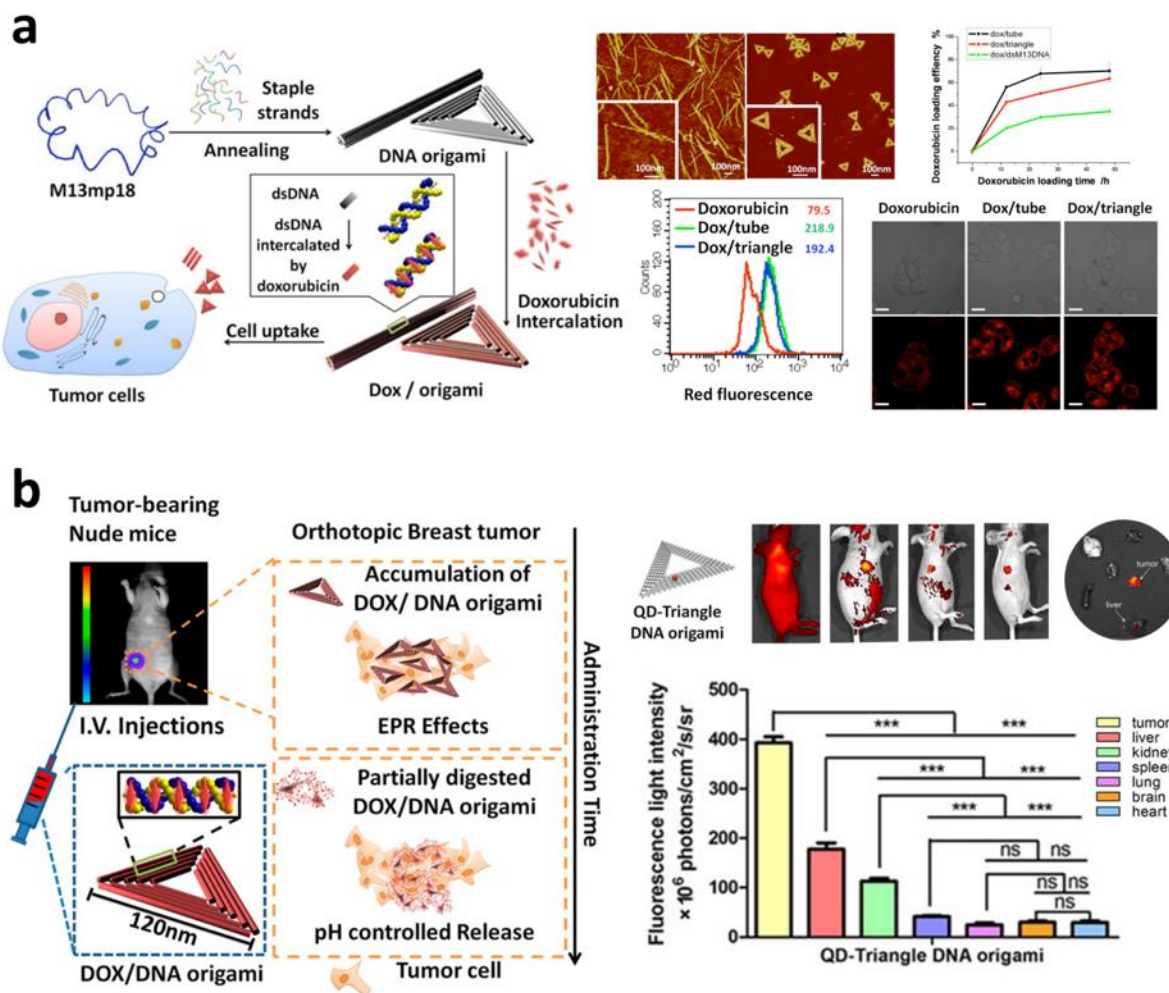


Figure 11. DNA origami as drug delivery system. Schematic illustration of a) DNA origami and doxorubicin (DOX) origami drug delivery system assembly and its interaction and anti-proliferation effect towards MCF7 cells, reprinted with permission from ref.[270], Copyright © 2012 American Chemical Society; b) the *in vivo* biodistribution and antitumor efficacy of DNA origami-DOX complex investigated in subcutaneous breast tumor model, reprinted with permission from ref.[271], Copyright © 2014 American Chemical Society.

Although the demonstrations of DOX aptamer-conjugated DNA delivery platform could kill cancer cells efficiently, DNA origami possessed more potential to deliver therapeutic levels of DOX than wireframe DNA structures because the tightly packed double-helices provide more anchor sites for base pair quenching and therefore increase the DOX loading.^[270] DOX had loading degree of approximately 50-60% in the triangular and tubular DNA origami assembled by viral ssDNA M13mp18 and the drug-loaded origami exhibited not only remarkable cytotoxicity to normal breast cancer cells, but importantly also conquered DOX-resistant cancer cells.^[270] The assumption is that DOX-loaded DNA origami inhibits lysosomal acidification, resulting in cellular redistribution of the drug in carcinoma tissue.^[270] (**Figure 11a**) Using the same structure, the first case study on using DNA origami as a safe drug delivery vehicle for *in vivo* cancer therapy was exemplified by Zhang et al,^[271] which also uncovered the shape effects of DNA origami to its distribution in cancer tissues. The triangle-shaped DNA origami exhibited much better tumor accumulation than square and tube shaped DNA origami, as indicated by the fluorescence signals. The triangle origami accumulated at the tumor site and reached the peak at 6 h and maintained high levels for 24 h, while tube and square origami exhibited relatively high fluorescence signal contrast at the tumor site since 12 h post injection.^[271] (**Figure 11b**)

Precise but simple logic delivery of DOX can be obtained with DNA origami delivery platform. It was demonstrated that by designing DNA origami nanostructures to have a certain twist density away to normal double helices increased binding affinity for

intercalators.^[272] This observation was applied to investigate whether such conformational change in the DNA origami would enable a change in the DOX loading and release properties. It turned out by designing the structures to exhibit different degrees of twist, not only the encapsulation efficiency and the release rate of the DOX was tuned but also increased the cytotoxicity and lower the intracellular elimination rate when compared to free DOX.^[273]

Although as a well-known mode drug for in cancer therapies, DOX has been shown multi-drug resistance. Variety of mechanisms may account for cancer cell resistant to anti-cancer treatment, the most common mechanism was the ejection of drug by molecular efflux pumps,^[274] especially ABC transporter.^[275] Other mechanisms include hypoxic induced resistance,^[276] the loose of drug transporter in cell surface. Due to structural similarity to DOX, daunorubicin share similar pharmacokinetics profile with DOX and bind with DNA by intercalation mechanism alike.^[277] Cancer cell also experienced daunorubicin resistance, most of them resulting from overexpression of efflux pump. Some research showed that this challenge can be addressed by DNA nanotechnology. The fabrication of a rod-like DNA origami loaded with daunorubicin led to increased cell uptake and retention in cells relative to free daunorubicin at equal concentrations in drug resistance leukemia cells.^[308]

To circumvent the drug-resistance of the generic chemotherapeutics, updated anti-cancer drugs are in urgent demanded. The metal complexes are promising candidates of next-generation cancer medicine, but the successful treatment with metal

complexes is precluded by the insufficient accumulation in tumor regions and the strong adverse effects due to their non-specificity *in vivo* distribution.^[278] While DNA origami conjugated with biotin could effectively load the ruthenium polypyridyl complexes (RuPOP) and achieve specific cellular uptake, increased drug retention and cytotoxicity against HepG2 cells.^[279]

Except the small chemical entities, macromolecules such as bioluminescent enzymes can also be loaded and delivered into HEK293 cells *in vitro* when they are attached to tubular DNA origami nanostructures. After the transfection process, the enzymes stay intact and remain their activity.^[280]

Single-layer DNA origami is an efficient method for programmable self-assembly of two-dimensional nanostructures, though they have been used in drug delivery applications, but the mechanical rigidity may compromise its efficiency. Multiple layers of such DNA sheets can assemble into a stack, enabling the construction of three dimensional shapes with greater mechanical rigidity than two-dimensional shapes. However, the folding of such 3D structure is time consuming. To accelerate the folding process, “targeted insertions” of intercalating agent, such as ethidium bromide on multi-layer DNA origami was applied.^[272] Implying anthracycline is another way of stabilizing the formation of the three dimensional DNA origami alike since ethidium and anthracycline are analogs sharing similar fused aromatic core.^[139] Therefore, we hypothesize the synchronous DOX loading and DNA origami assembly may favor the formation of drug-origami three dimensional structures. Intercalation with small

ligands also improved bioavailability of DNA origami. The nature of the origami scaffold is largely limited to its negatively charged deoxyribonucleic acids because the strongly negative charges backbones stop them from diffusing across cell membranes. Yet, by insertion of acridine-containing intercalators with side chains of either esterified fatty acids or oligo(ethylene glycol) into DNA origami, the surface charge was altered to positive without influencing the DNA origami's structural intactness, thus greatly stimulated the cellular uptake,^[281] and is worthy of further applications such as drug loading.

Enlightened by the mechanisms of viruses' infection, artificial virus shell structure has been utilized to decorate DNA nanostructure to advance nano-medication.^[40] (**Figure 12a)** By coating virus capsid proteins on DNA origami surface through electrostatic interactions, and the subsequent packing of DNA origami inside the viral capsid, the cellular delivery efficiency of DNA origami was enhanced by up to 13-folds towards human HEK293 cells.^[40] Virus-inspired enveloped DNA nano-octahedron to achieve *in vivo* stability has also been confirmed in mice mode. Importantly, the immune activation of the DNA nanostructure decreased for more than 100 folds below controls, and bioavailability improved 17 times.^[57] (Figure 12b) Although no following study was done to illustrate the drug delivery capacity yet, it is highly likely that virus capsid modified/coating DNA nanostructures is a promising platform for translation-ready biomedical applications. When DNA origami tubes covered with up to 62 cytosine-phosphate-guanine (CpG) sequences, it induced higher immunostimulation

than equal amounts of CpG oligonucleotides complexed with a standard carrier system Lipofectamine,^[269] demonstrating the Immunostimulationa DNA origami over lipid transfection reagent.

The structural stability of 3D DNA box origami is a key factor for drug delivery/release as needed, especially if aim for clinical applications. The degradation kinetics of 3D DNA box origami in serum was investigated by Dong's group using high-speed atomic force microscope in real time. It turned out that both rapid collapse and slow degradation contributed to the digestion process in serum, but origami box degradation occurred mainly in the collapse phase.^[282]

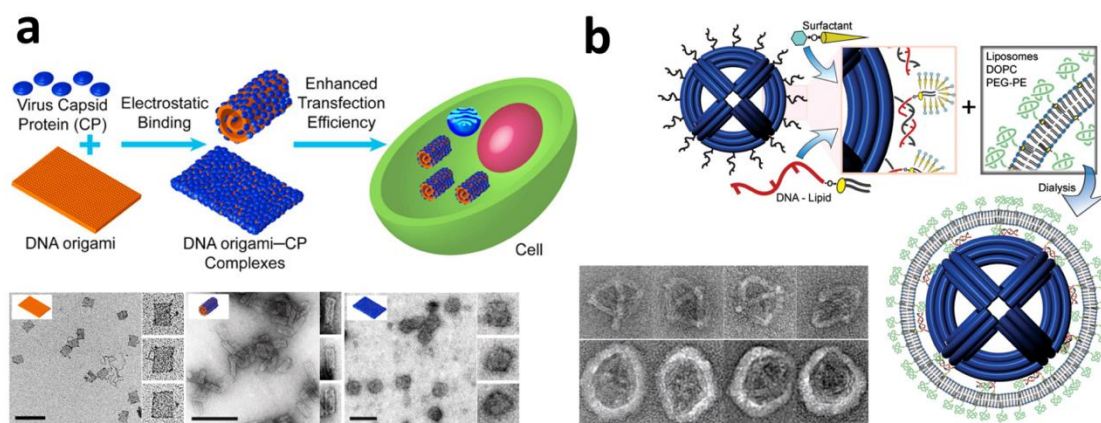


Figure 12. Hybrid DNA nanostructure for drug delivery. Schematic illustration of a) self-assembly of DNA origami with virus capsid protein (CP), TEM images showing the morphology of the DNA origami-CP (fraction of CP: 0, 0.08 and 0.64), scale bar = 200 nm, reprinted with permission from ref.[40], Copyright © 2014 American Chemical Society; b) assembly of DNA nano-octahedron (N-DNO) with similar geometry of a viral protein capsid shell, TEM images of purified N-DNO and encapsulated

DNO, scale bar = 50 nm, reprinted with permission from ref.[57], Copyright © 2014 American Chemical Society.

3.4.1.2. DNA origami for bio-sensing

The characteristics of DNA origami nanostructures, and the associated benefits, offer potential advantages for use in sensing applications. Driven by specific molecular interactions (nucleic acid hybridization, protein-ligand binding, *etc.*), binding based DNA origami constructs for bio-sensing undergo conformational changes to alter the shape or profile of the sensor.^[283] These exquisite changes can be investigated by single-molecule force spectroscopy, such as optical tweezers, magnetic tweezers and atomic force microscopy (AFM).^[284] Attributed to the detailed understood Watson-Crick base pairing with high specificity, one should not feel surprised that DNA origami nanostructures have been widely used for detecting specific nucleic acid sequences. After the incorporation of the complementary nucleic acid sequences of three target different genes (Rag1, Myc, and Actb) into DNA origami chip and optimization of their relative positions, the AFM detection sensitivity of target mRNAs' hybridization with probes segment was down to the 200 pM levels, depending upon nucleic acid tile concentration.^[285] (**Figure 13a**) Similar work was reported by Fan and He's group that an index-free DNA origami chip using the asymmetric origami map enabled detection of the target sequence not only use base complementary but streptavidin-biotin binding interaction by functionalization of oligonucleotides to

provide a clearer AFM signal.^[286] (Figure 13b) The subsequent work of the same group also developed DNA origami biosensors to detect single-nucleotide polymorphisms, enabling the single-base mismatch detection between two DNA.^[287] (Figure 13c) The work continued by Seeman's group offered the direct readout that identified the probe molecule nucleotide which is complementary to the specific nucleotide mutation in the target sequence.^[288] (Figure 13d)

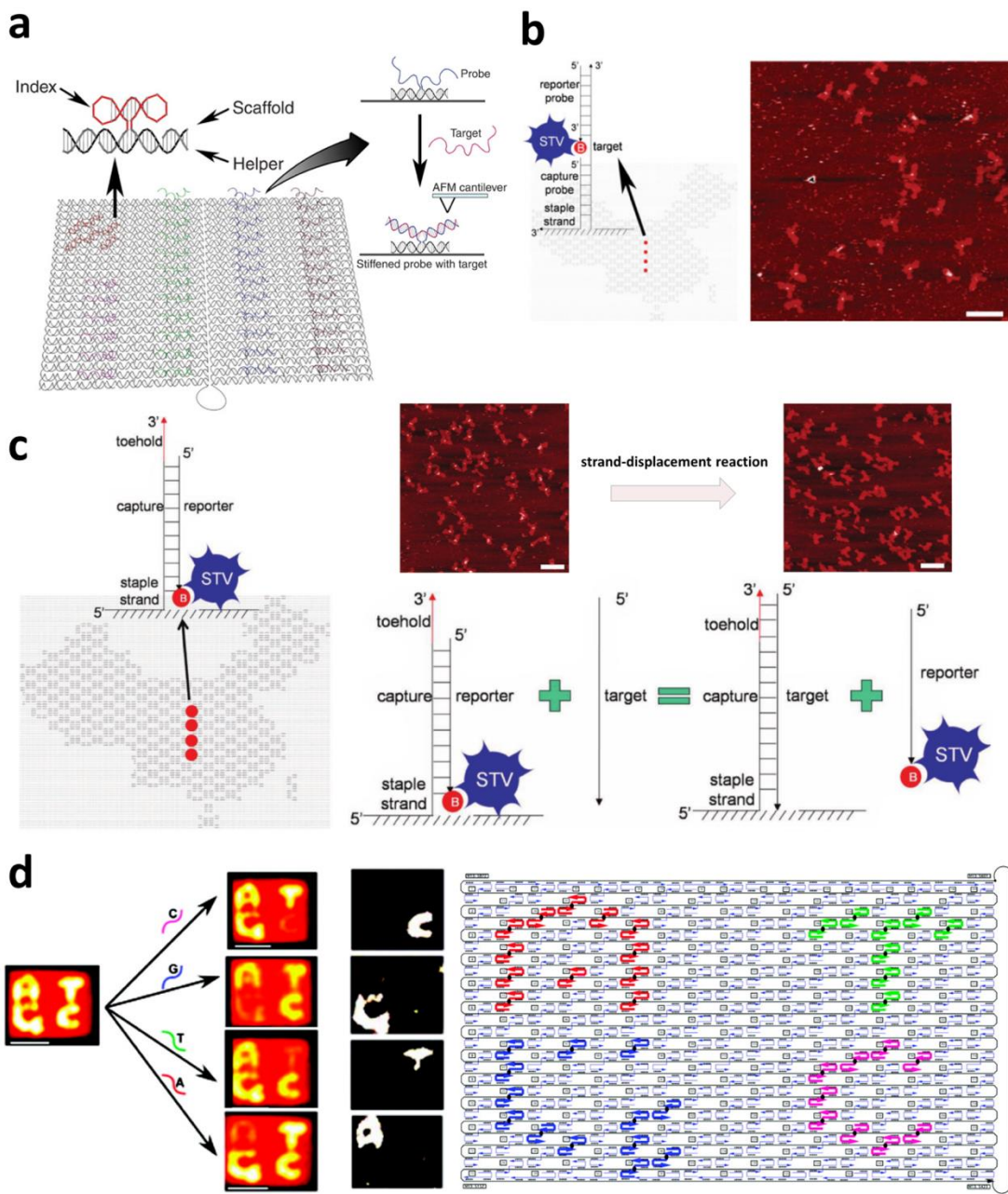


Figure 13. DNA probe tiles for bio-sensing. Schematic illustration of a) DNA probe tiles design and mechanism for target detection, reprinted with permission from ref.[285], Copyright © 2008 American Association for the Advancement of Science; b) Index-free nanoscale DNA chip with asymmetric origami map and its sandwich strategy for target detection, scale bar = 250 nm, reprinted with permission from ref.[286], Copyright © 2010 WILEY-VCH Verlag GmbH & Co. KGaA, Weinheim; c)

DNA-origami chip platform for target-labeling-free single-nucleotide polymorphism (SNP) genotyping, reprinted with permission from ref.[287], Copyright © 2010 Wiley-VCH Verlag GmbH & Co. KGaA, Weinheim; d) kinetic methods with atomic force microscopy of DNA origami patterns, reprinted with permission from ref.[288], Copyright © 2011 American Chemical Society.

The entire structure conformational change of DNA origami as the signal output was also related with sensing specific DNA sequences detection. A “pliers”-shaped origami nanostructure transition between three distinct parallel, anti-parallel, and cross-shaped conformations in the presence of their targets was triggered by three independent mechanisms: “pinching”, “zipping”, and “unzipping”,^[289] whereas a parallelogram structured origami experienced vertex angles between edges in the presence of the effector molecules.^[290] Cross form is the dominant species of the DNA origami pliers when no additional interaction was applied, but introduction of nine pairs of 12-mer sequence triggered transition of DNA origami pliers from open cross into closed parallel form under acidic conditions due to the quadruplexes formation upon protonation of cytosine between the sequence and DNA origami, showing potential application of the system to single-molecular pH sensors.^[291]

Unlike the clear understanding of specific nucleic acids and DNA nanostructures interface, the sensing of protein by DNA origami is currently limited to a select number of targets, predominately the proteins that directly interact with DNA. DNA binding protein human O⁶-alkylguanine-DNA alkyltransferase (hAGT) is responsible for the

repair of the O⁶-methylguanine and was considered relevant as a prognosis marker of cancer.^[292] Fàbrega's group developed a fluorescence method using a DNA G-quadruplex, the thrombin binding aptamer (TBA), as a molecular beacon for the detection of hAGT activity.^[293] The work was continued to visualize enzymatic activity of hAGT on an origami platform by combining the capabilities of the α -thrombin recognition/binding to TBA and the single-molecule features of the DNA origami applied to the detection of DNA repair.^[294] Taking the advantage of aptamers' high binding specificity to target protein and innate compatibility with origami,^[295] a malaria diagnostic approach was developed by incorporation of twelve DNA aptamers specific for the malaria biomarker Plasmodium falciparum lactate dehydrogenase(*Pf*LDH) into a rectangular DNA origami, by doing so the assembled aptamers remained their ability to specifically binding to target protein.^[186]

3.4.2. DNA tetrahedron

3.4.2.1. DNA tetrahedron for drug delivery

Comparing to DNA origami, tetrahedral DNA nanostructures (TDNs) is far smaller (less than 10 nm on a side) in size but capable of functioning equally, and it is more flexible for *in vivo* drug delivery.^[296] In addition, it can be self-assembled simply from DNA strands and prepared at high yield.^[37] Caveolin-dependent pathways endocytosis provide TDNs rapid internalization into mammalian cells, followed by transportation to the lysosomes in a highly ordered, microtubule dependent manner.^[297] TDNs can be further functionalized with nucleus-targeting signaling peptides that directed their entry

into the cellular nuclei,^[297] which advanced TDNs based drug delivery nanocarriers for intracellular targeted therapy. Another study confirmed that TDNs delivered DOX could reverse drug-resistant in cancer cells with enhanced uptake and bypassing efflux process, whereas free DOX is virtually non-cytotoxic due to the resistant.^[298]

Although a variety of materials have been explored for delivering siRNA, the performance is usually compromised using conventional liposomal and polymeric nanoparticles delivery vehicles due to their heterogeneity in size, composition and surface chemistry.^[299] (**Figure 14a**) Lee et al prepared self-assembled DNA tetrahedral nanoparticles with precisely controlled size to deliver siRNAs into tumor cells. Impressively, self-assembled DNA tetrahedral nanoparticles showed a longer blood circulation time *in vivo* ($t_{1/2} \approx 24.2$ min) than the naked siRNA ($t_{1/2} \approx 6$ min).^[300] Not only small drug molecules but macro therapeutics can be delivered by TDNs. The small DNA tetrahedral displaying a loop antisense DNA showed improved cell uptake and gene silencing when compared to linear DNA due to improved stability against degradation by nucleases in C2C12 myoblast cells study.^[301] And then Lee et al used similar setup, but focus on delivery siRNA attached to the tetrahedral. In this study, they also incorporated FA at several sides in the structure, to act as tumor target ligand. With this system, they were able to obtain over 50% reduction of firefly luciferase expression in HeLa cells and also 60% reduction in bioluminescence intensity in mouse model.^[300] (**Figure 14b**)

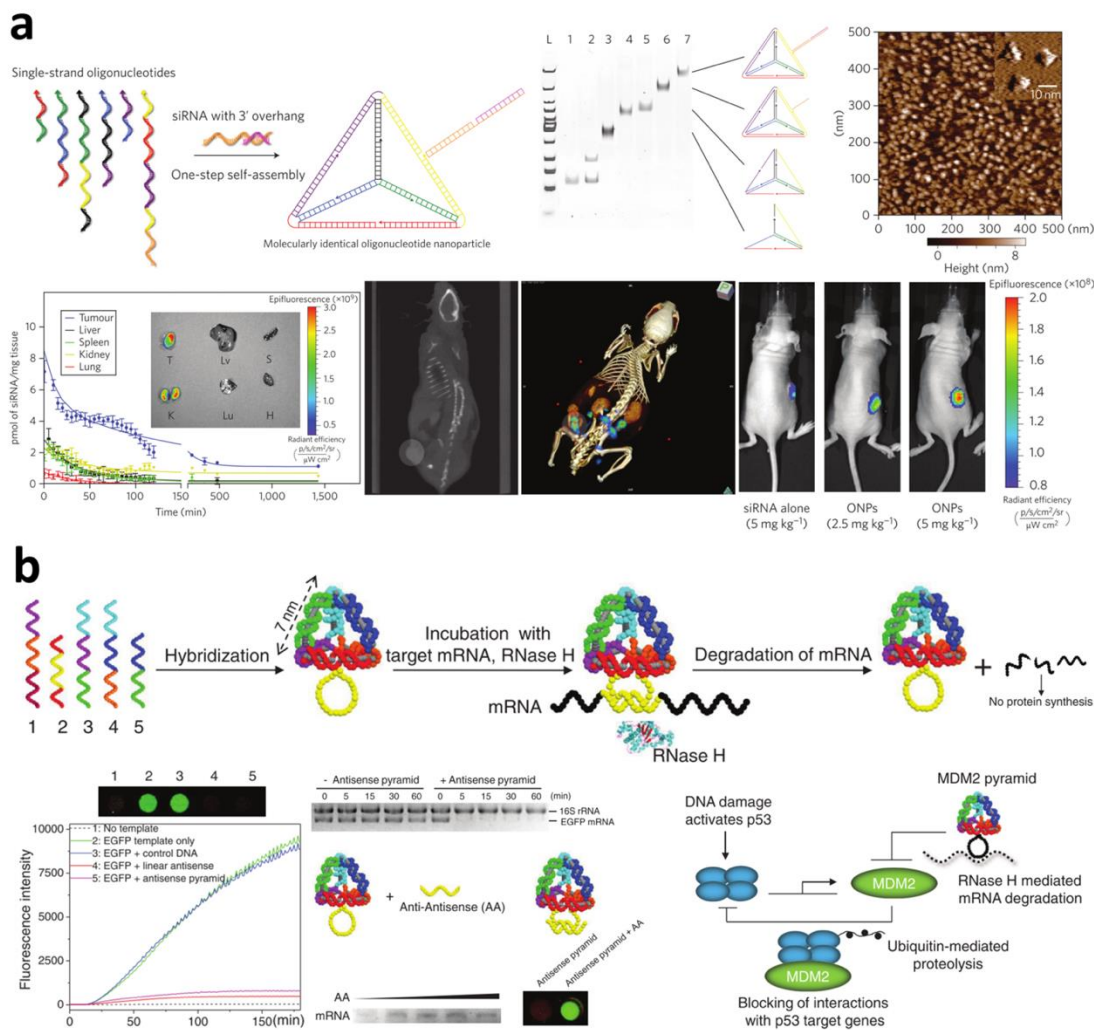


Figure 14. DNA tetrahedron for drug delivery. a) Self-assembly of oligonucleotide nanoparticles (ONPs) with site-specific hybridization of siRNA, and its pharmacokinetic profiles in tumor xenograft mouse model, reprinted with permission from ref.[302], Copyright © 2012 Macmillan Publishers Limited.; b) The fabrication of DNA tetrahedron with ssDNA antisense loop and *in vitro* activity evaluation, reprinted with permission from ref.[300], Copyright © 2011 Wiley-VCH Verlag GmbH & Co. KGaA, Weinheim.

3.4.2.2. DNA tetrahedron for bio-imaging

Beside commonly served as drug delivery vehicles, TDNs can also be functionalized with different molecules for *in vivo* imaging. For example, fluorescently labeled TDNs were used for *in vivo* sentinel lymph node imaging.^[298] Since TDNs' bio-distribution remains elusive, Fan's group has developed a TDN based dual-modality probe for mice imaging that combines both near-infrared (NIR) and single-photon emission computed tomography (SPECT).^[296] Although cancerous mRNA in living cells is promising to be used for cancer biomarker, the accurate detection and imaging of tumor-related mRNA remains challenging due to the complex biological matrices that result in inevitable noise signal.^[303] To achieve sensitive biomarker detection, He et al developed fluorescence resonance energy transfer-based DNA tetrahedron nanotweezer for highly reliable detection of tumor-related mRNA in living cells.

3.4.2.3. DNA tetrahedron for bio-sensing

Although aptamers inherit excellent properties for building biosensors (also denoted as aptasensors), its efficiency and sensitivity was often limited by some prerequisites: aptamer need to be perpendicularly to substrate surface, and have optimized density and distribution of the DNA strands on the surface.^[304] Moreover, chemical labeling of the DNA aptamer with a probe at the end is not efficient and possibly to decrease its affinity toward its target. While with the help of TDNs, the aptamers maintained the orientation and the density was adjustable,^[305] therefore may lead to synergic biological effects.^[306]

Molecular probes, especially fluorescent ones have been a powerful tool for detecting biologically relevant morphological details as well as monitoring various physiological processes in living systems because of their high noninvasivity, sensitivity, specificity, and disposed to fast analysis with spatial resolution.^[307] Consequently, fluorescent bio-sensing and bio-imaging now become a routine approach by tagging non-fluorescent molecules of interest with a fluorescent moiety to visualize these molecules.^[308] As such, fluorescent bio-sensing of DNA tetrahedron provides a promising tool to the early diagnosis of diseases as well as quantitative monitoring of drug delivery and release process.

3.4.3. DNA molecular beacon

Molecular beacons (MB) are oligonucleotide probe, typically 25 nucleotides long, which can report the presence of specific nucleic acids in solutions.^[50] The middle 15 nucleotides, complementary to the target DNA is loop of MB, while the five nucleotides at each terminus, complementary to each other rather than to the target DNA, form stem of MB. As a result, MB appears hairpin shaped molecule.^[50]

Tumor mRNA as a specific marker is proportional to various stages of tumor progression, providing new avenues to evaluate tumor response to treatment. An AuNP-DNA MB-DOX assembly was designed in a way that DOX intercalated in stem region of MB while MB loop base pair with tumor mRNA. When MB selectively bound to tumor mRNA of breast cancer cyclin D1 mRNA, MB double-strand opened and the conjugated DOX released. As such The controllable DOX release obtained

depend on concentration of mRNA expressed on cancer cells.^[309] (**Figure 15a**) The drug loading capability and controlled release of MB often combined with other molecular modification to realize more comprehensive functions. In some cancer cells the folate receptor (FR) was highly overexpressed. As a homing agent to such diseased cells, folate was covalently connected to carbon nanotube-mediated platinum (Pt)(IV) prodrug which was successfully delivered into FR(+) cancer cells by endocytosis pathway.^[310] With the understanding of folate specificity and the role of MB vehicle, folic acid functionalized single-stranded DNA and DNA MB was branched on the surface of AuNP to endow the nanoparticle not only the function of DOX carrier but exquisite control over site-specific functionalization.^[311] (**Figure 15b**)

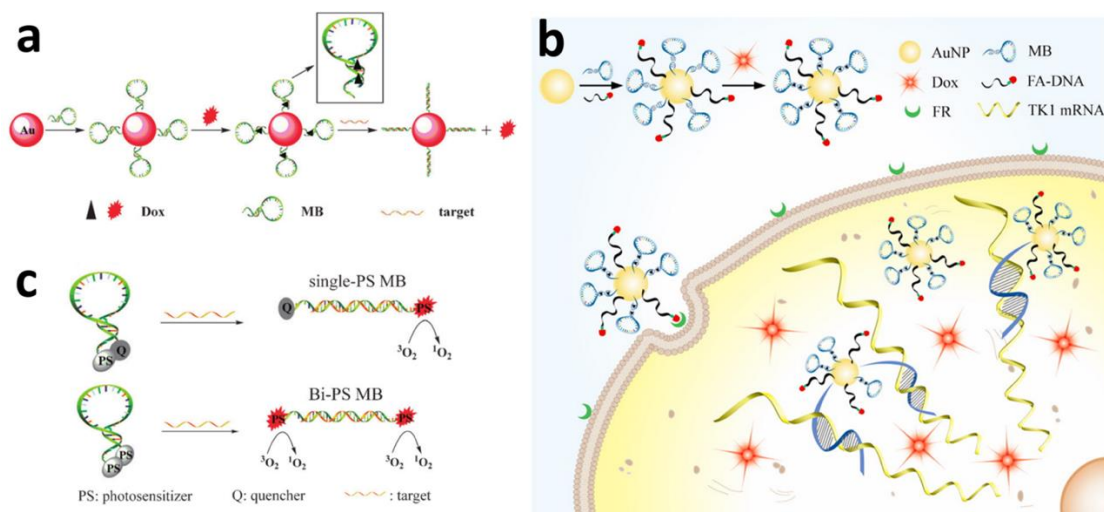


Figure 15. Molecular beacon for drug delivery. a) schematic illustration of the assembly of AuNP-MB (DOX), reprinted with permission from ref.[309], Copyright © 2011 The Royal Society of Chemistry; b) Schematic illustration of the assembly and cell uptake of dual-targeted nanocarrier, folic acid functionalized single-stranded DNA for active targeting, MB as drug carrier for activated release with

intracellular mRNA, reprinted with permission from ref.[311], Copyright © 2013 American Chemical Society; c) mRNA triggered a single MB with one-photosensitizer (PS) motif and two PS moieties, reprinted with permission from ref.[312], Copyright © 2011 The Royal Society of Chemistry.

MB can recognize the specific DNA/RNA with high selectivity, but its sensitivity depends on the ratio of the fluorescence in the open *versus* closed form and often this was a limitation. To increase this signal-to-background ratio, two photosensitizer molecules were assembled onto the opposite ends of a single MB instead of one.^[312] (Figure 15c)

Pei's group reported programmably regulation of the polyA-based aptamer nanobeacon (PAaptNB) for ATP analysis by adjusting the polyA length. For instance, with 30 bases attached, the PAaptNB detect a 10 µM detection limit of ATP, which is about 10-fold improvement compared with the conventional thiol-based aptamer nanobeacon.^[313]

3.4.4. DNA nanoflowers

DNA nanoflowers (NFs), the DNA nanogels by their nature of hydrogel, were self-assembled by co-precipitation of magnesium pyrophosphate and DNA generated via rolling-circle replication (RCR).^[178] Unlike conventional approaches to DNA nanostructure that the construction need of Watson-Crick base pairing, NFs assembly depends on liquid crystallization and dense packaging of building blocks.^[178] As a result, NFs are resistant to nuclease degradation, denaturation or dissociation at extremely low concentrations, may largely due to the dense DNA packaging in NFs.

The bio-stability is fundamental for biomedical applications. With rational design, drug-loading sites could be easily integrated into NF particles, especially double-stranded CG or GC rich sequences with preference to intercalate DOX. Plus the incorporation of cancer cell-targeting aptamers sgc8 and fluorescent bio-imaging agents, multifunctional NFs was assembled and the capability of intracellular imaging and targeted drug delivery was clearly demonstrated.^[314]

The specificity of NFs to cancer cell can achieve by the attachment of aptamers, such as KK1B10 for leukemia,^[315] sgc8 for breast cancer. Porous and densely packed infrastructures can provide NFs a high DOX loading capacity as high as 71.4% (*wt/wt*).^[316] NFs are size tunable. If NFs are within an appropriate size range, they can be internalized by many cancer cells. It has been reported MFs size can be as small as 200 nm in diameters.^[314] Collectively, these features account for multidrug resistance circumvention of NF-DOX, which was transported to the cytosol. Moreover, NFs protected DOX from efflux by P-gp, while free DOX was rapidly pumped out by adjacent P-gp.^[316]

The use of molecular dyes with different emissions represents an attractive technique for multi-fluorescent bio-imaging, especially for those dyes that experience a single-excitation wavelength offering multiple resolvable emission spectra. For instance, Hu et al reported an approach for making aptamer conjugated fluorescent resonance energy transfer (FRET)-NFs through RCR for single-excitation multiplexed imaging and traceable targeted anti-cancer drug DOX delivery.^[178]

3.4.5. DNA nanotubes

Double-crossover (DX) lattices curve back upon themselves to form hollow nanotubes.

These DNA nanotubes are somewhat similar in size and shape to carbon nanotubes while lack of the electrical conductance.^[317] Many researchers have constructed DNA nanotubes using a method that relies on spontaneous assembly of DNA in solution^[318, 317] and thermodynamics and kinetics constant of DNA nanotube based on polymeric self-assembly theory has been determined.^[319] The new building-block approach managed to yield fewer structural flaws and made it possible to better control the size and patterns of the DNA structures. The new method producing more dynamic and robust nanotubes were also reported.^[179] The diameters and patterns of DNA nanotube was also controllable using hierarchical DNA sub-tiles.^[320]

Comparing to other biomolecular nanostructures, such as peptide-amphiphilic nanofiber,^[321] and DNA tile,^[105] DNA nanotubes are more easily modified and connected to other structures. Johns Hopkins researchers have fabricated DNA nanotubes to assemble themselves into bridge-like structures arched between two molecular landmarks.^[322] Some studies of this self-assembling bridge process, which may be used to connect therapeutics to living cells, has already started. It was observed only microinjection of CpG-decorated DNA nanotubes but not of plain DNA nanotubes or CpG oligonucleotides induced a significant recruitment of leukocytes into the muscle tissue as well as activated the NF- κ B pathway in surrounding cells.^[321] (**Figure 16a)**

Same to other type of nanotubes structures, DNA nanotubes (NTs) hold promise for a number of materials' applications because of their high encapsulation potential inherited from its hollow structures. Triangular DNA nanotubes with alternating larger and smaller capsules along the tube length lines with positioning of the AuNP into the large capsules of these tubes 65 nm apart and the nanotube can be opened in the presence of complementary eraser DNA strand.^[323] (Figure 16b) This approach could lead to the applications of precise organization of one-dimensional nanomaterials, such as gene-triggered selective delivery of drugs and biological sensing. Molecular dynamics simulation uncovers that π - π interactions is the driving force of absorption of anti-cancer drugs, including DOX, daunorubicin, Paclitaxel (PTX) and vinblastine (VIN) by the DNA-NTs and the stability of DNA-NTs was improved with the absorption of anti-cancer drugs.^[324] (Figure 16c) DNA-NTs as combinatorial vehicles dual-functionalized by folate and Cy3 specifically bind to cancer cells through folate-folate receptor (FR) interaction and be further taken into the cancer cells for fluorescence imaging.^[325] (Figure 16d)

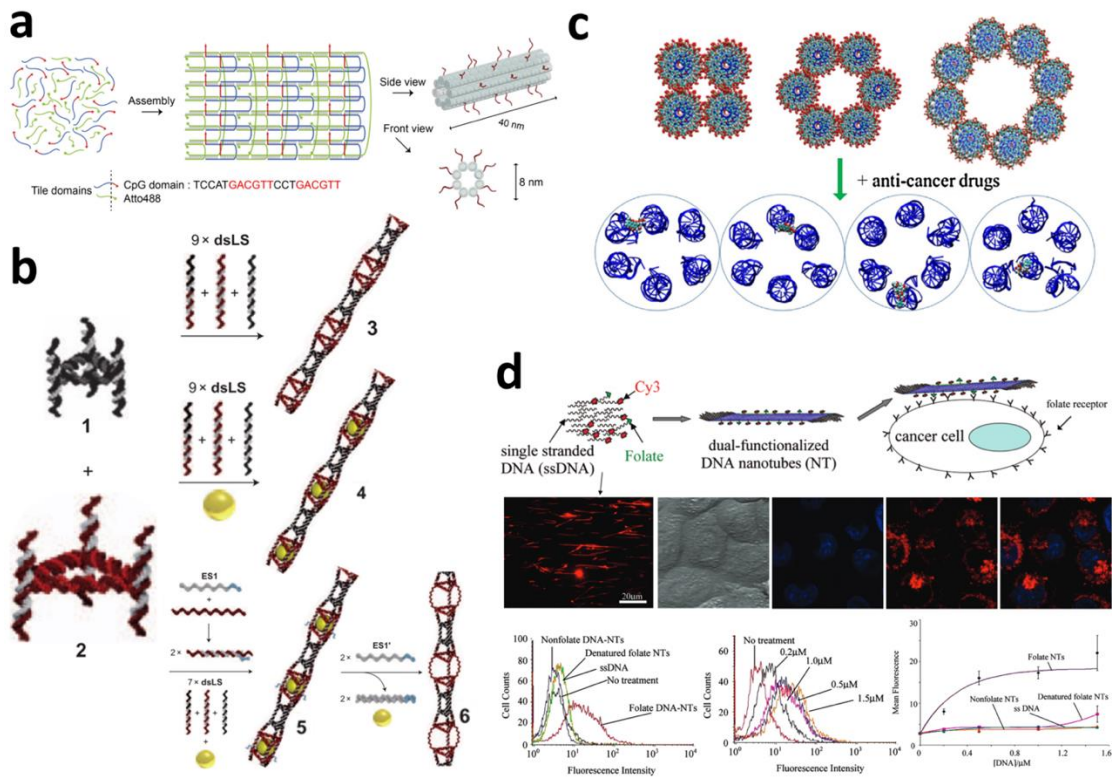


Figure 16. DNA nanotubes for drug delivery. a) CpG-decorated DNA nanotubes as carrier systems for CpG delivery, reprinted with permission from ref. [321], Copyright © 2015 Elsevier Ltd. b) Fabrication of triangular DNA nanotubes, small triangles 1 and large triangles 2 with appropriate linking strands, reprinted with permission from ref.[323], Copyright © 2010 Macmillan Publishers Limited.; c) DNA nanotubes composed of poly(AT)20 as anti-cancer drug carrier, reprinted with permission from ref.[324], Copyright © 2017 Elsevier B.V. d) Assembly of DNA nanotubes containing Cy3 and folate and its targeted cell delivery, reprinted with permission from ref.[325], Copyright © 2008 American Chemical Society.

An unsuccessfully case reported DNA nanotubes carrying siRNAs to GFP-expressing HeLa cells via folate targeting. Although the nanostructures entered the cells via an

endosomal pathway, but the nanostructures and their siRNA cargo were not capable of reaching the cytoplasm for knockdown and gene silencing, attributing to the DNA nanotube degradation in cell media.^[326]

3.4.6. DNA Dendrimer

Similar to other dendrimer, DNA dendrimer consist of several branched DNA units connected with each other using DNA ligase.^[180b] DNA dendrimers have been paid more and more attention due to highly branched, globular, and nanosized structures with outstanding monodispersity and stability, which therefore offered DNA dendrimers great potential to serve as candidate nanocarriers.

There was indication that the arrangement of CpG DNA into a branched, dendritic form significantly increased the immunostimulatory activity of CpG DNA, attributed to the cellular uptake of DNA dendrimers by RAW264.7 cells.^[327] The therapeutic application of DNA dendrimer for delivery, however, was limited by the use of ligase. Therefore enzyme-free method to prepare large DNA dendrimers was desired, and further to achieve pH responsiveness by introducing DNA molecular motors into the scaffold between the core and the first layer.^[328]

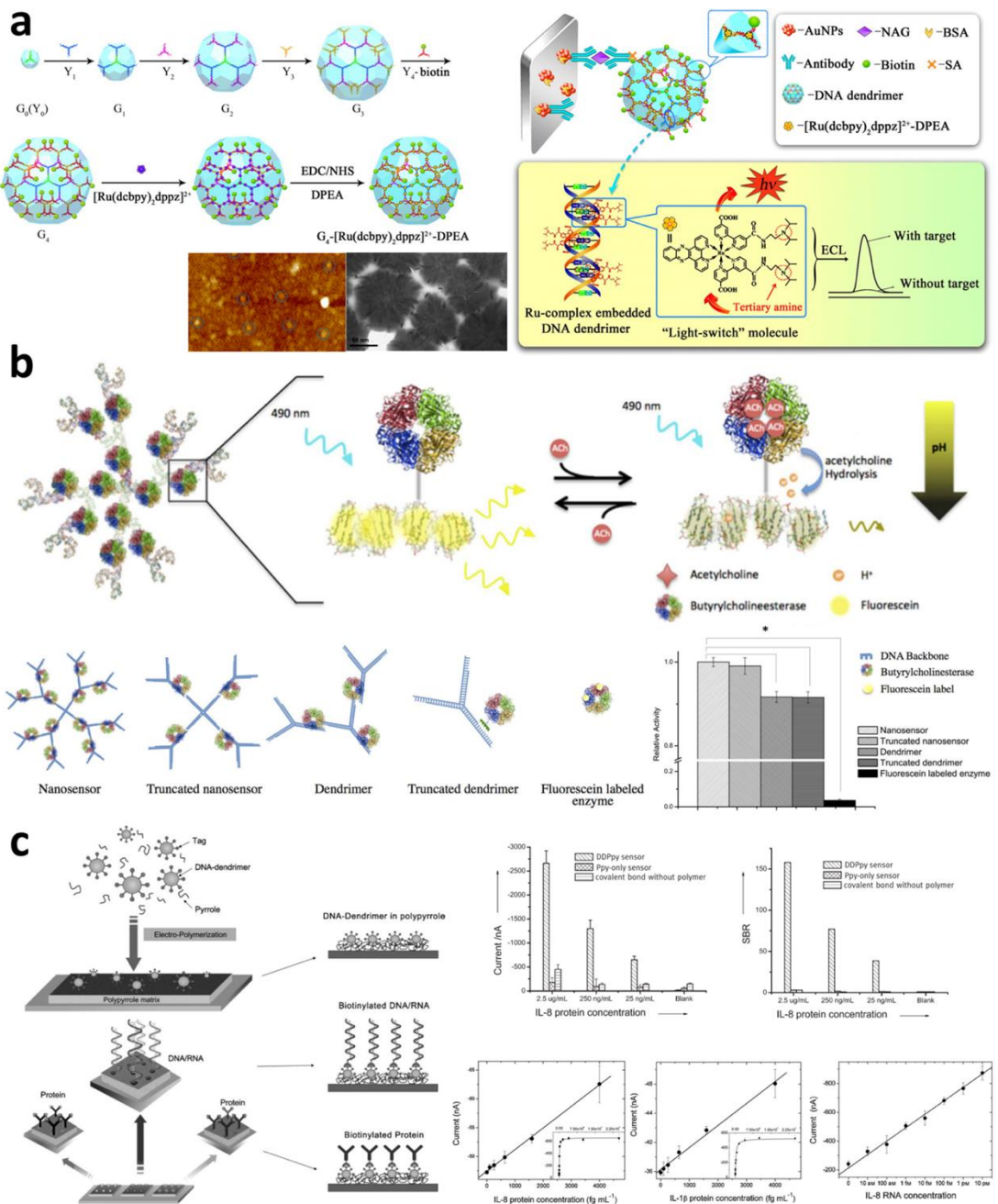


Figure 17. DNA dendrimer-based biosensors. a) Schematic illustration of the preparation of $G_4\text{-}[Ru(dcbpy)_2dppz]^{2+}\text{-N,N-diisopropylethylenediamine}$ (DPEA) and the response mechanism of this immunosensor, reprinted with permission from ref.[329], Copyright © 2016 American Chemical Society; b) The proposed mechanism of DNA dendrimer-based nanosensors, reprinted with permission from ref.[330], Copyright © 2015 Nature Publishing Group; c) Schematic illustration of the formation of DNA

dendrimer and polypyrrole (DDPpy)-based electrochemical sensors, IL-8, IL-1 β and IL-8mRNA as marker for efficiency testing, reprinted with permission from ref.[331], Copyright © 2009 Wiley-VCH Verlag GmbH & Co. KGaA, Weinheim.

Mohri et al has prepared self-assembling DNA dendrimers without needing of DNA ligases to deliver immunostimulatory CpG DNA to immune cells.^[180b] The histidine-dependent DNAzyme or anti-ATP aptamer-embedded DNA dendrimers maintained the catalytic activity of the DNAzyme or the recognition function of the anti-aptamer toward ATP in solution. When compared to free DNAzyme and aptamer, the dendritic nanocarriers exhibit excellent biocompatibility and cell membrane permeability, with enhanced intracellular stability. The applications of such sensing systems were used for imaging of histidine or ATP in living cells with satisfactory results.^[180a] The multifunctional DNA dendrimer constructed from functional building blocks with predesigned hybridization including fluorophore fluorescein isothiocyanate, targeting DNA aptamers sgc8 and intercalated anticancer drug DOX realized high affinity targeting, bio-imaging and drug delivery.^[332] The use of DNA dendrimers as templates to direct the assembly of nanoparticle groupings, such as quantum dots,^[333] nanodiamonds,^[334] silver^[335] and gold^[336] nanoparticles, was also reported for nanophotonic and sensing applications. Biotin labeled DNA dendrimer (the fourth generation, G4) with large amount of DNA duplex provided sufficient intercalated sites for “light-switch” molecule Ru(II) [Ru(dcbpy)₂dppz]²⁺ to improve its

luminous efficiency and expand the detection limit of *N*-acetyl- β -D-glucosaminidase to 0.028 pg mL⁻¹, a dramatic improvement comparing to the traditional probe molecule.^[329] (**Figure 17a**) DNA dendritic complex was reported to increase siRNA-based gene silencing efficiency for 13.8% with lower cytotoxicity than commercial cationic lipid transfection agents lipofectamine.^[337] The butyrylcholinesterase and fluorescein were incorporated into DNA dendrimer scaffolds based nanosensors which enabled the detection of acetylcholine in brain with the ability to quantify the spatiotemporal fluctuations of neurotransmitter release and overcome the current nanoscale size constraints of the synapse to sense.^[330] (Figure 17b) The human mutant-type p53 gene segment triggered the formation of DNA dendrimers from hairpin DNA probes by hybridization chain reaction and enabled the detection of mutated gene at concentrations ranging from 0.08 nM to 8 nM due to distinct optical reorientation appearance of liquid crystal characteristics of the dendrimer.^[338] Attributing to dendrimer's signal amplification effects, the limit of the detectable polynucleotide kinase activity by using gold electrode modified with magnetite microspheres coated with titanium dioxide nanoparticles and a DNA dendrimer was extended to 0.003 U mL⁻¹.^[339] DNA dendrimer was introduced into the interfacial film on the electrochemical sensors' surface to improve limit of detection of salivary biomarkers for oral cancer to 100-200 fg·mL⁻¹, which is three orders of magnitude better than that without the DNA dendrimer interface,^[331] indicating the bio/abiotic interface greatly accelerate the signal transduction process. (Figure 17c) By

crosslinking DNA dendrimer with streptavidin-coupled linker DNA into a nanostructure and combing a label-free quartz crystal microbalance (QCM) technology, a mass-sensitive QCM bio-sensing platform was fabricated, offering high selectivity and sensitivity with the detection limit of 0.062 nM 28 nt KRAS gene.^[340]

3.4.7. DNA as matrix

Self-assembled DNA nanostructures of high programmability and complexity provide excellent matrices to organize heteroelements at the nanoscale to construct interactive biomolecular complexes and networks.^[341] And in turn, it is hoped that these DNA-directed assemblies can lead to unique and improved functional properties which can be applied to many fields, such as molecules delivery and precise molecule detection.

A cocoon-like DOX-loaded self-degradable DNA matrix with maximum capacity of 66.7% DOX loading was reported, which introduced deoxyribonuclease (DNase) into the nanostructure to achieve self-degradation for promoting drug release. Yet DNase was encapsulated into a nanocapsule with a polymeric shell that was cross-linked by acid-degradable crosslinkers. When the assemble was internalized by cancer cells and enters the acidic endolysosome, the polymeric shell degraded and resulted in the exposure of DNase I, which rapidly degraded DNA scaffold, thereby releasing the intercalated DOX for enhanced anticancer efficacy.^[342] (**Figure 18a**)

Except the small therapeutics, DNA nanostructures were also used to organize biological molecules/assemblies. For instance, DNA origami was assembled into three

dimensions to construct DNA cubic box with a cavity that is large enough to contain antibody and can be opened by external oligonucleotides DNA ‘keys’,^[39] indicating application of logic sensors related with multiple-sequence signals or for the controlled release of cargos.

The relationship between wound healing and cancer has long been identified. There is recognition that the inflammatory processes during wound healing following tumor resection may promote cancer progression therefore blocking specific inflammatory signals, alone or in combination with other stem cell pathway by antibody, such as anti-programmed cell death protein (anti-PD-1), which can decrease cancer stem cell populations in a therapeutic setting.^[343] However, several factors may compromise therapy efficacy, such as autoimmune disorders, lacking costimulation tumor microenvironment. To address these limitations, a DNA nanococoon delivery carrier for the controlled release of anti-PD-1 antibody and CpG oligodeoxynucleotides (CpG ODNs) in response to inflammation conditions was developed. CpG ODNs trigger express of Toll-like receptor 9 improved the anti-cancer activity of cancer treatments in general, anti-PD1 was released when inflammation related matrix metalloproteinases act.^[344] (Figure 18b)

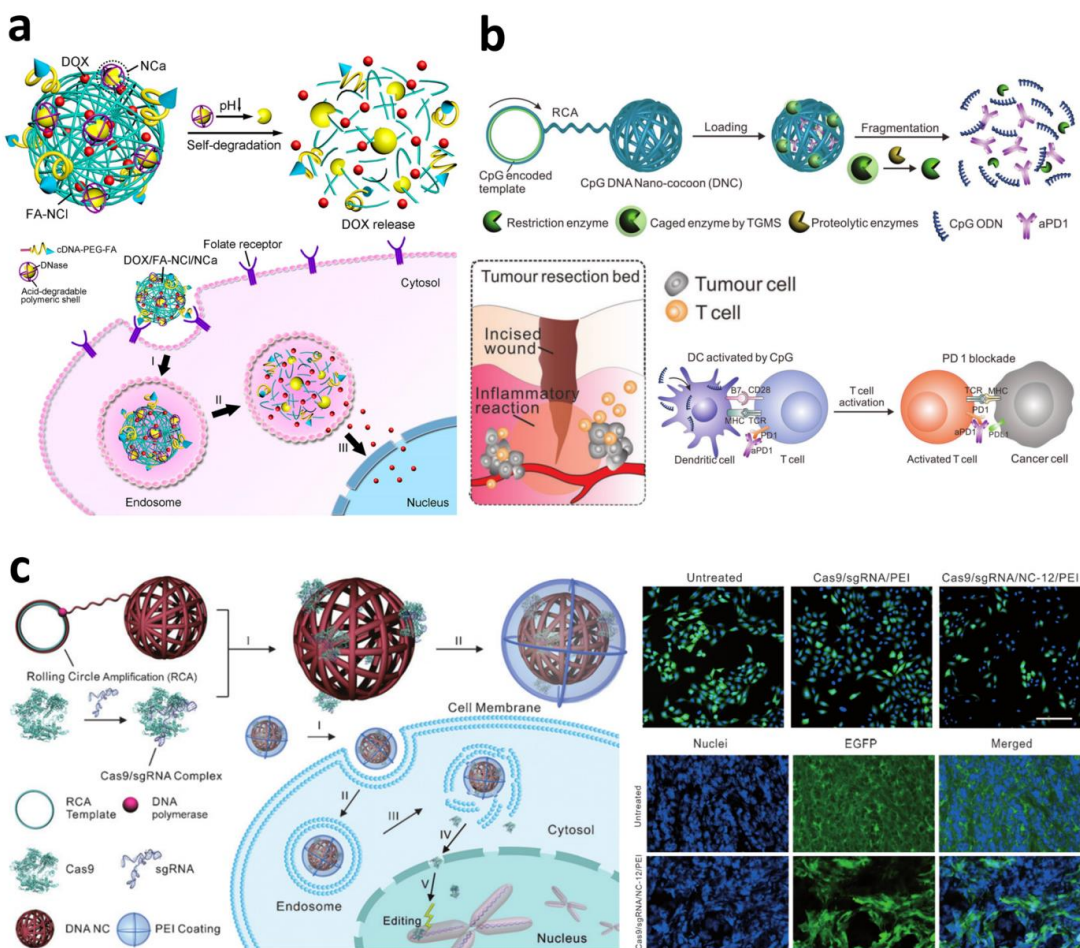


Figure 18. DNA as matrix for drug delivery. a) The cocoon-like DNA nanoclew (NCI), embedding with acid-triggered nanocapsule (NCA) and schematic illustration of efficient delivery of DOX for cancer therapy, reprinted with permission from ref.[342], Copyright © 2014 American Chemical Society; b) Schematic illustration of DNA nanococoon (DNC)-based drug delivery system, the CpG and aPD1 released under an inflammation condition, reprinted with permission from ref.[344], Copyright © 2016 WILEY-VCH Verlag GmbH & Co. KGaA, Weinheim; c) The assembly of yarn-like DNA nanoclew (NC) based CRISPR–Cas9 delivery system, and its corresponding *in vitro* and *in vivo* delivery, reprinted with permission from ref.[345], Copyright © 2015 WILEY-VCH Verlag GmbH & Co. KGaA, Weinheim.

Zhao et al reported DNA nanocaged enzymes not only increased substrate turnover but also protected the enzyme against protease, and the size of a protein and its activity enhancement was significant inverse correlated.^[346] Furthermore, detailed protocols for assembly DNA nanostructures as scaffolds to organize the spatial arrangements of multi-enzyme cascades with control of their relative distance, compartmentalization and mass transport of substrates were also published.^[347]

The CRISPR-Cas9 system experienced translation towards human therapeutics, while the delivery still poses the central challenge. One strategy is to use Cas9/sgRNA DNA nanoclews (NCs) complex for delivery, in which DNA NCs being partially complementary to the sgRNA. It was assumed binding and releasing of the Cas9/sgRNA complex were balanced due to this complementary arrangement, hence guide sequence greatly enhanced the extent of gene editing.^[345] (Figure 18c)

3.4.8. DNA hybrid

The population variations in expression of a single biomarker in certain diseases and/or from the lack of specificity to a particular disease of the target biomarker may lead to ‘false positive’ diagnosis, therefore measurements of a panel of biomarkers in parallel are typically needed for early disease detection and personalized therapy.^[348] A variety of platforms to monitor multi-target have been established in biomedical field. Among them, multifunctional DNA nanovectors reveal compelling potential for optimized therapy. Use of DNA alone to build up 2- and 3-D nanostructures paves the way for

versatile applications. However, the realization of more advanced functionality required the hybrid of DNA with other materials or technologies, resulting in new nanostructures and devices.^[349]

3.4.8.1. DNA hybrid with porous nanoparticles

Abnormal DNA methylation implied occurrence and development of many serious human diseases, such as cancer was precisely controlled by DNA methyltransferases (MTases).^[350] Therefore, it is of great value to precisely detection of DNA MTases for biomedical research and clinical diagnosis of cancers. Given the in-deep insights of mesoporous silica (MSN) but far more clear and application of controllable release of DNA by MSN, Wang et al built a DNA MTases responsive probe with double DNAs (DNA1/2) loaded in MSN, which not only served as a nano-carrier of loading DNA but also as an amplifier of surface-enhanced Raman scattering signal for high sensitivity, good selectivity, and fast analysis.^[351] A nanocarrier based on MSN-coated Cu_{1.8}S nanoparticles employing aptamer-modified GC-rich DNA-helix as gatekeepers was loaded with DOX and another anticancer drug, and showed synergistic therapeutic effect due to the denaturation of DNA double strand triggered by high photothermal conversion of Cu_{1.8}S.^[190d]

MicroRNA 21 (miR-21), one of the oncogenic miRNAs, was reported to be overexpressed in various human cancers, and inhibition of its expression by delivering antisense oligonucleotides (anti-miR-21) could lead to caspase-dependent apoptosis.^[188] Zhang et al reported the fabrication of a drug delivery system that was

based on DNA-hybrid-capped MSN-coated quantum dots (MSQDs): The DNA hybrid served as gatekeeper by forming 12 base pairs between parts of anti-miR-21. Under the guiding of surface aptamer AS1411, the nanocarrier exclusively entered tumor cell. Subsequently, the overexpressed miR-21 in tumor cell unlocked the gate through the complementary base paring with anti-miR-21 strand, and consequently triggered the release of DOX from MSN.^[188]

Biocompatibility, multifunctionality, stimuli responsiveness, and high drug loading are key requirements for the next generation of drug delivery vehicles. To receive all these properties in a single carrier, the microfluidic technology, porous silicon nanoparticles (PSi NPs) and giant liposomes were assembled as a nano-in-micro platform (PSi NPs@giant liposomes), which not only co-load and co-deliver hydrophilic and hydrophobic drugs but also combined with DNA nanostructures, AuNRs, and magnetic nanoparticles. Consequently, this platform showed magnetic and thermal responsive, high drug loading capacity, alike sustain the release of the therapeutics with tunable therapeutics ratio.^[216] Kong et al also fabricated an all-in-one platform in which PSi, AuNRs, and DNA origami were combined in double emulsion. It was believed AuNRs exhibit high affinity to DNA nanostructure and DOX, thus enhanced the loading of the DNA and DOX inside the double emulsion. In the end, a remarkable inhibition against multidrug resistance was observed for the therapeutics combination with DNA origami compared to any of the drugs used alone.^[352]

3.4.8.2. DNA hybrid with silver/gold nanoparticles

The spherical silver nanoparticles with an average diameter smaller than 10 nm consisted of Ag as the core coated by thin layer of DNA increased antibacterial efficiency for 4 folds (inhibitory concentrations decreased from 20 ppm to 5 ppm)^[353] against *E. coli* when applied to modify cotton based fabrics.^[354] This was presumably attributing to highly surficial negative charges of Ag nanoparticles, which favored the immobilization onto fabric surfaces *via* electrostatic interactions. It was also showed that the molecular beacon hybrid Au nanoprobes could detect 16S rRNA of *E. coli* at a concentration of 10^2 cfu.ml⁻¹, with which the sensitivity was enhanced by three orders of magnitude than using molecular beacon directly.^[355] Signal-switchable interlocked DNA nanostructures have attracted a growing of interests. For instance, by the functionalization of AuNP/DNA rotaxane hybrid nanostructures ring with fluorophore modified nucleic acids in different orientations, the switchable fluorescence properties were achieved.^[356] To improve fluorescence based applications, reducing photo bleaching is critical. Pellegrotti et al reported a DNA origami-based hybrids containing individual fluorophores and AuNPs at a controlled separation distance of 8.5 nm, by changing nanoparticles' size the mean number of photons emitted by the fluorophores increased before photo bleaching.^[357]

3.4.8.3. DNA hybrid with oligonucleotides

The biologically significant DNA itself can be internalized into cells efficiently. For example, uptake of DNA encoding a luciferase reporter gene from hybrid polymeric nanoparticle/DNA complexes with DNA either adsorbed on the surface, or

encapsulated, or both was found to be 500-600 times more efficient as unbound one to be delivered to HEK293 cells.^[267] Afonin et al reported RNA/DNA hybrid nanocubes consisting of either RNA or DNA cores (composed of six strands) with six attached RNA-DNA hybrid duplexes were able to conditionally activate the RNA interference in various human cells and also demonstrated that DNA-RNA nanocubes were less immunogenic than RNA-RNA and RNA-DNA nanocubes.^[358]

At low positive to negative charge ratio (N/P = 6), the hybrid non-viral system consisted of condensed plasmid DNA by generation 4 nanoglobules and lipid ECO, combined through electrostatic interactions between the positively charged head group of ECO and the anionic surface of the G4/pDNA complexes, efficiently delivered gene into RPE cells for treating ocular genetic disorders.^[359]

Aptamers' targeting abilities has been widely exploited, but its potential to improve drug loading and release from nanocarriers was thoroughly unexplored. Plourde et al hence utilized drug-binding aptamers to load DOX into cationic liposomes and optimization of the charge and drug/aptamer ratios resulted in ≥ 80% encapsulation efficiency, ten folds improvement than classical passively-encapsulating liposomal formulations.^[360]

3.4.8.4. Other DNA hybrid

CpGs are promising for cancer immunotherapy, but their delivery into antigen-presenting cells often was sub-optimized by unfavorable pharmacokinetics. To confront the challenge, Zhu et al presented DNA-magnesium pyrophosphate (Mg_2PPi)

hybrid nano-vaccines (hNVs) for efficient antigen-presenting cells' (APCs) uptake, prolonged tumor retention, and potent immunostimulation. The prolonged cancer immunotherapy mainly attributed to the protection of hNVs from nuclease degradation and thermal denaturation by Mg₂PPi.^[361]

The high DOX loading efficiency of graphene oxide (GO) nanosheets attributing to supramolecular π-π stacking has been widely exploited.^[362] These observations were further developed into GO crosslinked hybrid nano-aggregates via two single-stranded DNA, ATP aptamer and DOX to form sandwich structure.^[363] In the presence of ATP, the formation of the stable ATP/ATP aptamer complex lead to the dissociation of the aggregates therefore the release of DOX.^[363] In a recent work, targeted detection and drug delivery were simultaneously performed by incorporating different functional units, such as aptamers, and disulfide linkages into magnetic nanoparticles/DNA-sphere.^[364]

3.4.9. DNA nanostructure devices

3.4.9.1. Controlled molecule release

Inspired by the performance of hemoglobin, Mariottini synthesized the first hemoglobin-like DNA-based nanodevice with up to four interacting binding sites that realized ligand loading and releasing over narrow concentration ranges, and the ligand affinity could be controlled via both allosteric effectors and by environmental cues (*i.e.*, temperature and pH).^[364] Jeong et al prepared a electro-responsive multilayer nanofilm on the surface of a chip-electrode, which enabled controlled release of DNA strand

responding to electrochemical inputs.^[365] The “sense-and-treat” localized drug delivery system in which the aptamer accompanied DNA tetrahedron to specifically destroy circulating tumor cells by synergetic chemotherapy with DOX and photodynamic therapy with generating toxic $^1\text{O}_2$. Comparing to aptamer only labeled with photosensitizer, the DNA nanodevice promoted cellular internalization of anticancer agents, increase drug loading capacity, and induced the synergistic therapies.^[41]

(Figure 19a)

“ β -cyclodextrin (β -CD)-ferrocene” host-guest system was introduced in surface-tethered DNA nano-device which could actualize function of directional loading, transporting and unloading of β -CD under the control of pH and electrochemical treatment.^[366] Therefore they are of great value in controllable molecular transport and release. Beside the typical physiochemical of molecular stimuli and cues for control and regulate molecular nano-devices and nano-machines function, biological molecules were also taken under considerations. The possibility to rationally controlled release of ligand and mediate enzymatic reaction based on DNA-based nano-devices catalyzed by transferases and hydrolases had been confirmed.^[367] (Figure 19b)

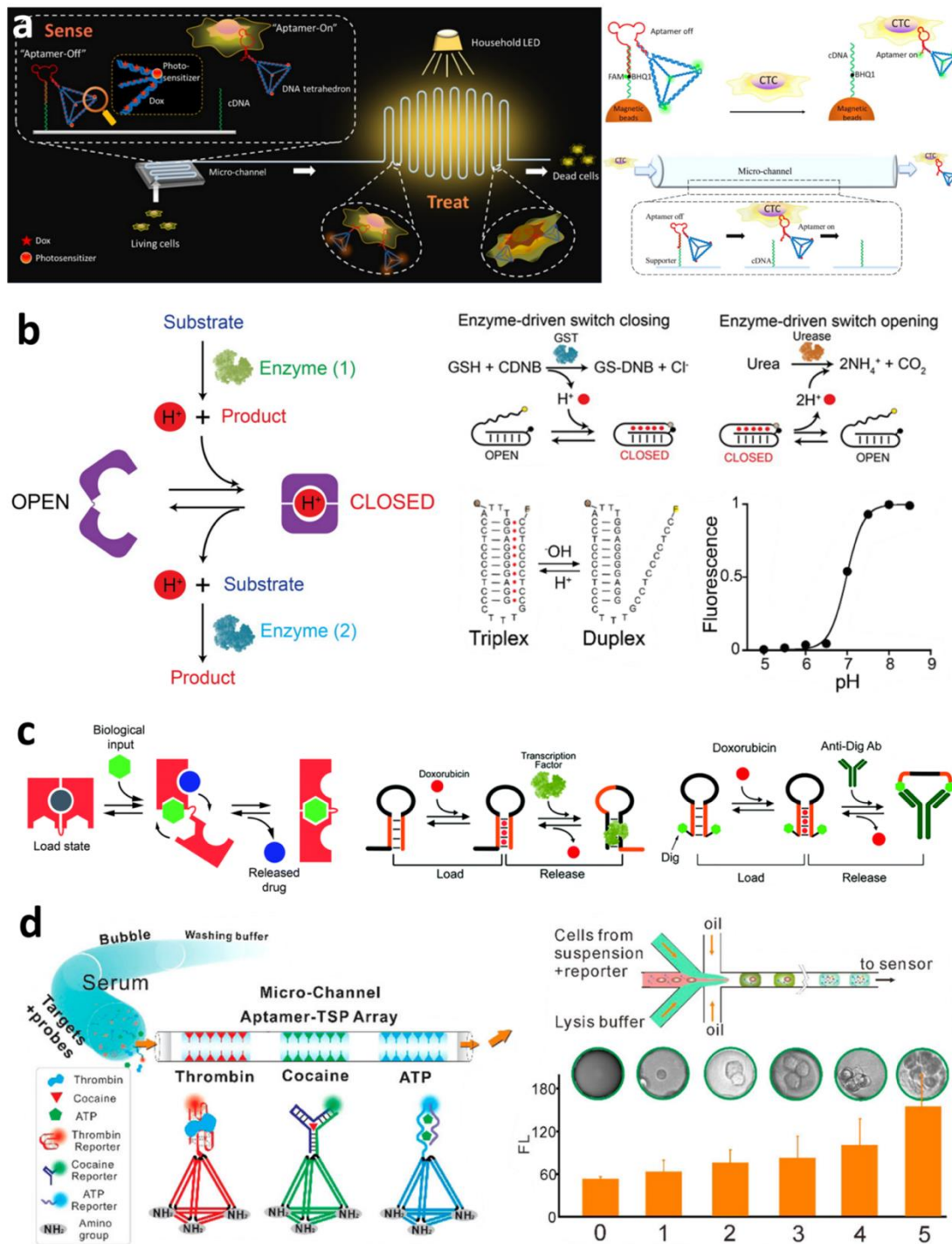


Figure 19. DNA nanodevice as drug delivery system. a) Scheme of the principle of “sense-and-treat” DNA nanodevice for synergetic destruction of circulating cancer cells, reprinted with permission from ref.[41], Copyright © 2016 American Chemical Society; b) DNA-based nanodevices with

configuration-switching DNA structures, the opening/closing switcher triggered by enzyme, reprinted with permission from ref.[367], Copyright © 2015 American Chemical Society; c) Allosteric DNA nano-switchers, triggered by biological inputs (TATA-binding protein, antibody), with permission from ref.[368], Copyright © 2017 The Royal Society of Chemistry; d) Construction of DNApull-based sensors and its application for measurement of cellular ATP level, reprinted with permission from ref.[369], Copyright © 2017 American Chemical Society.

Rossetti et al reported DNA-based nano-switches allosterically regulated by antibodies and transcription factors were able to release DOX in a controlled fashion as such the binding of the specific biological targets to the nano-switch pushes the conformational conversion from DOX “Load” towards the “Release” state.^[368] (Figure 19c) Recently, DNA-affibody nanoparticles bind with DOX which mimicked the antibody was prepared. These nanoparticles not only played the role as a support to anchor to antibody molecules but also act as a vehicle to non-covalently bind DOX for drug delivery. Comparing to reference antibody trastuzumab, the nanoparticle had a smaller size (95 kDa) than the reference antibody trastuzumab (150 kDa) but represented more than two-folds activity toward BT474 cell.^[370]

Shawn et al have used DNA origami to build a nanosized robot that acted as a drug delivery vehicle. The nanorobot came in the form of an open clamshell whose two halves were connected by special DNA duplex. The duplex could recognize specific proteins present on the surface of cells. When the robot came into contact with the right

cells, the duplex zipper opened the container and delivered its payload. As a testing case, nanorobots loaded with combinations of antibody to human CD33 and antibody to human CDw328 Fab' fragments were used in two different types of cell-signaling stimulation in tissue culture, the robots induced growth arrest in NKL cells in a dose-dependent fashion.^[371]

3.4.9.2. DNA device for cellular molecules detection

Pei's group recently reported an DNA nanostructure scaffold supported aptamer pull-down (DNaPull) assay serve as a sensitive analytical platform for analyzing a variety of bioactive molecules, including cell fuel ATP with limit of detection (LOD) of 1 μM, a drug cocaine (1 μM of LOD), and a biomarker thrombin (0.1 nM of LOD). This convective flux based assay was run in < 5 min, which is an 18-fold improvement compared to typical diffusive flux.^[369] (Figure 19d) By just change the probe attached at vertex, the same DNA tetrahedral-structured platform implemented sensitive and selective detection of multiple heavy-metal ions (*i.e.*, Hg²⁺, Ag⁺, and Pb²⁺) within 5 min, the detection limit was down to at least 20 nM.^[175] The LOD of thrombin was further improved to 1.7 pM due to aptamer/protein molecular machines' drastically amplified electrochemical responses signal.^[372] A reusable aptasensor of thrombin based on DNA machine on the basis of resonance light scattering technique was reported and could be repeatedly used for at least 6 cycling times by heat triggering conformation transfer and releasing of thrombin.^[373] The quantitative detection of ATP was realized using radiometric surface-enhanced Raman scattering strategy where thiolated

3'-Rox-labeled complementary DNA (cDNA) was fixed on the gold nanoparticle surface and then hybridized with the 3'-Cy5-labeled ATP-binding aptamer probe to form a rigid double-stranded DNA.^[374]

The unmoral expression of specific maker at the boundaries of eukaryotic cells was usually considered as the implication of disease. To more precisely target diseased cells, profiling the high or low expression levels of multiple biomarkers is needed since most identified cell-surface markers are not exclusively expressed on the target population of diseased cells.^[375] DNA aptamers can selectively recognize a wide range of targets, including biomarkers. Three aptamers, Sgc8c, Sgc4f, and TC01, respectively target three overexpressed markers on the surface of cancer cell were assembled into “nano-claw” sensor and was assigned capability of autonomously analyzing multiple cell molecular signature inputs and realizing targeted therapeutic effects.^[376]

3.4.9.3. Molecular probes

By using The dual-cyclical nucleic acid strand-displacement polymerization amplification strategy to the generation of DNA nanomachine, the bio-sensing signal was exponentially amplified, enabling the quantification of p53 gene in the wide concentration range from 0.05 to 150 nM with the detection limit of 50 pM and easily distinguishing the mutant gene from the wild-type.^[377]

A single AuNP coated with the self-assembly of intelligent layered DNA circuits underwent a variety of Boolean logic gate operations, served as a programmable strategy to sequentially tune the size of nanoparticles, as well as a new fingerprint

spectrum technique for intelligent multiplex bio-sensing.^[378] Gold nanostar enhanced surface Plasmon resonance detection of an tetracycline (TC) to as low as 10 aM concentration via TC-specific aptamer-antibody probe (antiTC) sandwich assay, which was >103 folds improvement in performance than sole antiTC.^[379]

Environmentally important organic pollutant such as bisphenol A could be detected by aptamer modified inorganic nanoparticles^[380] and the combination of truncated aptamer, complementary signalling DNA, quantum dots (QD), and magnetic beads,^[381] as well as palm-size NanoAptamer analyzer.^[382] DNA nano-devices composed of sensing, normalizing and targeting modules could quantify chloride transport in organelles of living cells in a pH-independent manner^[383].

3.4.10. DNA nanopore/channel

Biological ion channels are pore-forming membrane proteins which function as molecular gatekeepers that control transport across cell membranes.^[384] The re-engineering of such systems and the extending to non-ionic cargo is technologically significant to molecule bio-sensing or drug delivery, but artificially fabricating those channels with a predictable structure remains challenge. DNA nanomaterial with excellent programmable self-assembly properties allow the validation of this principle-of-concept.

Some fundamental observations disclosed that DNA nanopores could achieve voltage-dependent switching between open and closed state. Smaller PEGs entering the pore^[385] as well as molecular simulations demonstrated DNA nanopores central tube

lumen adopted a cylindrical shape while the mouth regions at the two DNA nanotube openings underwent gating-like motions,^[386] which underlined the DNA nanopores' potential applications in bio-sensing and drug delivery. Howorka's group reported a biomimetic DNA-based channel which could control cargo transportation across a bilayer selectively. Seven concatenated DNA consisted of the molecular valve experience conformational change could unlock the membrane-spanning channel by adding the key oligonucleotides.^[384]

Combination of DNA origami structures with glass nanocapillaries to form DNA origami nanopores actualized the both physical and chemical control of DNA translocation. Tuning the pore size could control the folding of dsDNA and specific introduction of binding sites in the DNA origami nanopore allowed selective detection of ssDNA as a function of the DNA sequence.^[387] DNA nanopore composed of a bundle of six DNA duplexes folded and functionalized with aptamer and cell-penetrating peptide with specific targeting and increased intracellular uptake by Ramos cells was recently reported.^[388] The DNA nanoprobe altered its structure from the open to close state in the presence of mRNA, thus bringing two distal fluorophores close enough to efficiently trigger fluorescence resonance energy transfer.^[303]

3.5. DNA-Nanoparticle superstructures

Driven by their compelling nanotechnological applications, including selective catalysis, biomineralization and drug delivery,^[389] multicompartiment superstructures in nanoscale have attracted tremendous attention, focusing on block copolymer

nanocomposites^[390] and micellar nanocontainers,^[391] and moving to DNA nanostructures.^[392] Among the different types of multicompartment architectures, “core-satellite” superstructures is a promising candidate^[393] because it is an effective way to increase the Raman scattering enhancement.^[394] Polyamines significantly enhanced the structural rigidity and plasmonic properties of DNA-assembled metal nanoparticles, which attributed to the ability of polyamines to condense DNA and cross-link DNA-coated nanoparticles.^[395]

Inorganic nanoparticles, such as gold, play an important role in diseases treatment, such nanoparticles will remain in the body for a long time because they do not biodegrade. This clearance difficulty *in vivo* have raised many concerns for safety reasons. Chou et al organized AuNPs into larger colloidal superstructures in which a central “core” AuNP was branched by multiple “satellite” AuNP through complementary DNA linker. It turned out this superstructure reduced AuNP retention by macrophages and improved *in vivo* tumor accumulation and whole-body elimination and further application to protect imaging or therapeutic agents against enzymatic degradation was also highlighted.^[396] (**Figure 20a**) This work was extended by creating AuNPs superstructures which partly covered with DNA chain and FA as targeting molecule. Depending on the DNA chain hybridization and overall particle configuration, the small AuNPs could link with “large core” (designated as morphology 1) to hide the FA or to expose it on the surface when connected with “medium core” (morphology 2), thus changing the way the particles interacted with cancer cells and it turned out the

cellular uptake of FA conjugated nanoassemblies of morphology 2 was 2.5 times higher

than that of morphology 1.^[397] (Figure 20b)

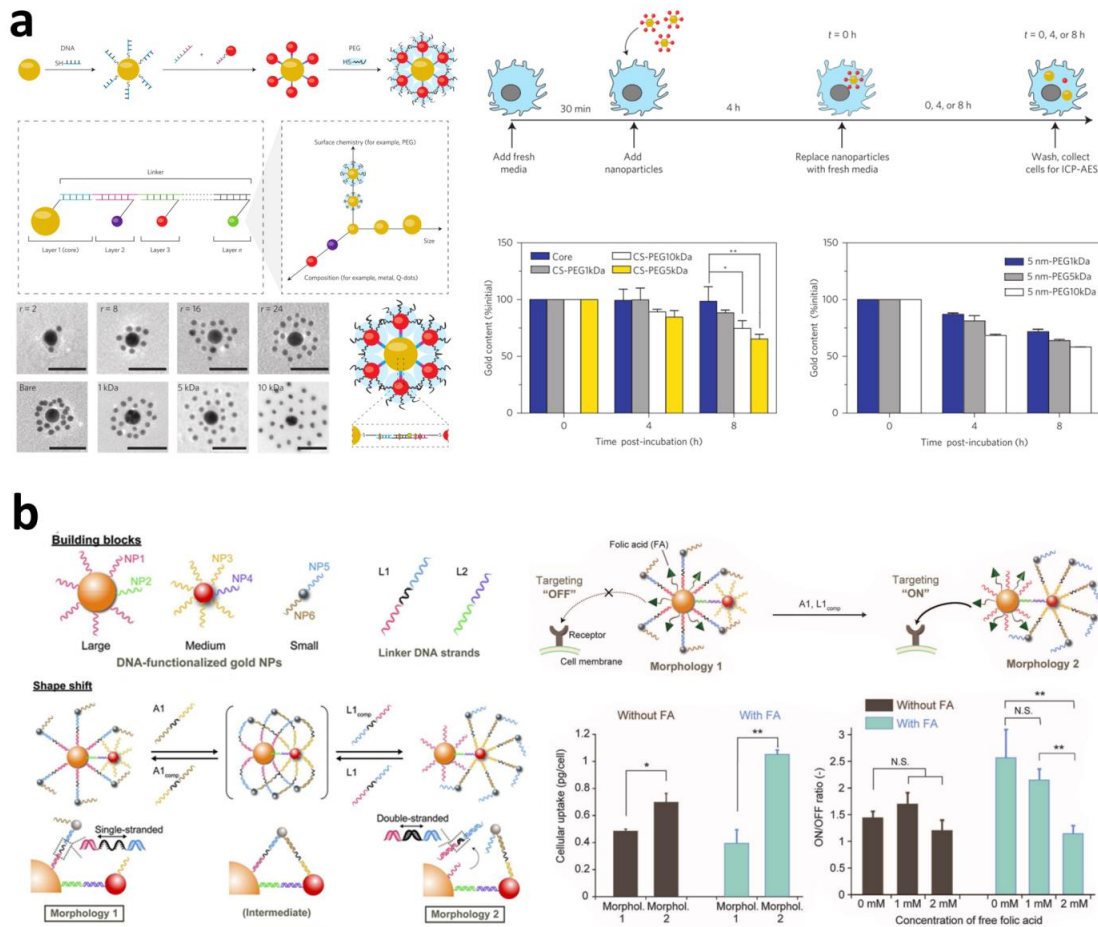


Figure 20. DNA assembly of nanoparticle superstructures. a) Schematic illustration of the design of “core-satellite” superstructures. Intracellular processing, renal elimination and tumor accumulation of superstructures, reprinted with permission from ref.[396], Copyright © 2014 Nature Publishing Group; b) The assembly of “core-satellite” superstructures mediated by DNA. Cellular uptake properties adjusted by the shape of the superstructure, reprinted with permission from ref.[397], Copyright © 2016 American Association for the Advancement of Science.

Except the investigation of bare AuNPs transportation profile based on this “core-satellite” platform, this superstructure was further functionalized into modular of drug-delivery system with few modifications and consist of three components: 1) AuNRs as central core, 2) DNA strands molecular linkers providing a natural capacity to associate with anti-cancer therapeutics DOX, and 3) peripheral gold spherical nanoparticles coating with PEG as navigators. It was showed that the DNA linker’s chemistry affected the loading capacity and DOX release rate and could be modulated using a photo-thermal core nanoparticle with specific DNA linker in this system.^[398]

Since the distance between core and satellite AuNP is adjustable by adding molecular stimuli (simple DNA strands),^[399] two-layer AuNP-DNA superstructures with same “core” loaded two types of cargos were made.^[400] Such system realized multistage cargo release with programmable degradation rates, because outer-layer structures prevented the serum factors responsible for assembly degradation from reaching the inner layer. In addition, the higher DNA density, shorter oligonucleotides, and thicker PEG layer on AuNPs the better the protection of DNA against serum degradation.^[400]

Through loading fluorescent dyes on DNA linker in this study, it is optimistic that such system can be transformed to multi-therapeutic delivery usages.

4. Conclusion and perspective

All living organisms preserve their genetic information in form of DNA. DNA structure was at first suggested by James Watson and Francis Crick as what is now accepted double-helix model more than six decades ago. In the 1980s, Seeman’s

pioneering work in the area of DNA nanotechnology assigned DNA as biomaterial usage. Since then, high self-recognition and programmability of DNA molecules were heavily investigated by creating considerable DNA nanostructures with pre-designed arrangement and DNA nanomachines with customized functionality. The report of DNA origami structure in 2006 by Rothemund proposed a new approach to fabricate self-assembled DNA nanostructures. Together with structural derivatives of DNA such as aptamer, hydrogel, tetrahedron, molecular beacon, nanoflow, nanotube, dendrimer, scaffold, device, hybrid even DNA-nanoparticle superstructures are reprehensive of DNA-based structures which are within our discussion in this review. Our review discussed the evolutionary trajectory of variety of the DNA-based nanostructures, and the structure based biomedical applications, including drug delivery, therapeutics, diagnosis, bio-imaging and bio-sensing.

In the area of drug delivery, current efforts on target delivery and sustained release formulations have been intensively exploited but still being pursued with more enthusiasms. The successful delivery of DNA-based structures into cells without visible toxicity paves the way to functionalized them as drug delivery vehicles and holds the promising desirability of overcoming the unfavorable merits of standard drug delivery materials, such as quality assurance of liposome^[401] and the incomplete and transient shielding effect of polyethylene glycol (PEG).^[402] Among all kinds of medications needed to be delivered through DNA related platform, cancer therapeutics are prioritized^[403] due to aggressive cancer lethality. And most of

therapeutics and chemo therapeutics in particular will indiscriminately suppress/kill all cells, which generally initiate the side effects.^[404] Furthermore, cancer development is stepwise and spatiotemporal dynamic, therefore multifunctional and programmable DNA based materials with controlled release of drug according to disease stages and location are highly demanded to minimize the side effects. Among versatile chemotherapeutics, DOX is considered as the most effective candidate against cancer but resistance to this agent is common.^[405] DOX is known to be fluorescent, which often been used to quantify its concentrations and track its pharmacokinetics trajectory through bio-imaging technology. The intercalation with DNA double helix supply DOX to perfect anchor through non-covalent π - π stacking interaction.^[406] Consequently, DOX became the perfect model drug for investigating the efficiency of different DNA-based delivery vehicles. As described above, multiple DNA-based materials in bulk scale, DNA origami, tetrahedron and hydrogel in particular have been successfully utilized for DOX and antisense delivery. To obtain controlled drug cargo release, liable linker has been introduced into the complex.^[407] Due to the excellent thermal transformation properties, gold nanomaterials was often incorporated with DNA-dominated vehicles to realized synergic treatments, such as NIR triggered drug release.

Beside serving as drug carrier, DNA tetrahedral nanostructures was also functionalized as bioprobe and made its dynamic range tunable by insertion of effector sequence.^[408] DNA aptamer derived aptasensors have been developed as a

class of agents for biomolecule detections due to their small size, and chemical stability over conventional biosensor such as antibody. Installment of aptamer in the vertex of tetrahedron realized fast and sensitive detection of multiple target molecules by just changing the molecular scavenger using only nano- to politer droplets.^[369] In addition, the programmability and multiplexed capability of other DNA nanostructures can be integrated with microfluidics, leading towards a miniaturized and high-throughput detection platform, such as a point-of-care diagnostic system.^[409] The robustness and addressability capability of DNA nanostructure favor their hybridization with gold nanoparticle to form superstructure for more advanced application. For instance, the nanopore hybrid DNA origami-Graphene actualized DNA Detection.^[410] Given the convenience in designing DNA nanostructures with different size, geometry, and functional groups, we speculate that self-assembled DNA-based material will be utilized for variety of application such as biosensor, diagnostics and theranostics.

Despite all the advantages, some obstacles need to be addressed. First of all, a better understanding of the pharmacokinetics of DNA nanostructures *in vivo* need to be developed, especially if competing with alternative delivery technologies based on liposomes, polymers, and others. Nuclease degradation is common to all DNA-based structures. In order to circumvent that, chemical modifications such as fluoro, amino, O-methyl base were commonly applied.^[411] Some DNA-based structures can resist nuclease action, but the circulation time of the objects need to be extended due to

renal filtration. This can be done by adjusting their modular properties or by conjugating bulky group such as cholesterol, protein, liposomes, organic or inorganic nanomaterials to DNA-based platforms. Additionally, potential immunostimulatory properties of DNA nanostructures should be taken into account as well. Finally, there has limited information about toxicity about these reagents. The negatively charged DNA based structures will intrinsically lead to nonspecific binding to protein in serum, which in most cases is unwanted. Lastly, arguably the relatively expensive synthesis of the starting materials especially when the building block nucleoside need to be modified to enable advanced applications. However, with rapid development of the entire research field and involvement of Contract Research Organization, it is undoubted that scaling-up of production and simultaneous knockdown of the price will occur. Thus, it is very likely that these challenges will be overcame in predictable future. Encouraged by the first approval of targeted anti-VEGF aptamer pegaptanib with brand name Macugen for ocular vascular disease,^[412] and clinical trial of bacterial virus Phi29 DNA-packaging nanomotor technique based biosensor which realize the detection and identification of trace target molecules under the atmosphere of high concentration impurities,^[413] we are optimistic that more DNA-based therapeutics will go to clinic trials, especially in the case of biosensors which have relative simpler processing steps to be approved by FDA comparing to classical medication.

Acknowledgements

We acknowledge financial support from the Academy of Finland (decision no. 297580), Jane and Aatos Erkko Foundation (grant no. 4704010), Sigrid Jusélius Foundation (decision no. 28001830K1), Social development of Jiangsu province (BE2015668), Shanghai Pujiang Talent Project (16PJ1402700), the National Science Foundation of China (Grants 21305151, and U1505243) and the China Postdoctoral Science Foundation (2015M581565, 2017T100283).

Received: ((will be filled in by the editorial staff))

Revised: ((will be filled in by the editorial staff))

Published online: ((will be filled in by the editorial staff))

References

- [1] a) J. Li, C. Fan, H. Pei, J. Shi, Q. Huang, *Adv. Mater.* **2013**, *25*, 4386; b) Z. G. Wang, B. Ding, *Adv. Mater.* **2013**, *25*, 3905.
- [2] a) V. Kumar, S. Palazzolo, S. Bayda, G. Corona, G. Toffoli, F. Rizzolio, *Theranostics* **2016**, *6*, 710; b) N. C. Seeman, *Mol. Biotechnol.* **2007**, *37*, 246; c) D. Yang, M. R. Hartman, T. L. Derrien, S. Hamada, D. An, K. G. Yancey, R. Cheng, M. Ma, D. Luo, *Acc. Chem. Res.* **2014**, *47*, 1902.
- [3] J. S. Kahn, Y. Hu, I. Willner, *Acc. Chem. Res.* **2017**, *50*, 680.
- [4] L. D. Hurst, A. R. Merchant, *Proc. Biol. Sci.* **2001**, *268*, 493.
- [5] C. Fonseca Guerra, F. M. Bickelhaupt, J. G. Snijders, E. J. Baerends, *J. Am. Chem. Soc.* **2000**, *122*, 4117.
- [6] Z. Wu, A. Ono, M. Kainosh, A. Bax, *J. Biomol. NMR* **2001**, *19*, 361.
- [7] E. D. Głowacki, M. Irimia-Vladu, S. Bauer, N. S. Sariciftci, *J. Mater. Chem. B* **2013**, *1*, 3742.
- [8] P. Yakovchuk, E. Protozanova, M. D. Frank-Kamenetskii, *Nucleic Acids Res.* **2006**, *34*, 564.
- [9] a) P. W. Rothemund, *Nature* **2006**, *440*, 297; b) F. Zhang, S. Jiang, S. Wu, Y. Li, C. Mao, Y. Liu, H. Yan, *Nat. Nanotechnol.* **2015**, *10*, 779.
- [10] J. D. C. Watson, F. H. C., *Nature* **1953**, *4356*, 77.
- [11] M. J. Campolongo, S. J. Tan, J. Xu, D. Luo, *Adv. Drug Delivery Rev.* **2010**, *62*, 606.
- [12] S. E. Halford, J. F. Marko, *Nucleic Acids Res.* **2004**, *32*, 3040.
- [13] B. R. Cairns, *Nature* **2009**, *461*, 193.
- [14] H. Masai, S. Matsumoto, Z. You, N. Yoshizawa-Sugata, M. Oda, *Annu. Rev. Biochem.* **2010**, *79*, 89.
- [15] W. L. Ward, K. Plakos, V. J. DeRose, *Chem. Rev.* **2014**, *114*, 4318.
- [16] M. H. Shamsi, H.-B. Kraatz, *J. Inorg. Organomet. Polym. Mater.* **2012**, *23*, 4.
- [17] X. Huang, M. A. El-Sayed, *J. Adv. Res.* **2010**, *1*, 13.
- [18] a) M. Cardenas, J. Barauskas, K. Schillen, J. L. Brennan, M. Brust, T. Nylander, *Langmuir* **2006**, *22*, 3294; b) Q. Wu, H. K. Kang, B. N. Oh, J. Kim, *J. Phys. Chem. C* **2012**, *116*, 8020.
- [19] A. G. Pershina, A. E. Sazonov, L. M. Ogorodova, *Bioorganicheskaiia khimiia* **2009**, *35*, 674.
- [20] a) J. C. Rohloff, A. D. Gelinas, T. C. Jarvis, U. A. Ochsner, D. J. Schneider, L. Gold, N. Janjic, *Mol Ther Nucleic Acids*. **2014**, *3*, e201; b) J. D. Vaught, C. Bock, J. Carter, T. Fitzwater, M. Otis, D. Schneider, J. Rolando, S. Waugh, S. K. Wilcox, B. E. Eaton, *J. Am. Chem. Soc.* **2010**, *132*, 4141.
- [21] D. M. Perrin, T. Garestier, C. Helene, *Nucleosides Nucleotides*. **1999**, *18*, 377.

- [22] L. Gold, D. Ayers, J. Bertino, C. Bock, A. Bock, E. N. Brody, J. Carter, A. B. Dalby, B. E. Eaton, T. Fitzwater, D. Flather, A. Forbes, T. Foreman, C. Fowler, B. Gawande, M. Goss, M. Gunn, S. Gupta, D. Halladay, J. Heil, J. Heilig, B. Hicke, G. Husar, N. Janjic, T. Jarvis, S. Jennings, E. Katilius, T. R. Keeney, N. Kim, T. H. Koch, S. Kraemer, L. Kroiss, N. Le, D. Levine, W. Lindsey, B. Lollo, W. Mayfield, M. Mehan, R. Mehler, S. K. Nelson, M. Nelson, D. Nieuwlandt, M. Nikrad, U. Ochsner, R. M. Ostroff, M. Otis, T. Parker, S. Pietrasiewicz, D. I. Resnicow, J. Rohloff, G. Sanders, S. Sattin, D. Schneider, B. Singer, M. Stanton, A. Sterkel, A. Stewart, S. Stratford, J. D. Vaught, M. Vrkjan, J. J. Walker, M. Watrobka, S. Waugh, A. Weiss, S. K. Wilcox, A. Wolfson, S. K. Wolk, C. Zhang, D. Zichi, *PloS one*. **2010**, 5, e15004.
- [23] B. N. Gawande, J. C. Rohloff, J. D. Carter, I. von Carlowitz, C. Zhang, D. J. Schneider, N. Janjic, *Proc. Natl. Acad. Sci. U. S. A.*, **2017**, 114, 2898.
- [24] I. Sacui, W. C. Hsieh, A. Manna, B. Sahu, D. H. Ly, *J. Am. Chem. Soc.* **2015**, 137, 8603.
- [25] S. Niewiadomski, Z. Beebejaun, H. Denton, T. K. Smith, R. J. Morris, G. K. Wagner, *Org. Biomol. Chem.* **2010**, 8, 3488.
- [26] A. Saha, S. Panda, S. Paul, D. Manna, *Chem. Commun.* **2016**, 52, 9438.
- [27] K. Sato, K. Seio, M. Sekine, *J. Am. Chem. Soc.* **2002**, 124, 12715.
- [28] Y. Zhang, A. Borrel, L. Ghemtio, L. Regad, G. Boije Af Gennas, A. C. Camproux, J. Yli-Kauhaluoma, H. Xhaard, *J. Chem. Inf. Model.* **2017**, 57, 499.
- [29] J. Li, L. Mo, C. H. Lu, T. Fu, H. H. Yang, W. Tan, *Chem. Soc. Rev.* **2016**, 45, 1410.
- [30] I. Jeddi, L. Saiz, *Sci. Rep.* **2017**, 7, 1178.
- [31] a) S. B. Dixit, D. L. Beveridge, *Bioinformatics*. **2006**, 22, 1007; b) X. J. Lu, W. K. Olson, *Nucleic Acids Res.* **2003**, 31, 5108.
- [32] J. N. Zadeh, B. R. Wolfe, N. A. Pierce, *J. Comput. Chem.* **2011**, 32, 439.
- [33] B. R. Wolfe, N. A. Pierce, *ACS Synth. Biol.* **2015**, 4, 1086.
- [34] B. R. Wolfe, N. J. Porubsky, J. N. Zadeh, R. M. Dirks, N. A. Pierce, *J. Am. Chem. Soc.* **2017**, 139, 3134.
- [35] R. M. Dirks, J. S. Bois, J. M. Schaeffer, E. Winfree, N. A. Pierce, *SIAM Review* **2007**, 49, 65.
- [36] A. D. Ellington, J. W. Szostak, *Nature* **1992**, 355, 850.
- [37] R. P. Goodman, I. A. Schaap, C. F. Tardin, C. M. Erben, R. M. Berry, C. F. Schmidt, A. J. Turberfield, *Science* **2005**, 310, 1661.
- [38] S. H. Um, J. B. Lee, N. Park, S. Y. Kwon, C. C. Umbach, D. Luo, *Nat. Mater.* **2006**, 5, 797.
- [39] E. S. Andersen, M. Dong, M. M. Nielsen, K. Jahn, R. Subramani, W. Mamdouh, M. M. Golas, B. Sander, H. Stark, C. L. Oliveira, J. S. Pedersen, V. Birkedal, F. Besenbacher, K. V. Gothelf, J. Kjems, *Nature* **2009**, 459, 73.
- [40] J. Mikkila, A. P. Eskelinen, E. H. Niemela, V. Linko, M. J. Frilander, P. Torma, M. A. Kostiainen, *Nano. Lett.* **2014**, 14, 2196.

- [41] N. Chen, S. Qin, X. Yang, Q. Wang, J. Huang, K. Wang, *ACS Appl. Mater. Interfaces* **2016**, *8*, 26552.
- [42] H. Pei, N. Lu, Y. Wen, S. Song, Y. Liu, H. Yan, C. Fan, *Adv. Mater.* **2010**, *22*, 4754.
- [43] S. I. Stupp, *Nano Lett.* **2010**, *10*, 4783.
- [44] C. Lin, Y. Liu, H. Yan, *Biochemistry* **2009**, *48*, 1663.
- [45] N. C. Seeman, *Annu. Rev. Biochem.* **2010**, *79*, 65.
- [46] M. Kircher, J. Kelso, *Bioessays* **2010**, *32*, 524.
- [47] S. M. Douglas, H. Dietz, T. Liedl, B. Hogberg, F. Graf, W. M. Shih, *Nature* **2009**, *459*, 414.
- [48] N. C. Seeman, *J. Theor. Biol.* **1982**, *99*, 237.
- [49] J. H. Chen, N. C. Seeman, *Nature* **1991**, *350*, 631.
- [50] S. Tyagi, F. R. Kramer, *Nat. Biotechnol.* **1996**, *14*, 303.
- [51] C. Mao, W. Sun, N. C. Seeman, *J. Am. Chem. Soc.* **1999**, *121*, 5437.
- [52] C. Mao, W. Sun, Z. Shen, N. C. Seeman, *Nature* **1999**, *397*, 144.
- [53] Y. Li, Y. D. Tseng, S. Y. Kwon, L. D'Espaux, J. S. Bunch, P. L. McEuen, D. Luo, *Nat. Mater.* **2004**, *3*, 38.
- [54] M. M. Maye, M. T. Kumara, D. Nykypanchuk, W. B. Sherman, O. Gang, *Nat. Nanotechnol.* **2010**, *5*, 116.
- [55] J. Li, H. Pei, B. Zhu, L. Liang, M. Wei, Y. He, N. Chen, D. Li, Q. Huang, C. Fan, *ACS Nano* **2011**, *5*, 8783.
- [56] H. Pei, F. Li, Y. Wan, M. Wei, H. Liu, Y. Su, N. Chen, Q. Huang, C. Fan, *J. Am. Chem. Soc.* **2012**, *134*, 11876.
- [57] S. D. Perrault, W. M. Shih, *ACS Nano* **2014**, *8*, 5132.
- [58] G. Zhu, J. Zheng, E. Song, M. Donovan, K. Zhang, C. Liu, W. Tan, *Proc. Natl. Acad. Sci. U. S. A.*, **2013**, *110*, 7998.
- [59] T. J. Fu, Y. C. Tse-Dinh, N. C. Seeman, *J. Mol. Biol.* **1994**, *236*, 91.
- [60] N. R. Kallenbach, R.-I. Ma, N. C. Seeman, *Nature* **1983**, *305*, 829.
- [61] R. I. Ma, N. R. Kallenbach, R. D. Sheardy, M. L. Petrillo, N. C. Seeman, *Nucleic Acids Res.* **1986**, *14*, 9745.
- [62] X. Wang, N. C. Seeman, *J. Am. Chem. Soc.* **2007**, *129*, 8169.
- [63] D. Liu, M. Wang, Z. Deng, R. Walulu, C. Mao, *J. Am. Chem. Soc.* **2004**, *126*, 2324.
- [64] T. J. Fu, N. C. Seeman, *Biochemistry* **1993**, *32*, 3211.
- [65] Y. Zhang, N. C. Seeman, *J. Am. Chem. Soc.* **1994**, *116*, 1661.
- [66] X. Zhang, H. Yan, Z. Shen, N. C. Seeman, *J. Am. Chem. Soc.* **2002**, *124*, 12940.
- [67] W. M. Shih, J. D. Quispe, G. F. Joyce, *Nature* **2004**, *427*, 618.
- [68] P. J. Paukstelis, J. Nowakowski, J. J. Birktoft, N. C. Seeman, *Chem Biol.* **2004**, *11*, 1119.

- [69] J. Zheng, J. J. Birktoft, Y. Chen, T. Wang, R. Sha, P. E. Constantinou, S. L. Ginell, C. Mao, N. C. Seeman, *Nature* **2009**, *461*, 74.
- [70] A. Kuzuya, R. Wang, R. Sha, N. C. Seeman, *Nano Lett.* **2007**, *7*, 1757.
- [71] E. Winfree, F. Liu, L. A. Wenzler, N. C. Seeman, *Nature* **1998**, *394*, 539.
- [72] J. Zheng, P. E. Constantinou, C. Micheel, A. P. Alivisatos, R. A. Kiehl, N. C. Seeman, *Nano Lett.* **2006**, *6*, 1502.
- [73] S. H. Park, P. Yin, Y. Liu, J. H. Reif, T. H. LaBean, H. Yan, *Nano Lett.* **2005**, *5*, 729.
- [74] R. P. Goodman, R. M. Berry, A. J. Turberfield, *Chem Commun* **2004**, 1372.
- [75] S. Rinker, Y. Liu, H. Yan, *Chem. Commun.* **2006**, 2675.
- [76] T. H. LaBean, H. Yan, J. Kopatsch, F. Liu, E. Winfree, J. H. Reif, N. C. Seeman, *J. Am. Chem. Soc.* **2000**, *122*, 1848.
- [77] D. Liu, S. H. Park, J. H. Reif, T. H. LaBean, *Proc. Natl. Acad. Sci. U. S. A.*, **2004**, *101*, 717.
- [78] Z. Shen, H. Yan, T. Wang, N. C. Seeman, *J. Am. Chem. Soc.* **2004**, *126*, 1666.
- [79] a) N. Chelyapov, Y. Brun, M. Gopalkrishnan, D. Reishus, B. Shaw, L. Adleman, *J. Am. Chem. Soc.* **2004**, *126*, 13924; b) B. Ding, R. Sha, N. C. Seeman, *J. Am. Chem. Soc.* **2004**, *126*, 10230.
- [80] Y. He, Y. Chen, H. Liu, A. E. Ribbe, C. Mao, *J. Am. Chem. Soc.* **2005**, *127*, 12202.
- [81] Y. He, Y. Tian, A. E. Ribbe, C. Mao, *J. Am. Chem. Soc.* **2006**, *128*, 15978.
- [82] J. Song, Z. Li, P. Wang, T. Meyer, C. Mao, Y. Ke, *Science* **2017**, 357.
- [83] H. Yan, S. H. Park, G. Finkelstein, J. H. Reif, T. H. LaBean, *Science* **2003**, *301*, 1882.
- [84] Y. He, Y. Tian, Y. Chen, Z. Deng, A. E. Ribbe, C. Mao, *Angew. Chem., Int. Ed.* **2005**, *44*, 6694.
- [85] a) C. M. Erben, R. P. Goodman, A. J. Turberfield, *J. Am. Chem. Soc.* **2007**, *129*, 6992; b) C. Zhang, M. Su, Y. He, Y. Leng, A. E. Ribbe, G. Wang, W. Jiang, C. Mao, *Chem. Commun.* **2010**, *46*, 6792.
- [86] F. F. Andersen, B. Knudsen, C. L. Oliveira, R. F. Frohlich, D. Kruger, J. Bungert, M. Agbandje-McKenna, R. McKenna, S. Juul, C. Veigaard, J. Koch, J. L. Rubinstein, B. Guldbrandtsen, M. S. Hede, G. Karlsson, A. H. Andersen, J. S. Pedersen, B. R. Knudsen, *Nucleic Acids Res.* **2008**, *36*, 1113.
- [87] F. A. Aldaye, H. F. Sleiman, *J. Am. Chem. Soc.* **2007**, *129*, 13376.
- [88] Y. He, M. Su, P. A. Fang, C. Zhang, A. E. Ribbe, W. Jiang, C. Mao, *Angew. Chem., Int. Ed.* **2010**, *49*, 748.
- [89] C. Zhang, M. Su, Y. He, X. Zhao, P. A. Fang, A. E. Ribbe, W. Jiang, C. Mao, *Proc. Natl. Acad. Sci. U. S. A.*, **2008**, *105*, 10665.
- [90] P. Yin, R. F. Hariadi, S. Sahu, H. M. Choi, S. H. Park, T. H. LaBean, J. H. Reif, *Science* **2008**, *321*, 824.

- [91] Z. Jin, W. Sun, Y. Ke, C. J. Shih, G. L. Paulus, Q. Hua Wang, B. Mu, P. Yin, M. S. Strano, *Nat. Commun.* **2013**, *4*, 1663.
- [92] Y. Ke, L. L. Ong, W. M. Shih, P. Yin, *Science* **2012**, *338*, 1177.
- [93] J. R. Burns, E. Stulz, S. Howorka, *Nano Lett.* **2013**, *13*, 2351.
- [94] Y. Ke, L. L. Ong, W. Sun, J. Song, M. Dong, W. M. Shih, P. Yin, *Nat. Chem.* **2014**, *6*, 994.
- [95] A. D. Ellington, J. W. Szostak, *Nature* **1990**, *346*, 818.
- [96] D. L. Robertson, G. F. Joyce, *Nature* **1990**, *344*, 467.
- [97] M. Cho, S. Soo Oh, J. Nie, R. Stewart, M. Eisenstein, J. Chambers, J. D. Marth, F. Walker, J. A. Thomson, H. T. Soh, *Proc. Natl. Acad. Sci. U. S. A.*, **2013**, *110*, 18460.
- [98] A. D. Keefe, S. Pai, A. Ellington, *Nat. Rev. Drug Discovery* **2010**, *9*, 537.
- [99] C. Tuerk, L. Gold, *Science* **1990**, *249*, 505.
- [100] Q. Yuan, D. Lu, X. Zhang, Z. Chen, W. Tan, *TrAC, Trends Anal. Chem.* **2012**, *39*, 72.
- [101] T. H. Ku, T. Zhang, H. Luo, T. M. Yen, P. W. Chen, Y. Han, Y. H. Lo, *Sensors (Basel, Switzerland)* **2015**, *15*, 16281.
- [102] A. Ruscito, M. C. DeRosa, *Front Chem.* **2016**, *4*, 14.
- [103] P. S. Pendergrast, H. N. Marsh, D. Grate, J. M. Healy, M. Stanton, *J. Biomol. Tech.* **2005**, *16*, 224.
- [104] J. Zhou, J. Rossi, *Nat. Rev. Drug Discovery* **2017**, *16*, 181.
- [105] X. Wu, J. Chen, M. Wu, J. X. Zhao, *Theranostics* **2015**, *5*, 322.
- [106] G. Zhu, S. Cansiz, M. You, L. Qiu, D. Han, L. Zhang, L. Mei, T. Fu, Z. Chen, W. Tan, *NPG Asia Mater.* **2015**, *7*, e169.
- [107] V. C. Ozalp, F. Eyidogan, H. A. Oktem, *Pharmaceuticals* **2011**, *4*, 1137.
- [108] Z. Cao, R. Tong, A. Mishra, W. Xu, G. C. Wong, J. Cheng, Y. Lu, *Angew. Chem., Int. Ed.* **2009**, *48*, 6494.
- [109] Y. Wu, K. Sefah, H. Liu, R. Wang, W. Tan, *Proc. Natl. Acad. Sci. U. S. A.*, **2010**, *107*, 5.
- [110] Y. Wang, Z. Li, D. Hu, C. T. Lin, J. Li, Y. Lin, *J. Am. Chem. Soc.* **2010**, *132*, 9274.
- [111] M. Chang, C. S. Yang, D. M. Huang, *ACS Nano* **2011**, *5*, 6156.
- [112] Z. Xiao, O. C. Farokhzad, *ACS Nano* **2012**, *6*, 3670.
- [113] E. Climent, R. Martinez-Manez, F. Sancenon, M. D. Marcos, J. Soto, A. Maquieira, P. Amoros, *Angew. Chem., Int. Ed.* **2010**, *49*, 7281.
- [114] Z. Li, Z. Liu, M. Yin, X. Yang, Q. Yuan, J. Ren, X. Qu, *Biomacromolecules* **2012**, *13*, 4257.
- [115] H. A. Alhadrami, R. Chinnappan, S. Eissa, A. A. Rahamn, M. Zourob, *Anal. Biochem.* **2017**, *525*, 78.

- [116] M. Jafari, M. Rezaei, H. Kalantari, M. Tabarzad, B. Daraei, *Biotechnol. Appl. Biochem.* **2017**.
- [117] J. Kosman, B. Juskowiak, *Anal. Chim. Acta* **2011**, 707, 7.
- [118] J. Fu, M. Liu, Y. Liu, H. Yan, *Acc. Chem. Res.* **2012**, 45, 1215.
- [119] C. J. Kearney, C. R. Lucas, F. J. O'Brien, C. E. Castro, *Adv. Mater.* **2016**, 28, 5509.
- [120] S. M. Douglas, A. H. Marblestone, S. Teerapittayanon, A. Vazquez, G. M. Church, W. M. Shih, *Nucleic Acids Res.* **2009**, 37, 5001.
- [121] Z. Li, M. Liu, L. Wang, J. Nangreave, H. Yan, Y. Liu, *J. Am. Chem. Soc.* **2010**, 132, 13545.
- [122] A. Rajendran, M. Endo, Y. Katsuda, K. Hidaka, H. Sugiyama, *ACS Nano* **2011**, 5, 665.
- [123] M. Endo, T. Sugita, A. Rajendran, Y. Katsuda, T. Emura, K. Hidaka, H. Sugiyama, *Chem. Commun.* **2011**, 47, 3213.
- [124] J. Song, J. M. Arbona, Z. Zhang, L. Liu, E. Xie, J. Elezgaray, J. P. Aime, K. V. Gothelf, F. Besenbacher, M. Dong, *J. Am. Chem. Soc.* **2012**, 134, 9844.
- [125] J. Song, Z. Zhang, S. Zhang, L. Liu, Q. Li, E. Xie, K. V. Gothelf, F. Besenbacher, M. Dong, *Small* **2013**, 9, 2954.
- [126] Z. Zhang, J. Song, F. Besenbacher, M. Dong, K. V. Gothelf, *Angew. Chem., Int. Ed.* **2013**, 52, 9219.
- [127] M. Tintore, R. Eritja, C. Fabrega, *ChemBioChem* **2014**, 15, 1374.
- [128] A. Kuzuya, M. Komiyama, *Chem. Commun.* **2009**, 4182.
- [129] Y. Ke, J. Sharma, M. Liu, K. Jahn, Y. Liu, H. Yan, *Nano Lett.* **2009**, 9, 2445.
- [130] S. M. Douglas, J. J. Chou, W. M. Shih, *Proc. Natl. Acad. Sci. U. S. A.* **2007**, 104, 6644.
- [131] Y. Ke, S. M. Douglas, M. Liu, J. Sharma, A. Cheng, A. Leung, Y. Liu, W. M. Shih, H. Yan, *J. Am. Chem. Soc.* **2009**, 131, 15903.
- [132] T. Liedl, B. Hogberg, J. Tytell, D. E. Ingber, W. M. Shih, *Nat. Nanotechnol.* **2010**, 5, 520.
- [133] H. Dietz, S. M. Douglas, W. M. Shih, *Science* **2009**, 325, 725.
- [134] P. Wang, S. Gaitanaros, S. Lee, M. Bathe, W. M. Shih, Y. Ke, *J. Am. Chem. Soc.* **2016**, 138, 7733.
- [135] M. J. Urban, P. K. Dutta, P. Wang, X. Duan, X. Shen, B. Ding, Y. Ke, N. Liu, *J. Am. Chem. Soc.* **2016**, 138, 5495.
- [136] Y. Ke, T. Meyer, W. M. Shih, G. Bellot, *Nat. Commun.* **2016**, 7, 10935.
- [137] C. Shen, X. Lan, X. Lu, T. A. Meyer, W. Ni, Y. Ke, Q. Wang, *J. Am. Chem. Soc.* **2016**, 138, 1764.
- [138] Y. Tian, T. Wang, W. Liu, H. L. Xin, H. Li, Y. Ke, W. M. Shih, O. Gang, *Nat. Nanotechnol.* **2015**, 10, 637.
- [139] D. Han, S. Pal, J. Nangreave, Z. Deng, Y. Liu, H. Yan, *Science* **2011**, 332, 342.

- [140] D. Han, S. Pal, Y. Liu, H. Yan, *Nat. Nanotechnol.* **2010**, *5*, 712.
- [141] a) R. D. Barish, R. Schulman, P. W. Rothemund, E. Winfree, *Proc. Natl. Acad. Sci. U. S. A.*, **2009**, *106*, 6054; b) K. Fujibayashi, R. Hariadi, S. H. Park, E. Winfree, S. Murata, *Nano Lett.* **2008**, *8*, 1791.
- [142] W. Liu, H. Zhong, R. Wang, N. C. Seeman, *Angew. Chem., Int. Ed.* **2011**, *50*, 264.
- [143] Z. Zhao, H. Yan, Y. Liu, *Angew. Chem., Int. Ed.* **2010**, *49*, 1414.
- [144] E. Pound, J. R. Ashton, H. A. Becerril, A. T. Woolley, *Nano Lett.* **2009**, *9*, 4302.
- [145] B. Hogberg, T. Liedl, W. M. Shih, *J. Am. Chem. Soc.* **2009**, *131*, 9154.
- [146] a) E. S. Andersen, M. Dong, M. M. Nielsen, K. Jahn, A. Lind-Thomsen, W. Mamdouh, K. V. Gothelf, F. Besenbacher, J. Kjems, *ACS Nano* **2008**, *2*, 1213; b) E. S. Andersen, A. Lind-Thomsen, B. Knudsen, S. E. Kristensen, J. H. Havgaard, E. Torarinsson, N. Larsen, C. Zwieb, P. Sestoft, J. Kjems, J. Gorodkin, *RNA* **2007**, *13*, 1850.
- [147] C. E. Castro, F. Kilchherr, D. N. Kim, E. L. Shiao, T. Wauer, P. Wortmann, M. Bathe, H. Dietz, *Nat Methods* **2011**, *8*, 221.
- [148] Veneziano, Rémi, Ratanalert, Sakul, Zhang, Kaiming, Zhang, Fei, Yan, Hao, Chiu, Wah, M. Bathe, *Science* **2016**.
- [149] X. Liu, C. H. Lu, I. Willner, *Acc. Chem. Res.* **2014**, *47*, 1673.
- [150] H. Pei, L. Liang, G. Yao, J. Li, Q. Huang, C. Fan, *Angew. Chem., Int. Ed.* **2012**, *51*, 9020.
- [151] X. Ma, A. C. Hortelao, T. Patino, S. Sanchez, *ACS Nano* **2016**, *10*, 9111.
- [152] F. C. Simmel, B. Yurke, *Phys. Rev. E: Stat., Nonlinear, Soft Matter Phys.* **2001**, *63*, 041913.
- [153] Y. Krishnan, F. C. Simmel, *Angew. Chem., Int. Ed.* **2011**, *50*, 3124.
- [154] W. U. Dittmer, F. C. Simmel, *Nano Lett.* **2004**, *4*, 689.
- [155] M. Marini, L. Piantanida, R. Musetti, A. Bek, M. Dong, F. Besenbacher, M. Lazzarino, G. Firrao, *Nano Lett.* **2011**, *11*, 5449.
- [156] H. Yan, X. Zhang, Z. Shen, N. C. Seeman, *Nature* **2002**, *415*, 62.
- [157] B. Chakraborty, R. Sha, N. C. Seeman, *Proc. Natl. Acad. Sci. U. S. A.*, **2008**, *105*, 17245.
- [158] C. Liu, N. Jonoska, N. C. Seeman, *Nano Lett.* **2009**, *9*, 2641.
- [159] B. Ding, N. C. Seeman, *Science* **2006**, *314*, 1583.
- [160] X. Qu, D. Zhu, G. Yao, S. Su, J. Chao, H. Liu, X. Zuo, L. Wang, J. Shi, L. Wang, W. Huang, H. Pei, C. Fan, *Angew. Chem., Int. Ed.* **2017**, *56*, 1855.
- [161] X.R. Wu, C.W. Wu, C. Zhang, *Chin. J. Polym. Sci.* **2016**, *35*, 1.
- [162] R. Chhabra, J. Sharma, Y. Liu, S. Rinker, H. Yan, *Adv. Drug Delivery Rev.* **2010**, *62*, 617.
- [163] Y. He, Y. Tian, A. E. Ribbe, C. Mao, *J. Am. Chem. Soc.* **2006**, *128*, 12664.

- [164] B. A. Williams, K. Lund, Y. Liu, H. Yan, J. C. Chaput, *Angew. Chem., Int. Ed.* **2007**, *46*, 3051.
- [165] a) M. Homann, H. U. Goringer, *Nucleic Acids Res.* **1999**, *27*, 2006; b) D. S. Wilson, J. W. Szostak, *Annu. Rev. Biochem.* **1999**, *68*, 611.
- [166] a) H. Li, J. D. Carter, T. H. LaBean, *Mater. Today* **2009**, *12*, 24; b) Y. Liu, C. Lin, H. Li, H. Yan, *Angew. Chem., Int. Ed.* **2005**, *44*, 4333.
- [167] R. Chhabra, J. Sharma, Y. Ke, Y. Liu, S. Rinker, S. Lindsay, H. Yan, *J. Am. Chem. Soc.* **2007**, *129*, 10304.
- [168] C. A. Mirkin, R. L. Letsinger, R. C. Mucic, J. J. Storhoff, *Nature* **1996**, *382*, 607.
- [169] a) R. J. Macfarlane, B. Lee, M. R. Jones, N. Harris, G. C. Schatz, C. A. Mirkin, *Science* **2011**, *334*, 204; b) D. Nykypanchuk, M. M. Maye, D. van der Lelie, O. Gang, *Nature* **2008**, *451*, 549.
- [170] J. I. Cutler, E. Auyeung, C. A. Mirkin, *J. Am. Chem. Soc.* **2012**, *134*, 1376.
- [171] a) J. Dobson, *Gene therapy* **2006**, *13*, 283; b) N. L. Rosi, D. A. Giljohann, C. S. Thaxton, A. K. Lytton-Jean, M. S. Han, C. A. Mirkin, *Science* **2006**, *312*, 1027; c) D. S. Seferos, D. A. Giljohann, H. D. Hill, A. E. Prigodich, C. A. Mirkin, *J. Am. Chem. Soc.* **2007**, *129*, 15477.
- [172] C. Fan, K. W. Plaxco, A. J. Heeger, *Proc. Natl. Acad. Sci. U. S. A.*, **2003**, *100*, 9134.
- [173] P. Zhan, P. K. Dutta, P. Wang, G. Song, M. Dai, S. X. Zhao, Z. G. Wang, P. Yin, W. Zhang, B. Ding, Y. Ke, *ACS Nano* **2017**, *11*, 1172.
- [174] A. S. Walsh, H. Yin, C. M. Erben, M. J. Wood, A. J. Turberfield, *ACS Nano* **2011**, *5*, 5427.
- [175] X. Qu, F. Yang, H. Chen, J. Li, H. Zhang, G. Zhang, L. Li, L. Wang, S. Song, Y. Tian, H. Pei, *ACS Appl. Mater. Interfaces* **2017**, *9*, 16026.
- [176] A. R. Chandrasekaran, *J. Chem. Technol. Biotechnol.* **2016**, *91*, 843.
- [177] J. Zheng, R. Yang, M. Shi, C. Wu, X. Fang, Y. Li, J. Li, W. Tan, *Chem. Soc. Rev.* **2015**, *44*, 3036.
- [178] R. Hu, X. Zhang, Z. Zhao, G. Zhu, T. Chen, T. Fu, W. Tan, *Angew. Chem., Int. Ed.* **2014**, *53*, 5821.
- [179] J. F. Rahbani, A. A. Hariri, G. Cosa, H. F. Sleiman, *ACS Nano* **2015**, *9*, 11898.
- [180] a) H. M. Meng, X. Zhang, Y. Lv, Z. Zhao, N. N. Wang, T. Fu, H. Fan, H. Liang, L. Qiu, G. Zhu, W. Tan, *ACS Nano* **2014**, *8*, 6171; b) K. Mohri, E. Kusuki, S. Ohtsuki, N. Takahashi, M. Endo, K. Hidaka, H. Sugiyama, Y. Takahashi, Y. Takakura, M. Nishikawa, *Biomacromolecules* **2015**, *16*, 1095.
- [181] J. R. Burns, K. Gopfrich, J. W. Wood, V. V. Thacker, E. Stulz, U. F. Keyser, S. Howorka, *Angew. Chem., Int. Ed.* **2013**, *52*, 12069.
- [182] A. Stornetta, M. Zimmermann, G. D. Cimino, P. T. Henderson, S. J. Sturla, *Chem. Res. Toxicol.* **2017**, *30*, 388.

- [183] R. M. Elder, A. Jayaraman, *Biophys J.* **2012**, *102*, 2331.
- [184] C. H. Stuart, D. A. Horita, M. J. Thomas, F. R. Salsbury, Jr., M. O. Lively, W. H. Gmeiner, *Bioconjugate Chem.* **2014**, *25*, 406.
- [185] a) S. Eissa, M. Zourob, *Sci. Rep.* **2017**, *7*, 1016; b) J. J. Trausch, M. Shank-Retzlaff, T. Verch, *Vaccine* **2017**.
- [186] M. Godonoga, T. Y. Lin, A. Oshima, K. Sumitomo, M. S. Tang, Y. W. Cheung, A. B. Kinghorn, R. M. Dirkzwager, C. Zhou, A. Kuzuya, J. A. Tanner, J. G. Heddle, *Sci. Rep.* **2016**, *6*, 21266.
- [187] X. Yang, N. Li, D. G. Gorenstein, *Expert Opin. Drug Discovery* **2011**, *6*, 75.
- [188] P. Zhang, F. Cheng, R. Zhou, J. Cao, J. Li, C. Burda, Q. Min, J.-J. Zhu, *Angew. Chem., Int. Ed.* **2014**, *126*, 2403.
- [189] a) A. V. Lakhin, V. Z. Tarantul, L. V. Gening, *Acta naturae* **2013**, *5*, 34; b) W. Niu, X. Chen, W. Tan, A. S. Veige, *Angew. Chem., Int. Ed.* **2016**, *55*, 8889.
- [190] a) L. L. Li, M. Xie, J. Wang, X. Li, C. Wang, Q. Yuan, D. W. Pang, Y. Lu, W. Tan, *Chem. Commun.* **2013**, *49*, 5823; b) C. Wu, D. Han, T. Chen, L. Peng, G. Zhu, M. You, L. Qiu, K. Sefah, X. Zhang, W. Tan, *J. Am. Chem. Soc.* **2013**, *135*, 18644; c) C. Zhang, X. Ji, Y. Zhang, G. Zhou, X. Ke, H. Wang, P. Tinnefeld, Z. He, *Anal. Chem.* **2013**, *85*, 5843; d) Y. Zhang, Z. Hou, Y. Ge, K. Deng, B. Liu, X. Li, Q. Li, Z. Cheng, P. Ma, C. Li, J. Lin, *ACS Appl. Mater. Interfaces* **2015**, *7*, 20696.
- [191] S. Taghavi, M. Ramezani, M. Alibolandi, K. Abnous, S. M. Taghdisi, *Cancer Lett.* **2017**, *400*, 1.
- [192] V. Bagalkot, O. C. Farokhzad, R. Langer, S. Jon, *Angew. Chem., Int. Ed.* **2006**, *45*, 8149.
- [193] Y. F. Huang, D. Shangguan, H. Liu, J. A. Phillips, X. Zhang, Y. Chen, W. Tan, *Chembiochem* **2009**, *10*, 862.
- [194] R. Wang, G. Zhu, L. Mei, Y. Xie, H. Ma, M. Ye, F.-L. Qing, W. Tan, *J. Am. Chem. Soc.* **2014**, *136*, 2731.
- [195] G. Zhu, G. Niu, X. Chen, *Bioconjugate Chem.* **2015**, *26*, 2186.
- [196] C. Perez-Arnaiz, N. Bustos, J. M. Leal, B. Garcia, *J. Phys. Chem. B* **2014**, *118*, 1288.
- [197] D. Shangguan, Z. Cao, L. Meng, P. Mallikaratchy, K. Sefah, H. Wang, Y. Li, W. Tan, *J. Proteome Res.* **2008**, *7*, 2133.
- [198] Z. Xiao, D. Shangguan, Z. Cao, X. Fang, W. Tan, *Chem.* **2008**, *14*, 1769.
- [199] S. Yoon, K.-W. Huang, V. Reebye, P. Mintz, Y.-W. Tien, H.-S. Lai, P. Sætrom, I. Reccia, P. Swiderski, B. Armstrong, A. Jozwiak, D. Spalding, L. Jiao, N. Habib, J. J. Rossi, *Mol. Ther.*, **24**, 1106.
- [200] S. Yoon, K.-W. Huang, V. Reebye, D. Spalding, T. M. Przytycka, Y. Wang, P. Swiderski, L. Li, B. Armstrong, I. Reccia, D. Zacharoulis, K. Dimas, T. Kusano, J. Shively, N. Habib, J. J. Rossi, *Mol. Ther.--Nucleic Acids*, **6**, 80.
- [201] D. Shangguan, Z. Cao, L. Meng, P. Mallikaratchy, K. Sefah, H. Wang, Y. Li, W. Tan, *J Proteome Res* **2008**, *7*, 2133.

- [202] Y. Kato, S. Ozawa, C. Miyamoto, Y. Maehata, A. Suzuki, T. Maeda, Y. Baba, *Cancer Cell Int.* **2013**, *13*, 89.
- [203] K. Ji, C. Lee, B. G. Janesko, E. E. Simanek, *Mol. Pharm.* **2015**, *12*, 2924.
- [204] R. Deng, H. Qu, L. Liang, J. Zhang, B. Zhang, D. Huang, S. Xu, C. Liang, W. Xu, *Anal. Chem.* **2017**, *89*, 2844.
- [205] F. Huang, M. You, T. Chen, G. Zhu, H. Liang, W. Tan, *Chem. Commun.* **2014**, *50*, 3103.
- [206] S. Xu, W. Wang, X. Li, J. Liu, A. Dong, L. Deng, *Eur. J. Pharm. Sci.* **2014**, *62*, 267.
- [207] I. A. N. J. MACDONALD, T. J. DOUGHERTY, *J. Porphyrins Phthalocyanines* **2001**, *05*, 105.
- [208] D. E. J. G. J. Dolmans, D. Fukumura, R. K. Jain, *Nat. Rev. Cancer* **2003**, *3*, 380.
- [209] J. Tu, T. Wang, W. Shi, G. Wu, X. Tian, Y. Wang, D. Ge, L. Ren, *Biomaterials* **2012**, *33*, 7903.
- [210] Z. Zhu, Z. Tang, J. A. Phillips, R. Yang, H. Wang, W. Tan, *J. Am. Chem. Soc.* **2008**, *130*, 10856.
- [211] K. Wang, M. You, Y. Chen, D. Han, Z. Zhu, J. Huang, K. Williams, C. J. Yang, W. Tan, *Angew. Chem. Int. Ed. Engl.* **2011**, *50*, 6098.
- [212] Q. Yuan, Y. Wu, J. Wang, D. Lu, Z. Zhao, T. Liu, X. Zhang, W. Tan, *Angew. Chem. Int. Ed. Engl.* **2013**, *52*, 13965.
- [213] J. Wang, G. Zhu, M. You, E. Song, M. I. Shukoor, K. Zhang, M. B. Altman, Y. Chen, Z. Zhu, C. Z. Huang, W. Tan, *ACS Nano* **2012**, *6*, 5070.
- [214] J. L. Hickey, R. A. Ruhayel, P. J. Barnard, M. V. Baker, S. J. Berners-Price, A. Filipovska, *J. Am. Chem. Soc.* **2008**, *130*, 12570.
- [215] J. E. Rosenberg, R. M. Bambury, E. M. Van Allen, H. A. Drabkin, P. N. Lara, Jr., A. L. Harzstark, N. Wagle, R. A. Figlin, G. W. Smith, L. A. Garraway, T. Choueiri, F. Erlandsson, D. A. Laber, *Investigational new drugs* **2014**, *32*, 178.
- [216] F. Zhang, A. Correia, E. Makila, W. Li, J. Salonen, J. J. Hirvonen, H. Zhang, H. A. Santos, *ACS Appl. Mater. Interfaces* **2017**, *9*, 10034.
- [217] a) M. A. Shahbazi, B. Herranz, H. A. Santos, *Biomatter* **2012**, *2*, 296; b) J. Tu, A. L. Boyle, H. Friedrich, P. H. Bomans, J. Bussmann, N. A. Sommerdijk, W. Jiskoot, A. Kros, *ACS Appl. Mater. Interfaces* **2016**, *8*, 32211; c) J. Tu, G. Du, M. Reza Nejadnik, J. Monkare, K. van der Maaden, P. H. H. Bomans, N. Sommerdijk, B. Slutter, W. Jiskoot, J. A. Bouwstra, A. Kros, *Pharm. Res.* **2017**; d) H. Zhang, D. Liu, M. A. Shahbazi, E. Makila, B. Herranz-Blanco, J. Salonen, J. Hirvonen, H. A. Santos, *Adv. Mater.* **2014**, *26*, 4497; e) H. Zhang, M. A. Shahbazi, E. M. Makila, T. H. da Silva, R. L. Reis, J. J. Salonen, J. T. Hirvonen, H. A. Santos, *Biomaterials* **2013**, *34*, 9210.
- [218] Y. Song, Y. Li, Q. Xu, Z. Liu, *Int. J. Nanomedicine* **2017**, *12*, 87.
- [219] M. D. Jansson, A. H. Lund, *Molecular Oncology* **2012**, *6*, 590.
- [220] X. Yang, X. Liu, Z. Liu, F. Pu, J. Ren, X. Qu, *Adv. Mater.* **2012**, *24*, 2890.

- [221] J. J. Trausch, M. Shank-Retzlaff, T. Verch, *Anal. Chem.* **2017**, *89*, 3554.
- [222] E. W. Ng, D. T. Shima, P. Calias, E. T. Cunningham, Jr., D. R. Guyer, A. P. Adamis, *Nat. Rev. Drug Discovery* **2006**, *5*, 123.
- [223] C. Forier, E. Boschetti, M. Ouhammouch, A. Cibiel, F. Duconge, M. Nogre, M. Tellier, D. Bataille, N. Bihoreau, P. Santambien, S. Chtourou, G. Perret, *J. Chromatogr. A* **2017**, *1489*, 39.
- [224] C. Kuehne, S. Wedepohl, J. Dernedde, *Sensors* **2017**, *17*.
- [225] M. You, G. Zhu, T. Chen, M. J. Donovan, W. Tan, *Journal of the American Chemical Society* **2015**, *137*, 667.
- [226] B. Yuan, X. Jiang, Y. Chen, Q. Guo, K. Wang, X. Meng, Z. Huang, X. Wen, *Talanta* **2017**, *170*, 56.
- [227] L. Hong, F. Zhou, D. Shi, X. Zhang, G. Wang, *Biosensors & bioelectronics* **2017**, *95*, 152.
- [228] S. Wan, L. Zhang, S. Wang, Y. Liu, C. Wu, C. Cui, H. Sun, M. Shi, Y. Jiang, L. Li, L. Qiu, W. Tan, *J. Am. Chem. Soc.* **2017**, *139*, 5289.
- [229] S. Wang, L. Zhang, S. Wan, S. Cansiz, C. Cui, Y. Liu, R. Cai, C. Hong, I. T. Teng, M. Shi, Y. Wu, Y. Dong, W. Tan, *ACS Nano* **2017**, *11*, 3943.
- [230] X. Jiang, H. Wang, H. Wang, Y. Zhuo, R. Yuan, Y. Chai, *Anal. Chem.* **2017**, *89*, 4280.
- [231] L. Zhang, S. Wan, Y. Jiang, Y. Wang, T. Fu, Q. Liu, Z. Cao, L. Qiu, W. Tan, *Journal of the American Chemical Society* **2017**, *139*, 2532.
- [232] G. Zhu, S. Zhang, E. Song, J. Zheng, R. Hu, X. Fang, W. Tan, *Angew. Chem. Int. Ed. Engl.* **2013**, *52*, 5490.
- [233] Y. Han, D. Diao, Z. Lu, X. Li, Q. Guo, Y. Huo, Q. Xu, Y. Li, S. Cao, J. Wang, Y. Wang, J. Zhao, Z. Li, M. He, Z. Luo, X. Lou, *Anal. Chem.* **2017**, *89*, 5270.
- [234] B. Wang, B. Park, B. Xu, Y. Kwon, *J. Nanobiotechnology* **2017**, *15*, 40.
- [235] S. Eissa, M. Zourob, *Anal. Chem.* **2017**, *89*, 3138.
- [236] a) Z. Lai, J. Tan, R. Wan, J. Tan, Z. Zhang, Z. Hu, J. Li, W. Yang, Y. Wang, Y. Jiang, J. He, N. Yang, X. Lu, Y. Zhao, *Oncol. Rep.* **2017**, *37*, 2688; b) M. S. Song, S. S. Sekhon, W. R. Shin, H. C. Kim, J. Min, J. Y. Ahn, Y. H. Kim, *Molecules (Basel, Switzerland)* **2017**, *22*.
- [237] L. Hu, L. Wang, W. Lu, J. Zhao, H. Zhang, W. Chen, *Int. J. Mol. Sci.* **2017**, *18*.
- [238] M. Sypabekova, A. Bekmurzayeva, R. Wang, Y. Li, C. Nogues, D. Kanayeva, *Tuberc.* **2017**, *104*, 70.
- [239] D. J. Scoville, T. K. Uhm, J. A. Shallcross, R. J. Whelan, *J. Nucleic Acids* **2017**, *2017*, 9879135.
- [240] a) L. ACS Appl Mater Interfaces Zhou, N. Gan, Y. Zhou, T. Li, Y. Cao, Y. Chen, *Talanta* **2017**, *167*, 544; b) M. Chen, N. Gan, T. Li, Y. Wang, Q. Xu, Y. Chen, *Anal. Chim. Acta* **2017**, *968*, 30.
- [241] J. L. Chavez, J. A. Hagen, N. Kelley-Loughnane, *Sensors* **2017**, *17*.

- [242] D. Lu, L. He, G. Zhang, A. Lv, R. Wang, X. Zhang, W. Tan, *Nanophotonics* **2017**, *6*.
- [243] T. G. Cha, B. A. Baker, J. Salgado, C. J. Bates, K. H. Chen, A. C. Chang, M. C. Akatay, J. H. Han, M. S. Strano, J. H. Choi, *ACS Nano* **2012**, *6*, 8136.
- [244] R. Ueki, S. Sando, *Chem. Commun. (Cambridge, U. K.)* **2014**, *50*, 13131.
- [245] R. Ueki, A. Ueki, N. Kanda, S. Sando, *Angew. Chem. Int. Ed. Engl.* **2016**, *55*, 579.
- [246] M. Nishikawa, K. Ogawa, Y. Umeki, K. Mohri, Y. Kawasaki, H. Watanabe, N. Takahashi, E. Kusuki, R. Takahashi, Y. Takahashi, Y. Takakura, *J Control Release* **2014**, *180*, 25.
- [247] A. Zinchenko, Y. Miwa, L. I. Lopatina, V. G. Sergeyev, S. Murata, *ACS Applied Materials & Interfaces* **2014**, *6*, 3226.
- [248] X. Zhou, C. Li, Y. Shao, C. Chen, Z. Yang, D. Liu, *Chem. Commun.* **2016**, *52*, 10668.
- [249] J. Li, C. Zheng, S. Cansiz, C. Wu, J. Xu, C. Cui, Y. Liu, W. Hou, Y. Wang, L. Zhang, I. T. Teng, H. H. Yang, W. Tan, *J. Am. Chem. Soc.* **2015**, *137*, 1412.
- [250] S. H. J. Song, K. Im, J. Hur, J. Nam, S. Hwang, G. O. Ahn, S. K. a. N. Park, *J. Mater. Chem. B*, 1537.
- [251] J. Song, K. Im, S. Hwang, J. Hur, J. Nam, G. O. Ahn, S. Hwang, S. Kim, N. Park, *Nanoscale* **2015**, *7*, 9433.
- [252] H. Kang, A. C. Trondoli, G. Zhu, Y. Chen, Y. J. Chang, H. Liu, Y. F. Huang, X. Zhang, W. Tan, *ACS Nano* **2011**, *5*, 5094.
- [253] Y. Nishida, S. Ohtsuki, Y. Araie, Y. Umeki, M. Endo, T. Emura, K. Hidaka, H. Sugiyama, Y. Takahashi, Y. Takakura, M. Nishikawa, *Nanomedicine* **2016**, *12*, 123.
- [254] M. Nishikawa, Y. Mizuno, K. Mohri, N. Matsuoka, S. Rattanakiat, Y. Takahashi, H. Funabashi, D. Luo, Y. Takakura, *Biomaterials* **2011**, *32*, 488.
- [255] B. Xiang, K. He, R. Zhu, Z. Liu, S. Zeng, Y. Huang, Z. Nie, S. Yao, *ACS Appl. Mater. Interfaces* **2016**, *8*, 22801.
- [256] N. Park, S. H. Um, H. Funabashi, J. Xu, D. Luo, *Nat. Mater.* **2009**, *8*, 432.
- [257] N. Park, J. S. Kahn, E. J. Rice, M. R. Hartman, H. Funabashi, J. Xu, S. H. Um, D. Luo, *Nat. Protoc.* **2009**, *4*, 1759.
- [258] M. M. Stanton, J. Samitier, S. Sanchez, *Lab Chip* **2015**, *15*, 3111.
- [259] A. Tellechea, E. A. Silva, J. Min, E. C. Leal, M. E. Auster, L. Pradhan-Nabzdyk, W. Shih, D. J. Mooney, A. Veves, *Int. J. Lower Extremity Wounds* **2015**, *14*, 146.
- [260] Y. Che, A. Zinchenko, S. Murata, *J. Colloid Interface Sci.* **2015**, *445*, 364.
- [261] L. Zhang, J. Lei, L. Liu, C. Li, H. Ju, *Anal. Chem.* **2013**, *85*, 11077.
- [262] D. Wang, Y. Hu, P. Liu, D. Luo, *Acc. Chem. Res.* **2017**, *50*, 733.
- [263] Y. Wang, Y. Shao, X. Ma, B. Zhou, A. Faulkner-Jones, W. Shu, D. Liu, *ACS Appl. Mater. Interfaces* **2017**, *9*, 12311.
- [264] W. M. Jacobs, D. Frenkel, *J. Am. Chem. Soc.* **2016**, *138*, 2457.

- [265] C. A. Hong, B. Jang, E. H. Jeong, H. Jeong, H. Lee, *Chem. Commun.* **2014**, *50*, 13049.
- [266] Y. R. Yang, Y. Liu, H. Yan, *Bioconjugate Chem.* **2015**, *26*, 1381.
- [267] Q. Zhong, D. M. D. Chinta, S. Pamujula, H. Wang, X. Yao, T. K. Mandal, R. B. Luftig, *Journal of Nanobiotechnology* **2010**, *8*, 6.
- [268] X. Shen, Q. Jiang, J. Wang, L. Dai, G. Zou, Z.-G. Wang, W.-Q. Chen, W. Jiang, B. Ding, *Chem. Commun.* **2012**, *48*, 11301.
- [269] V. J. Schuller, S. Heidegger, N. Sandholzer, P. C. Nickels, N. A. Suhartha, S. Endres, C. Bourquin, T. Liedl, *Acs Nano* **2011**, *5*, 9696.
- [270] Q. Jiang, C. Song, J. Nangreave, X. Liu, L. Lin, D. Qiu, Z. G. Wang, G. Zou, X. Liang, H. Yan, B. Ding, *J. Am. Chem. Soc.* **2012**, *134*, 13396.
- [271] Q. Zhang, Q. Jiang, N. Li, L. Dai, Q. Liu, L. Song, J. Wang, Y. Li, J. Tian, B. Ding, Y. Du, *ACS Nano* **2014**, *8*, 6633.
- [272] Y. Ke, G. Bellot, N. V. Voigt, E. Fradkov, W. M. Shih, *Chem. Sci.* **2012**, *3*, 2587.
- [273] Y.-X. Zhao, A. Shaw, X. Zeng, E. Benson, A. M. Nyström, B. Höglberg, *ACS Nano* **2012**, *6*, 8684.
- [274] S. AbuHammad, M. Zihlif, *Genomics* **2013**, *101*, 213.
- [275] H. Glavinas, P. Krajcsi, J. Cserepes, B. Sarkadi, *Current drug delivery* **2004**, *1*, 27.
- [276] G. F. Davies, A. Berg, S. D. Postnikoff, H. L. Wilson, T. G. Arnason, A. Kusalik, T. A. Harkness, *PLoS One* **2014**, *9*, e84611.
- [277] B. Pang, X. Qiao, L. Janssen, A. Velds, T. Groothuis, R. Kerkhoven, M. Nieuwland, H. Ovaa, S. Rottenberg, O. van Tellingen, J. Janssen, P. Huijgens, W. Zwart, J. Neefjes, **2013**, *4*, 1908.
- [278] M. Frezza, S. Hindo, D. Chen, A. Davenport, S. Schmitt, D. Tomco, Q. P. Dou, *Curr. Pharm Des.* **2010**, *16*, 1813.
- [279] Y. Huang, W. Huang, L. Chan, B. Zhou, T. Chen, *Biomaterials* **2016**, *103*, 183.
- [280] A. Ora, E. Jarvihaavisto, H. Zhang, H. Auvinen, H. A. Santos, M. A. Kostiainen, V. Linko, *Chem. Commun.* **2016**, *52*, 14161.
- [281] J. Brglez, P. Nikolov, A. Angelin, C. M. Niemeyer, *Chem.* **2015**, *21*, 9440.
- [282] Z. Jiang, S. Zhang, C. Yang, J. Kjems, Y. Huang, F. Besenbacher, M. Dong, *Nano Res.* **2015**, *8*, 2170.
- [283] P. Wang, T. A. Meyer, V. Pan, P. K. Dutta, Y. Ke, *Chem.* **2017**, *2*, 359.
- [284] K. C. Neuman, A. Nagy, *Nat. Methods* **2008**, *5*, 491.
- [285] Y. Ke, S. Lindsay, Y. Chang, Y. Liu, H. Yan, *Science* **2008**, *319*, 180.
- [286] Z. Zhang, Y. Wang, C. Fan, C. Li, Y. Li, L. Qian, Y. Fu, Y. Shi, J. Hu, L. He, *Adv. Mater.* **2010**, *22*, 2672.
- [287] Z. Zhang, D. Zeng, H. Ma, G. Feng, J. Hu, L. He, C. Li, C. Fan, *Small* **2010**, *6*, 1854.

- [288] H. K. Subramanian, B. Chakraborty, R. Sha, N. C. Seeman, *Nano Lett.* **2011**, *11*, 910.
- [289] A. Kuzuya, Y. Sakai, T. Yamazaki, Y. Xu, M. Komiyama, *Nat. Commun.* **2011**, *2*, 449.
- [290] Y. Ke, T. Meyer, W. M. Shih, G. Bellot, *Nat. Commun.* **2016**, *7*, 10935.
- [291] A. Kuzuya, R. Watanabe, Y. Yamanaka, T. Tamaki, M. Kaino, Y. Ohya, *Sensors* **2014**, *14*, 19329.
- [292] R. Pepponi, G. Marra, M. P. Fuggetta, S. Falcinelli, E. Pagani, E. Bonmassar, J. Jiricny, S. D'Atri, *J. Pharmacol. Exp. Ther.* **2003**, *304*, 661.
- [293] M. Tintoré, A. Aviñó, F. M. Ruiz, R. Eritja, C. Fàbrega, *Journal of Nucleic Acids* **2010**, *2010*, 632041.
- [294] M. Tintore, I. Gallego, B. Manning, R. Eritja, C. Fabrega, *Angew. Chem., Int. Ed.* **2013**, *52*, 7747.
- [295] H. K. Walter, J. Bauer, J. Steinmeyer, A. Kuzuya, C. M. Niemeyer, H. A. Wagenknecht, *Nano Lett.* **2017**, *17*, 2467.
- [296] D. Jiang, Y. Sun, J. Li, Q. Li, M. Lv, B. Zhu, T. Tian, D. Cheng, J. Xia, L. Zhang, L. Wang, Q. Huang, J. Shi, C. Fan, *ACS Appl. Mater. Interfaces* **2016**, *8*, 4378.
- [297] L. Liang, J. Li, Q. Li, Q. Huang, J. Shi, H. Yan, C. Fan, *Angew. Chem., Int. Ed.* **2014**, *53*, 7745.
- [298] K. R. Kim, Y. D. Lee, T. Lee, B. S. Kim, S. Kim, D. R. Ahn, *Biomaterials* **2013**, *34*, 5226.
- [299] D. Chitkara, S. Singh, A. Mittal, *Ther. Delivery* **2016**, *7*, 245.
- [300] H. Lee, A. K. Lytton-Jean, Y. Chen, K. T. Love, A. I. Park, E. D. Karagiannis, A. Sehgal, W. Querbes, C. S. Zurenko, M. Jayaraman, C. G. Peng, K. Charisse, A. Borodovsky, M. Manoharan, J. S. Donahoe, J. Truelove, M. Nahrendorf, R. Langer, D. G. Anderson, *Nat. Nanotechnol.* **2012**, *7*, 389.
- [301] J. W. Keum, J. H. Ahn, H. Bermudez, *Small* **2011**, *7*, 3529.
- [302] a) V. Luc, Z. Alexei, *J. Phys. A: Math. Theor.* **2011**, *44*, 085201; b) K. A. Whitehead, R. Langer, D. G. Anderson, *Nat. Rev. Drug Discovery* **2009**, *8*, 129.
- [303] L. He, D. Q. Lu, H. Liang, S. Xie, C. Luo, M. Hu, L. Xu, X. Zhang, W. Tan, *ACS Nano* **2017**, *11*, 4060.
- [304] H. Pei, X. Zuo, D. Pan, J. Shi, Q. Huang, C. Fan, *NPG Asia Mater.* **2013**, *5*, e51.
- [305] N. N. Bu, A. Gao, X. W. He, X. B. Yin, *Biosensors & bioelectronics* **2013**, *43*, 200.
- [306] P. Sun, N. Zhang, Y. Tang, Y. Yang, X. Chu, Y. Zhao, *International Journal of Nanomedicine* **2017**, *12*, 2657.
- [307] H. Zhu, J. Fan, J. Du, X. Peng, *Acc. Chem. Res.* **2016**, *49*, 2115.
- [308] T. Ueno, T. Nagano, *Nat. Methods* **2011**, *8*, 642.
- [309] G. Qiao, L. Zhuo, Y. Gao, L. Yu, N. Li, B. Tang, *Chem. Commun.* **2011**, *47*, 7458.

- [310] S. Dhar, Z. Liu, J. Thomale, H. Dai, S. J. Lippard, *J. Am. Chem. Soc.* **2008**, *130*, 11467.
- [311] W. Pan, H. Yang, T. Zhang, Y. Li, N. Li, B. Tang, *Anal. Chem.* **2013**, *85*, 6930.
- [312] Y. Gao, G. Qiao, L. Zhuo, N. Li, Y. Liu, B. Tang, *Chem. Commun.* **2011**, *47*, 5316.
- [313] L. Chen, J. Chao, X. Qu, H. Zhang, D. Zhu, S. Su, A. Aldalbahi, L. Wang, H. Pei, *ACS Appl. Mater. Interfaces* **2017**, *9*, 8014.
- [314] G. Zhu, R. Hu, Z. Zhao, Z. Chen, X. Zhang, W. Tan, *J. Am. Chem. Soc.* **2013**, *135*, 16438.
- [315] K. Sefah, Z. Tang, D. Shangguan, H. Chen, D. Lopez-Colon, Y. Li, P. Parekh, J. Martin, L. Meng, W. Tan, *Leuk.* **2009**, *23*, 235.
- [316] L. Mei, G. Zhu, L. Qiu, C. Wu, H. Chen, H. Liang, S. Cansiz, Y. Lv, X. Zhang, W. Tan, *Nano Res.* **2015**, *8*, 3447.
- [317] A. M. Mohammed, R. Schulman, *Nano Lett.* **2013**, *13*, 4006.
- [318] a) M. Glaser, J. Schnauß, T. Tschirner, B. U. S. Schmidt, M. Moebius-Winkler, J. A. Käs, D. M. Smith, *New J. Phys.* **2016**, *18*, 055001; b) A. A. Hariri, G. D. Hamblin, Y. Gidi, H. F. Sleiman, G. Cosa, *Nat. Chem.* **2015**, *7*, 295.
- [319] R. F. Hariadi, B. Yurke, E. Winfree, *Chem. Sci.* **2015**, *6*, 2252.
- [320] X. Shi, X. Wu, T. Song, X. Li, *Nanoscale* **2016**, *8*, 14785.
- [321] S. Sellner, S. Kocabey, K. Nekolla, F. Krombach, T. Liedl, M. Rehberg, *Biomaterials* **2015**, *53*, 453.
- [322] A. M. Mohammed, P. Sulc, J. Zenk, R. Schulman, *Nat. Nanotechnol.* **2017**, *12*, 312.
- [323] P. K. Lo, P. Karam, F. A. Aldaye, C. K. McLaughlin, G. D. Hamblin, G. Cosa, H. F. Sleiman, *Nat. Chem.* **2010**, *2*, 319.
- [324] L. Liang, J. W. Shen, Q. Wang, *Colloids and surfaces. B, Biointerfaces* **2017**, *153*, 168.
- [325] S. Ko, H. Liu, Y. Chen, C. Mao, *Biomacromolecules* **2008**, *9*, 3039.
- [326] S. Kocabey, H. Meinl, I. S. MacPherson, V. Cassinelli, A. Manetto, S. Rothenfusser, T. Liedl, F. S. Lichtenegger, *Nanomater.* **2014**, *5*, 47.
- [327] K. Mohri, M. Nishikawa, N. Takahashi, T. Shiomi, N. Matsuoka, K. Ogawa, M. Endo, K. Hidaka, H. Sugiyama, Y. Takahashi, Y. Takakura, *ACS Nano* **2012**, *6*, 5931.
- [328] T. Zhou, P. Chen, L. Niu, J. Jin, D. Liang, Z. Li, Z. Yang, D. Liu, *Angew. Chem., Int. Ed.* **2012**, *51*, 11271.
- [329] H. Wang, Y. Yuan, Y. Zhuo, Y. Chai, R. Yuan, *Anal. Chem.* **2016**, *88*, 5797.
- [330] R. Walsh, J. M. Morales, C. G. Skipwith, T. T. Ruckh, H. A. Clark, *Sci. Rep.* **2015**, *5*, 14832.
- [331] F. Wei, W. Liao, Z. Xu, Y. Yang, D. T. Wong, C. M. Ho, *Small* **2009**, *5*, 1784.

- [332] H. Zhang, Y. Ma, Y. Xie, Y. An, Y. Huang, Z. Zhu, C. J. Yang, *Sci. Rep.* **2015**, *5*, 10099.
- [333] G. Tikhomirov, S. Hoogland, P. E. Lee, A. Fischer, E. H. Sargent, S. O. Kelley, *Nat. Nanotechnol.* **2011**, *6*, 485.
- [334] T. Zhang, A. Neumann, J. Lindlau, Y. Wu, G. Pramanik, B. Naydenov, F. Jelezko, F. Schuder, S. Huber, M. Huber, F. Stehr, A. Hogele, T. Weil, T. Liedl, *J. Am. Chem. Soc.* **2015**, *137*, 9776.
- [335] D. Zhu, J. Chao, H. Pei, X. Zuo, Q. Huang, L. Wang, W. Huang, C. Fan, *ACS Appl. Mater. Interfaces* **2015**, *7*, 11047.
- [336] a) P. Chen, T. Zhang, T. Zhou, D. Liu, *RSC Adv.* **2016**, *6*, 70553; b) T. Zhou, Y. Wang, Y. Dong, C. Chen, D. Liu, Z. Yang, *Bioorganic & medicinal chemistry* **2014**, *22*, 4391.
- [337] Y. Lv, R. Peng, Y. Zhou, X. Zhang, W. Tan, *Chem. Commun.* **2016**, *52*, 1413.
- [338] H. Tan, X. Li, S. Liao, R. Yu, Z. Wu, *Biosensors & bioelectronics* **2014**, *62*, 84.
- [339] G. Wang, L. Chen, X. He, Y. Zhu, X. Zhang, *Analyst* **2014**, *139*, 3895.
- [340] Y. Zhao, S. Hu, H. Wang, K. Yu, Y. Guan, X. Liu, N. Li, F. Liu, *Anal. Chem.* **2017**, *89*, 6907.
- [341] A. V. Pinheiro, D. Han, W. M. Shih, H. Yan, *Nat. Nanotechnol.* **2011**, *6*, 763.
- [342] W. Sun, T. Jiang, Y. Lu, M. Reiff, R. Mo, Z. Gu, *J. Am. Chem. Soc.* **2014**, *136*, 14722.
- [343] K. M. Arnold, L. M. Opdenaker, D. Flynn, J. Sims-Mourtada, *Cancer Growth Metastasis* **2015**, *8*, 1.
- [344] C. Wang, W. Sun, G. Wright, A. Z. Wang, Z. Gu, *Adv. Mater.* **2016**, *28*, 8912.
- [345] W. Sun, W. Ji, J. M. Hall, Q. Hu, C. Wang, C. L. Beisel, Z. Gu, *Angew. Chem., Int. Ed.* **2015**, *54*, 12029.
- [346] Z. Zhao, J. Fu, S. Dhakal, A. Johnson-Buck, M. Liu, T. Zhang, N. W. Woodbury, Y. Liu, N. G. Walter, H. Yan, *Nat. Commun.* **2016**, *7*, 10619.
- [347] J. Fu, Y. R. Yang, S. Dhakal, Z. Zhao, M. Liu, T. Zhang, N. G. Walter, H. Yan, *Nat. Protoc.* **2016**, *11*, 2243.
- [348] S. Campuzano, P. Yanez-Sedeno, J. M. Pingarron, *Sensors* **2017**, *17*.
- [349] E. D. Mentovich, K. Livanov, D. K. Prusty, M. Sowwan, S. Richter, *J. Nanobiotechnology* **2012**, *10*, 21.
- [350] S. A. Wajed, P. W. Laird, T. R. DeMeester, *Ann. Surg.* **2001**, *234*, 10.
- [351] X. Wang, M. Cui, H. Zhou, S. Zhang, *Chem. Commun.* **2015**, *51*, 13983.
- [352] F. Kong, H. Zhang, X. Qu, X. Zhang, D. Chen, R. Ding, E. Makila, J. Salonen, H. A. Santos, M. Hai, *Adv. Mater.* **2016**, *28*, 10195.
- [353] S. Chernousova, M. Epple, *Angew. Chem., Int. Ed.* **2013**, *52*, 1636.

- [354] T. Takeshima, Y. Tada, N. Sakaguchi, F. Watari, B. Fugetsu, *Nanomater.* **2015**, *5*, 284.
- [355] J. Cao, C. Feng, Y. Liu, S. Wang, F. Liu, *Biosensors & bioelectronics* **2014**, *57*, 133.
- [356] A. Cecconello, C. H. Lu, J. Elbaz, I. Willner, *Nano Lett.* **2013**, *13*, 6275.
- [357] J. V. Pellegrotti, G. P. Acuna, A. Puchkova, P. Holzmeister, A. Gietl, B. Lalkens, F. D. Stefani, P. Tinnefeld, *Nano Lett.* **2014**, *14*, 2831.
- [358] K. A. Afonin, M. Viard, I. Kagiampakis, C. L. Case, M. A. Dobrovolskaia, J. Hofmann, A. Vrzak, M. Kireeva, W. K. Kasprzak, V. N. KewalRamani, B. A. Shapiro, *ACS Nano* **2015**, *9*, 251.
- [359] D. Sun, H. Maeno, M. Gujrati, R. Schur, A. Maeda, T. Maeda, K. Palczewski, Z. R. Lu, *Macromol. Biosci.* **2015**, *15*, 1663.
- [360] K. Plourde, R. M. Derbali, A. Desrosiers, C. Dubath, A. Vallee-Belisle, J. Leblond, *J. Controlled Release* **2017**, *251*, 82.
- [361] G. Zhu, Y. Liu, X. Yang, Y. H. Kim, H. Zhang, R. Jia, H. S. Liao, A. Jin, J. Lin, M. Aronova, R. Leapman, Z. Nie, G. Niu, X. Chen, *Nanoscale* **2016**, *8*, 6684.
- [362] Y. Chen, P. Xu, Z. Shu, M. Wu, L. Wang, S. Zhang, Y. Zheng, H. Chen, J. Wang, Y. Li, J. Shi, *Adv. Funct. Mater.* **2014**, *24*, 4386.
- [363] R. Mo, T. Jiang, W. Sun, Z. Gu, *Biomaterials* **2015**, *50*, 67.
- [364] Y. Guo, Y. Wang, S. Li, L. Niu, D. Wei, S. Zhang, *Chem. Commun.* **2017**, *53*, 4826.
- [365] D. Mariottini, A. Idili, A. Vallee-Belisle, K. W. Plaxco, F. Ricci, *Nano Lett.* **2017**, *17*, 3225.
- [366] Z. Wang, Y. Xu, H. Wang, F. Liu, Z. Ren, Z. Wang, *Sci. Rep.* **2016**, *6*, 28292.
- [367] E. Del Grosso, A. M. Dallaire, A. Vallee-Belisle, F. Ricci, *Nano Lett.* **2015**, *15*, 8407.
- [368] M. Rossetti, S. Ranallo, A. Idili, G. Palleschi, A. Porchetta, F. Ricci, *Chem. Sci.* **2017**, *8*, 914.
- [369] X. Qu, H. Zhang, H. Chen, A. Aldalbahi, L. Li, Y. Tian, D. A. Weitz, H. Pei, *Anal. Chem.* **2017**, *89*, 3468.
- [370] Y. Zhang, S. Jiang, D. Zhang, X. Bai, S. M. Hecht, S. Chen, *Chem. Commun.* **2017**, *53*, 573.
- [371] S. M. Douglas, I. Bachelet, G. M. Church, *Science* **2012**, *335*, 831.
- [372] J. Yang, B. Dou, R. Yuan, Y. Xiang, *Anal. Chem.* **2017**, *89*, 5138.
- [373] Y. Hou, J. Liu, M. Hong, X. Li, Y. Ma, Q. Yue, C. Z. Li, *Biosensors & bioelectronics* **2017**, *92*, 259.
- [374] Y. Wu, F. Xiao, Z. Wu, R. Yu, *Anal. Chem.* **2017**, *89*, 2852.
- [375] R. Schiess, B. Wollscheid, R. Aebersold, *Mol Oncol* **2009**, *3*, 33.
- [376] M. You, L. Peng, N. Shao, L. Zhang, L. Qiu, C. Cui, W. Tan, *Journal of the American Chemical Society* **2014**, *136*, 1256.

- [377] J. Xu, Z. S. Wu, W. Shen, H. Xu, H. Li, L. Jia, *Biosensors & bioelectronics* **2015**, *73*, 19.
- [378] B. Yang, X. B. Zhang, L. P. Kang, Z. M. Huang, G. L. Shen, R. Q. Yu, W. Tan, *Nanoscale* **2014**, *6*, 8990.
- [379] S. Kim, H. J. Lee, *Anal. Chem.* **2017**, *89*, 6624.
- [380] a) A. Azadbakht, M. Roushani, A. R. Abbasi, Z. Derikvand, *Anal. Biochem.* **2016**, *512*, 58; b) S. Beiranvand, A. Azadbakht, *Mater. Sci. Eng., C* **2017**, *76*, 925.
- [381] E. H. Lee, H. J. Lim, S. D. Lee, A. Son, *ACS Appl. Mater. Interfaces* **2017**, *9*, 14889.
- [382] H. J. Lim, B. Chua, A. Son, *Biosensors & bioelectronics* **2017**, *94*, 10.
- [383] S. Saha, V. Prakash, S. Halder, K. Chakraborty, Y. Krishnan, *Nat. Nanotechnol.* **2015**, *10*, 645.
- [384] J. R. Burns, A. Seifert, N. Fertig, S. Howorka, *Nat. Nanotechnol.* **2016**, *11*, 152.
- [385] A. Seifert, K. Gopfrich, J. R. Burns, N. Fertig, U. F. Keyser, S. Howorka, *ACS Nano* **2015**, *9*, 1117.
- [386] V. Maingi, M. Lelimousin, S. Howorka, M. S. Sansom, *ACS Nano* **2015**, *9*, 11209.
- [387] S. Hernandez-Ainsa, N. A. Bell, V. V. Thacker, K. Gopfrich, K. Misiunas, M. E. Fuentes-Perez, F. Moreno-Herrero, U. F. Keyser, *ACS Nano* **2013**, *7*, 6024.
- [388] X. L. Guo, D. D. Yuan, T. Song, X. M. Li, *Anal. Bioanal. Chem.* **2017**, *409*, 3789.
- [389] R. Savic, L. Luo, A. Eisenberg, D. Maysinger, *Science* **2003**, *300*, 615.
- [390] a) H. Khan, S. Chen, H. Zhou, S. Wang, W. Zhang, *Macromolecules* **2017**, *50*, 2794; b) S. Li, X. He, Q. Li, P. Shi, W. Zhang, *ACS Macro Lett.* **2014**, *3*, 916.
- [391] a) Z. Li, E. Kesselman, Y. Talmon, M. A. Hillmyer, T. P. Lodge, *Science* **2004**, *306*, 98; b) J. N. Marsat, M. Heydenreich, E. Kleinpeter, H. V. Berlepsch, C. Böttcher, A. Laschewsky, *Macromolecules* **2011**, *44*, 2092.
- [392] A. Czogalla, H. G. Franquelim, P. Schwille, *Biophys J.* **2016**, *110*, 1698.
- [393] C. Duan, W. Li, F. Qiu, A.-C. Shi, *ACS Macro Lett.* **2017**, *6*, 257.
- [394] J. Prasad, I. Zins, R. Branscheid, J. Becker, A. H. R. Koch, G. Fytas, U. Kolb, C. Sönnichsen, *J. Phys. Chem. C* **2015**, *119*, 5577.
- [395] L. Y. Chou, F. Song, W. C. Chan, *J. Am. Chem. Soc.* **2016**, *138*, 4565.
- [396] L. Y. Chou, K. Zagorovsky, W. C. Chan, *Nat. Nanotechnol.* **2014**, *9*, 148.
- [397] S. Ohta, D. Glancy, W. C. Chan, *Science* **2016**, *351*, 841.
- [398] V. Raeesi, L. Y. T. Chou, W. C. W. Chan, *Adv. Mater.* **2016**, *28*, 8511.
- [399] M. M. Maye, M. T. Kumara, D. Nykypanchuk, W. B. Sherman, O. Gang, *Nat Nano* **2010**, *5*, 116.
- [400] K. Zagorovsky, L. Y. T. Chou, W. C. W. Chan, *Proceedings of the National Academy of Sciences* **2016**, *113*, 13600.

- [401] L. Sercombe, T. Veerati, F. Moheimani, S. Y. Wu, A. K. Sood, S. Hua, *Front. Pharmacol.* **2015**, 6.
- [402] P. Mishra, B. Nayak, R. K. Dey, *Asian J. Pharm. Sci.* **2016**, 11, 337.
- [403] A. K. Mitra, V. Agrahari, A. Mandal, K. Cholkar, C. Natarajan, S. Shah, M. Joseph, H. M. Trinh, R. Vaishya, X. Yang, Y. Hao, V. Khurana, D. Pal, *J. Controlled Release* **2015**, 219, 248.
- [404] R. Xu, G. Zhang, J. Mai, X. Deng, V. Segura-Ibarra, S. Wu, J. Shen, H. Liu, Z. Hu, L. Chen, Y. Huang, E. Koay, Y. Huang, J. Liu, J. E. Ensor, E. Blanco, X. Liu, M. Ferrari, H. Shen, *Nat. Biotechnol.* **2016**, 34, 414.
- [405] F. Xu, F. Wang, T. Yang, Y. Sheng, T. Zhong, Y. Chen, *Cancer Cell Int.* **2014**, 14, 538.
- [406] C. A. Frederick, L. D. Williams, G. Ughetto, G. A. van der Marel, J. H. van Boom, A. Rich, A. H. Wang, *Biochem.* **1990**, 29, 2538.
- [407] F. Zhang, J. Nangreave, Y. Liu, H. Yan, *J. Am. Chem. Soc.* **2014**, 136, 11198.
- [408] P. Song, M. Li, J. Shen, H. Pei, J. Chao, S. Su, A. Aldalbahi, L. Wang, J. Shi, S. Song, L. Wang, C. Fan, X. Zuo, *Anal. Chem.* **2016**, 88, 8043.
- [409] Z. H. Fan, W. Tan, *Nanomedicine* **2013**, 8, 1731.
- [410] A. Barati Farimani, P. Dibaeinia, N. R. Aluru, *ACS Appl. Mater. Interfaces* **2017**, 9, 92.
- [411] D. D. Dickey, G. S. Thomas, J. P. Dassie, P. H. Giangrande, *Methods Mol. Biol.* **2016**, 1364, 209.
- [412] E. S. Gragoudas , A. P. Adamis , E. T. J. Cunningham , M. Feinsod , D. R. Guyer *N. Engl. J. Med.* **2004**, 351, 2805.
- [413] J. Geng, S. Wang, H. Fang, P. Guo, *ACS Nano* **2013**, 7, 3315.